Supporting Information for

Alkali metal mediated hydroboration and cyano sillylation of carbonyl compounds

Adimulam Harinath,[a] Jayeeta Bhattacharjee,[a] Hari Pada Nayek[b] and Tarun K. Panda*[a]

Department of Chemistry, Indian Institute of Technology Hyderabad, Kandi, Sangareddy, 502285, Telangana, India. Fax: + 91(40) 2301 6032; Tel: + 91(40) 2301 6036; E-mail: tpanda@iith.ac.in

Table of Contents

X-ray crystallographic analyses: Single crystals of complexes **1-4** were grown from a concentrated solution of THF/n-pentane (3:1) in an argon-filled atmosphere at -35 °C. However, single crystals of **LH.HCl** was obtained from a solution of ethanol at -35 °C. A crystal of suitable dimensions of complexes **1-4** was mounted on a CryoLoop (Hampton Research Corp.) with a layer of light mineral oil and placed in a nitrogen stream at 150(2) K. The crystals of **LH.HCl** was measured at 298 K. All measurements were made on an Rigaku Supernova X-calibur Eos CCD detector with graphite monochromatic Cu-Kα (1.54184 Å) radiation. The data for the compounds LH.HCl and sodium complex **2** are not satisfactory and R factors are high. Thus only figures of LH.HCl (Fig FS2) and complex 2 (Fig FS3) were used for comparison only. Crystal data and structure refinement parameters of complexes **1**, **3** and **4** are summarized in Table TS1. The structures were solved by direct methods (SIR2004)[1] and refined on F^2 by full-matrix least-squares methods, using SHELXL-97.[2] Non-hydrogen atoms were anisotropically refined. H-atoms were included in the refinement on calculated positions riding on their carrier atoms. The function minimized was $[\sum w(Fo^2 - Fc^2)^2]$ ($w = 1 / [\sigma^2 (Fo^2) + (aP)^2 + bP]$), where $P = (\mathrm{Max}(Fo^2,0) + 2Fc^2) / 3$ with $\sigma^2(Fo^2)$ from counting statistics. The function $R1$ and $wR2$ were $(\Sigma||Fo| - |Fc||) / \Sigma|Fo|$ and $[\Sigma w(Fo^2 - Fc^2)^2 / \Sigma(wFo^4)]^{1/2}$, respectively. The ORTEP-3 program was used to draw the molecules of **LH.HCl**, **1**, **2**, and **4**. However, Diamond 3 program was used to draw the molecule of **3**. Crystallographic data (excluding structure factors) for the structures reported in this paper have been deposited with the Cambridge Crystallographic Data Centre as supplementary publication no. CCDC 1844011 (**1**), 1844012 (**3**), 1844010 (**4**). Copies of the data can be obtained free of charge on application to CCDC, 12 Union Road, Cambridge CB21EZ, UK (fax: + (44)1223-336-033; email: deposit@ccdc.cam.ac.uk).

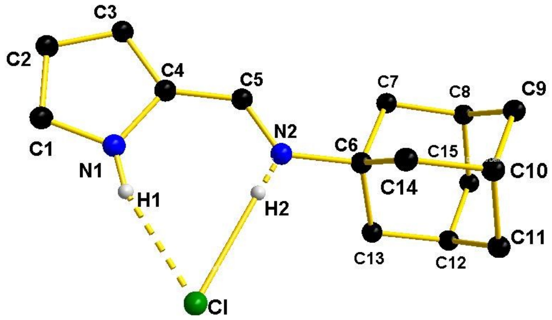

Figure FS1. Molecular solid-state structure of **LH.HCl**. The R factors of the complex **LH.HCl** are slightly high due to poor data set. Nevertheless the Fig FS1 confirms the formation of the ligand **LH**.

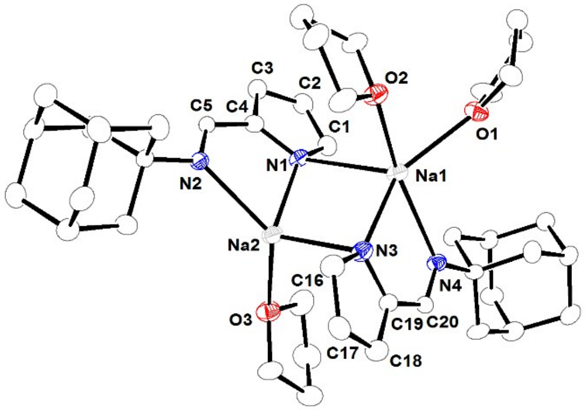

Figure FS2. Solid state structure of sodium complex **2**. The R factors of the complex **2** are slightly high due to poor data set. Nevertheless the Fig FS2 confirms the four fold and five fold coordination around the sodium ions.

Table TS1. Crystallographic data and refinement parameters of **1**, **3** and **4**.

Crystal Parameters	**1**	**3**	**4**
CCDC No.	1844011	1844012	1844010
Empirical formula	$C_{38}H_{54}N_2Li_2O_2$	$C_{19}H_{27}N_2OK$	$C_{46}H_{70}N_4O_4Mg$
Formula weight	612.73	338.53	767.37
T (K)	150(2) K	152(2) K	150(2) K
λ (Å)	1.54184 A	1.54184 A	1.54184 A
Crystal system	monoclinic	triclinic	monoclinic
Space group	$P\ 2_1/c$	*P* -1	$P\ 2_1/c$
a(Å)	11.4708(4)	7.3434(12)	11.1013(4)
b (Å)	10.5272(3)	11.2646(17)	37.9808(18)
c(Å)	14.4429(4)	11.9562(19)	10.1334(3)
α (°)	90.00	86.178(13)	90.00
β (°)	105.612(3)	72.192(15)	94.099(3)
γ (°)	90.00	76.218(14)	90.00
V(Å^3)	1679.71(9)	914.5(3)	4261.7(3)
Z	2	2	4
D_{calc} g cm^{-3}	1.211	1.229	1.196
μ (mm^{-1})	0.567	2.575	0.723
F(000)	664	364	1672
Theta range for data collection	4.001 to 70.59 Deg	3.883 to 70.713 deg	3.99 to 70.85 deg.
Limiting indices -	$-13 \leq h \leq 13$, $-12 \leq k \leq 9$, $-17 \leq l \leq 13$	-8<=h<=8, -7<=k<=13, -14<=l<=13.	-9<=h<=13, -40<=k<=46, -11<=l<=12.
Reflections collected / unique	6112 / 3151 [R(int) = 0.0220]	3359 / 2592 [R(int) = 0.0349]	17729 / 8061 [R(int) = 0.0531]
Completeness to theta	99.5 %	76.3 %	98.0 %
Absorption corraction	Semi-empirical from equivalents	Semi-empirical from equivalents	Semi-empirical from equivalents
Max. and min. transmission	1.00000 and 0.68112	1.00000 and 0.83710	1.00000 and 0.65420
Refinement method	Full-matrix least-squares on F^2	Full-matrix least-squares on F^2	Full-matrix least-squares on F^2
Data / restraints / parameters	3151 / 0 / 216	2592 / 0 / 215	8061 / 0 / 496
Goodness-of-fit on F^2	1.123	1.084	1.047

Final R indices [I>2sigma(I)]	R1 = 0.0475, wR2 = 0.1388	R1 = 0.0732, wR2 = 0.1893	R1 = 0.0738, wR2 = 0.1870
R indices (all data)	R1 = 0.0511, wR2 = 0.1413	R1 = 0.0957, wR2 = 0.2186	R1 = 0.0976, wR2 = 0.2089
Absolute structure parameter			
Largest diff. peak and hole	0.267 and -0.305 e.A^-3	0.683 and -0.666 e.A^-	0.550 and -0.359 e.A^-3

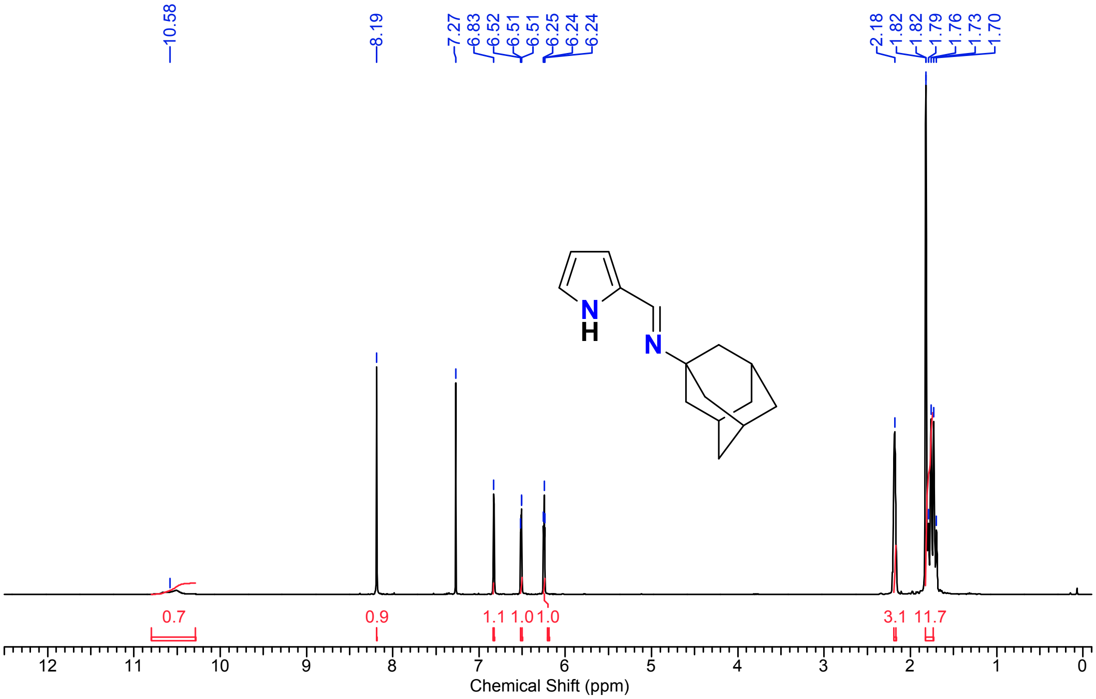

Figure FS3. ^{1}H NMR spectra of complex **L1.**

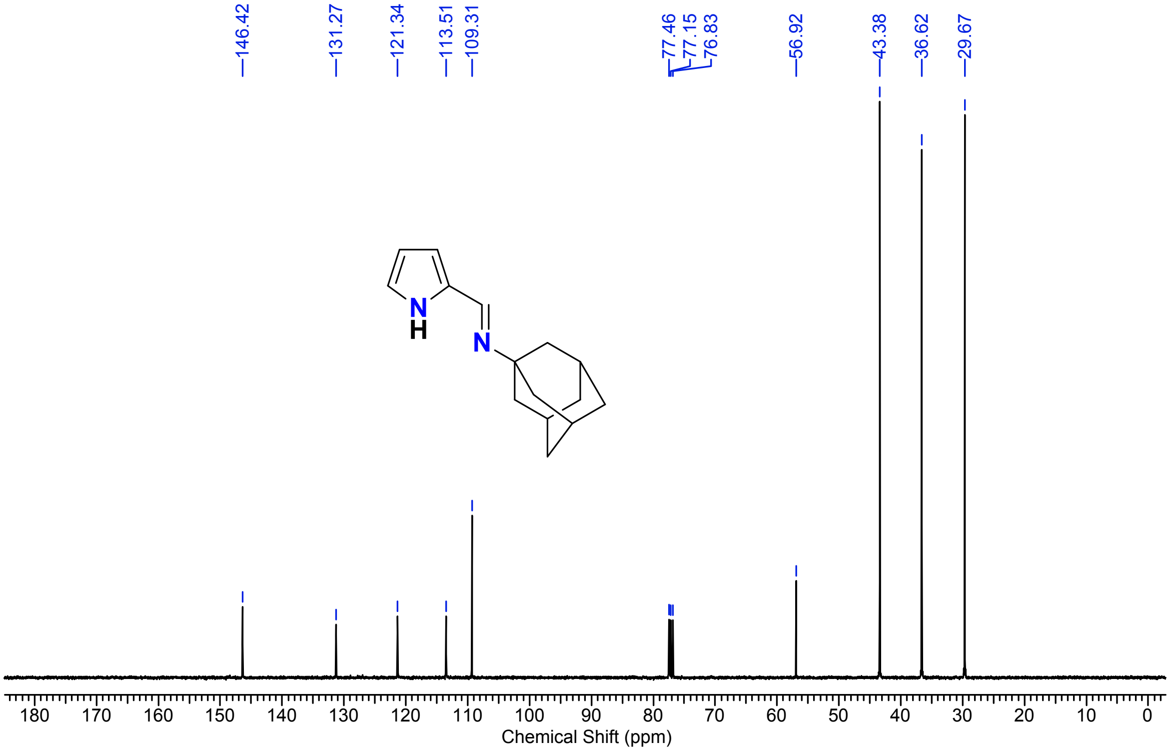

Figure FS4. ^{13}C NMR spectra of complex **L1.**

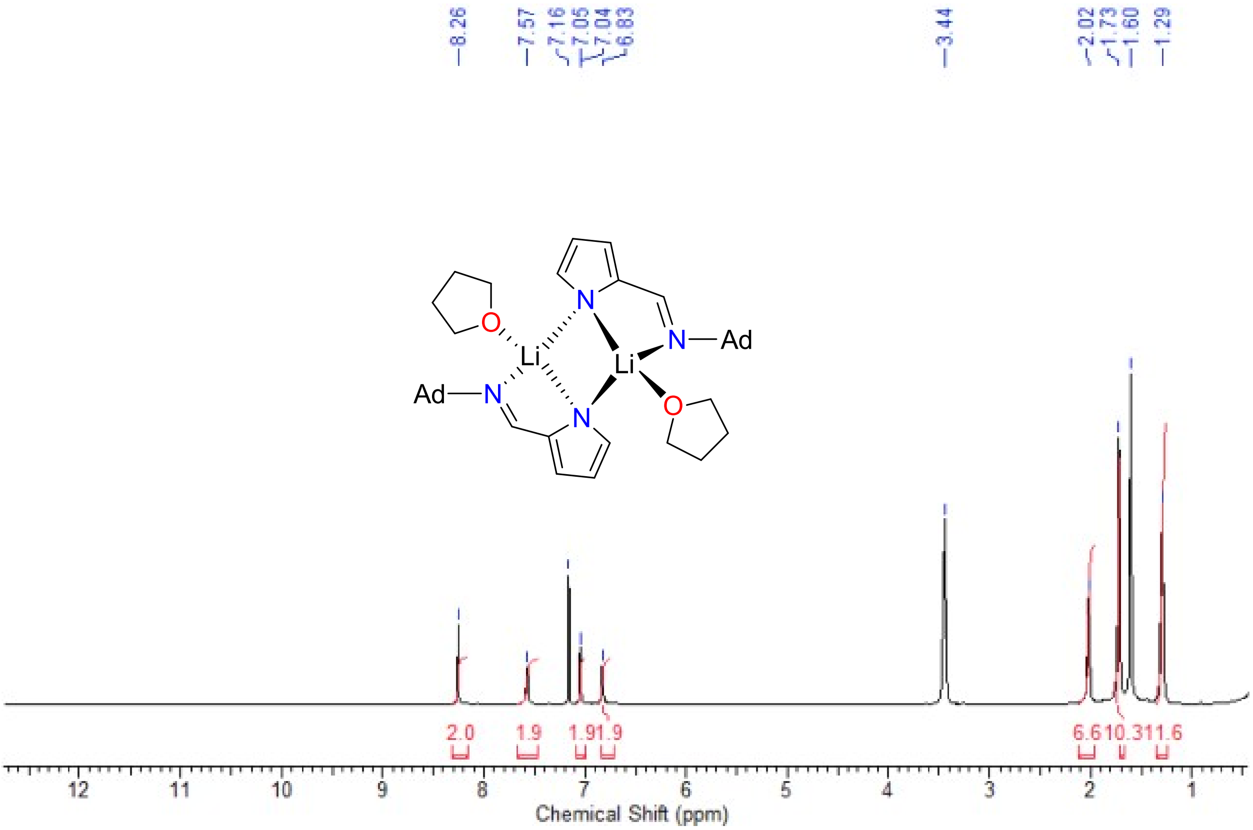

Figure FS5. ^{1}H NMR spectra of complex **1.**

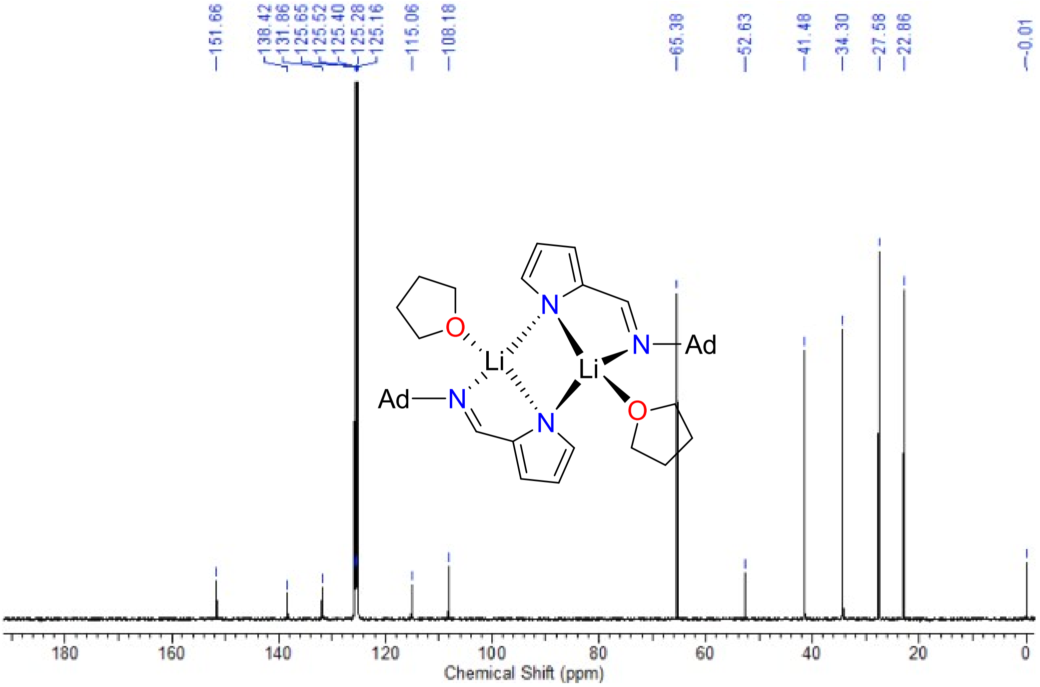

Figure FS6. ^{13}C NMR spectra of complex **1**.

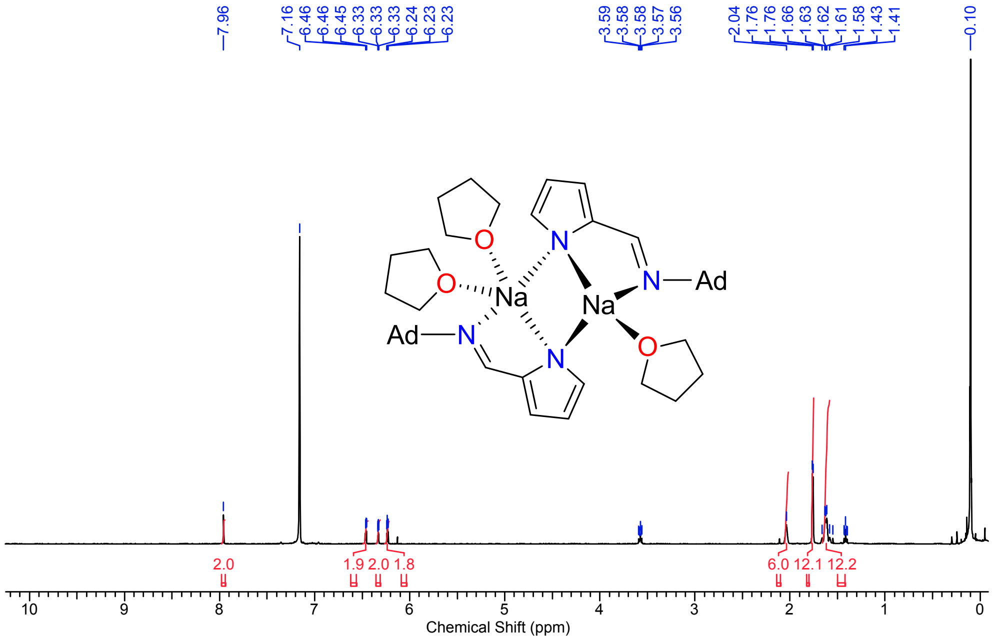

Figure FS7. ^{13}C NMR spectra of complex **2.**

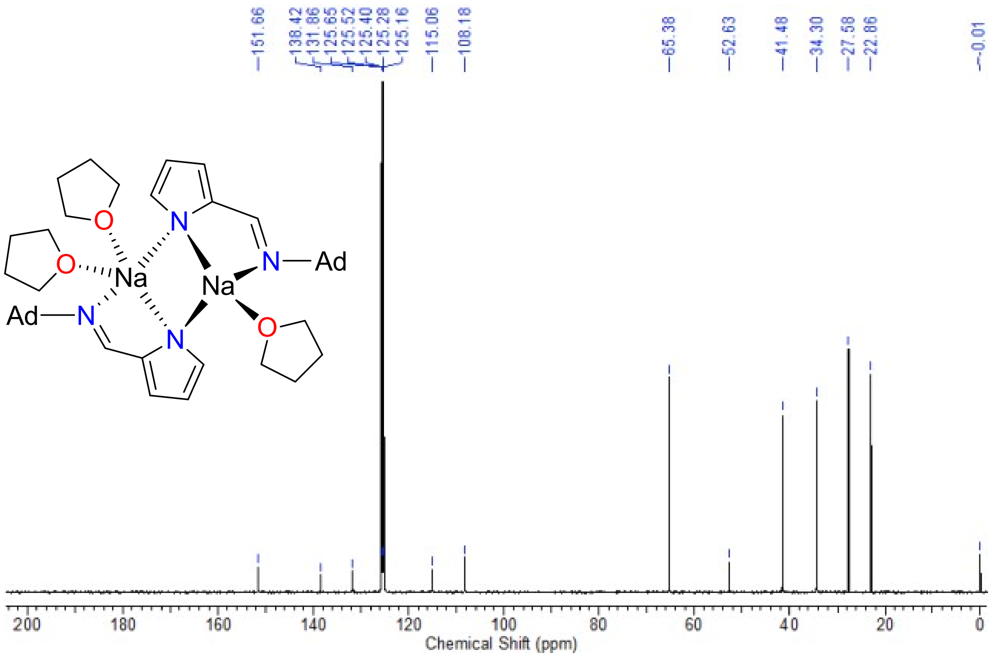

Figure FS8. ^{13}C NMR spectra of complex **2**.

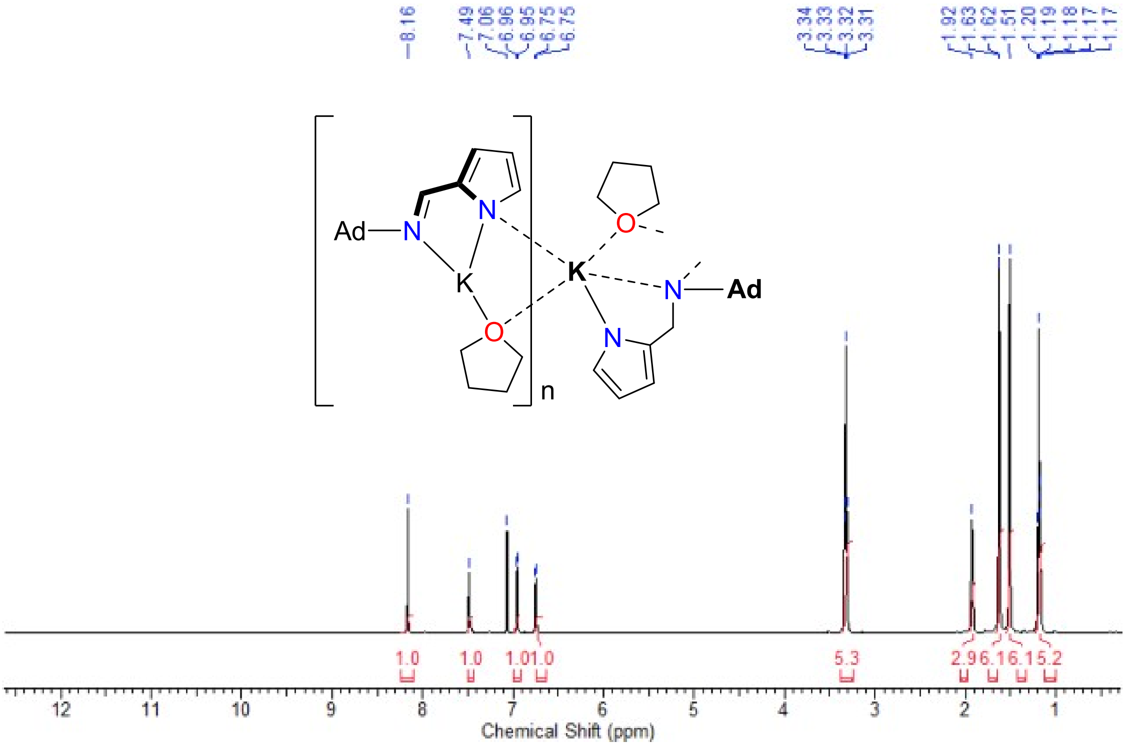

Figure FS9: ^{1}H NMR spectra of complex **3.**

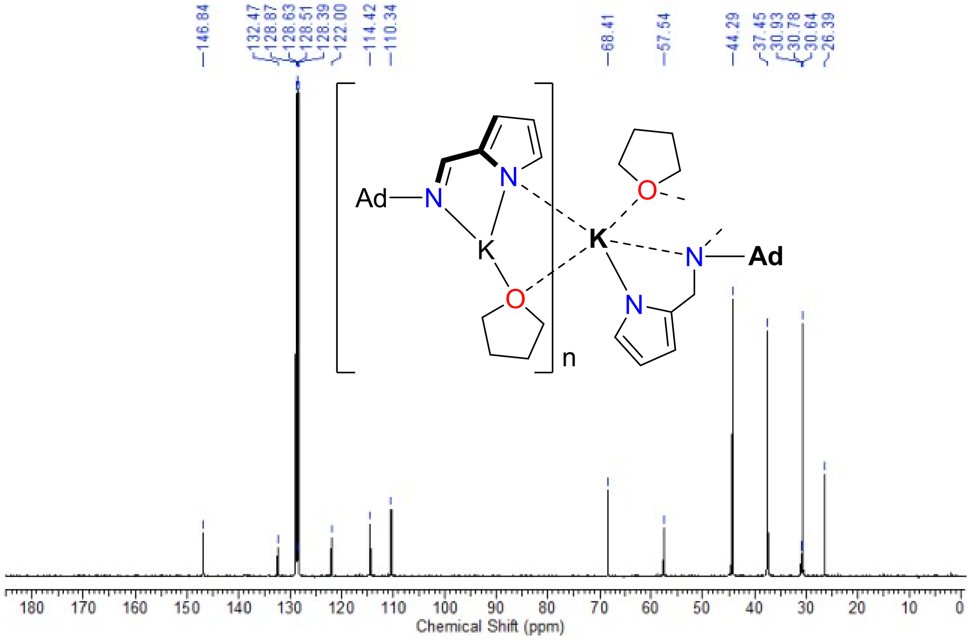

Figure FS10. ^{13}C NMR spectra of complex **3**.

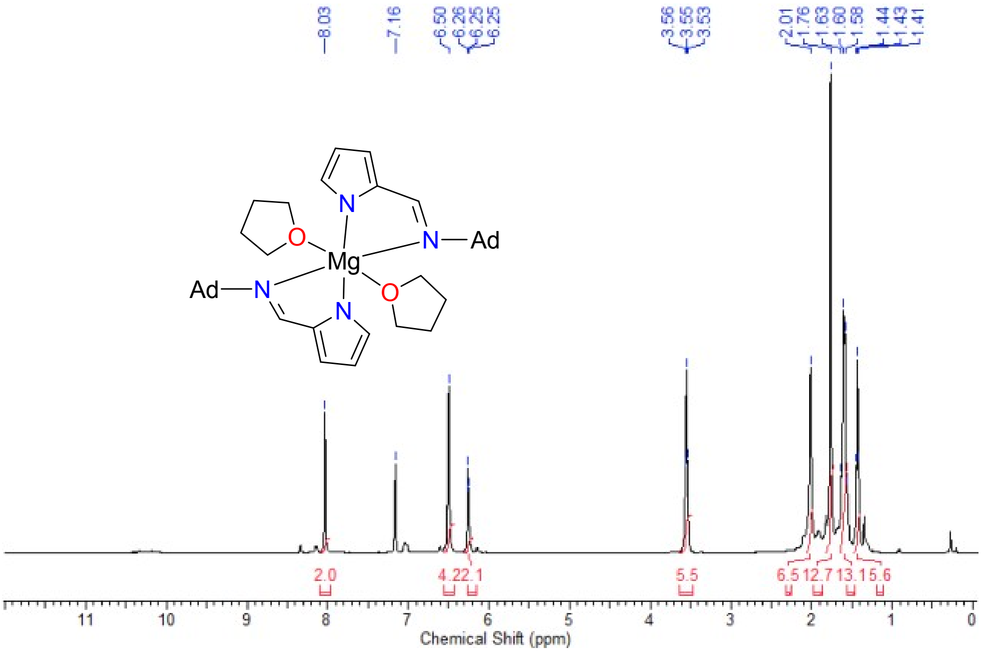

Figure FS11. ^{1}H NMR spectra of Magnesium complex **4.**

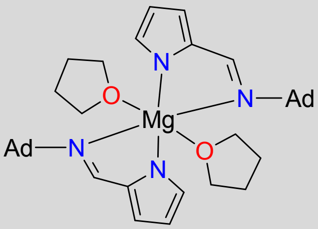

Figure FS12. ^{13}C NMR spectra of magnesium complex **4**.

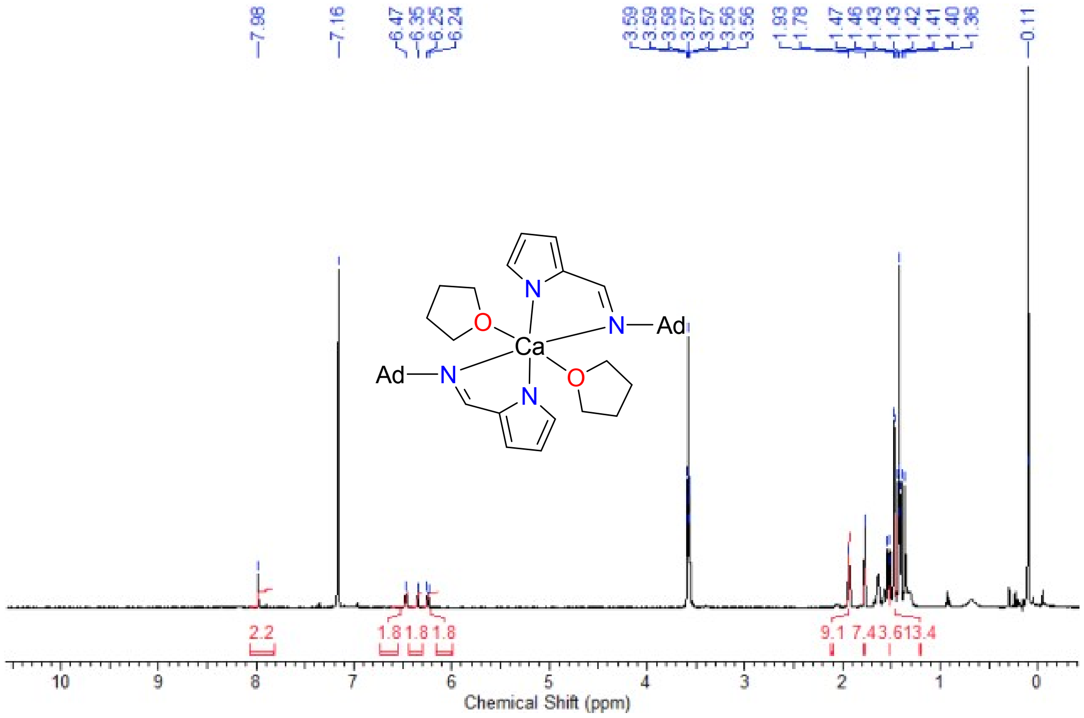

Figure FS13. ^{1}H NMR spectra of calcium complex **5.**

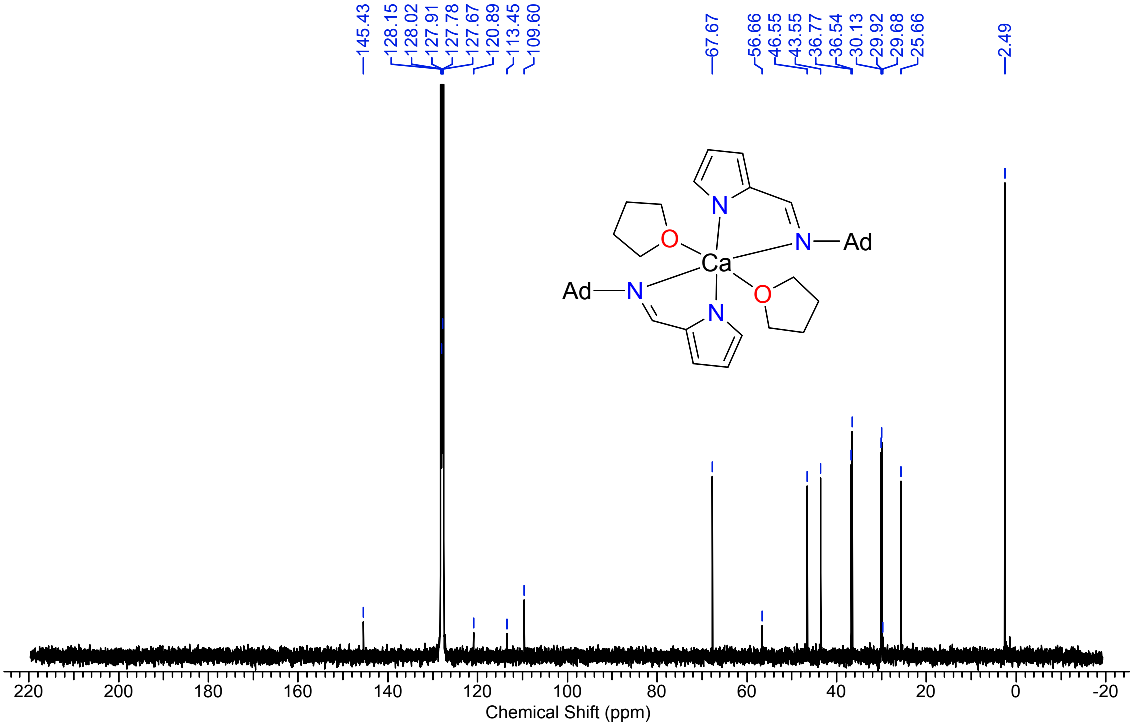

Figure FS14. ^{13}C NMR spectra of Calcium complex **5**.

Typical procedure for hydroborylation of carbonyl compounds:

Hydroboylation of carbonyl compounds were carried out using the following standard protocol. In the glove box, the chosen pre-catalyst (0.03 mmol) was loaded into a Schlenk tube, and subsequently the aldehyde or ketone (1 mmol) followed by pinacolborane (1 mmol) were added. The reaction was stirred in an oil bath at the desired temperature (30°C). Substrate conversion was monitored by examination of the ^{1}H NMR, which indicates the formation of new CH_2 (for aldehydes) CH (ketones) peak and disappearance of aldehyde proton.

Typical procedure for TMSCN addition to carbonyl compounds:

TMSCN addition of carbonyl compounds were carried out using the following standard protocol. In the glove box, the chosen pre-catalyst (0.03 mmol) was loaded into a Schlenk tube, and subsequently the aldehyde or ketone (1 mmol) followed by TMSCN (1 mmol) were added. The reaction was stirred in an oil bath at the desired temperature (30°C).

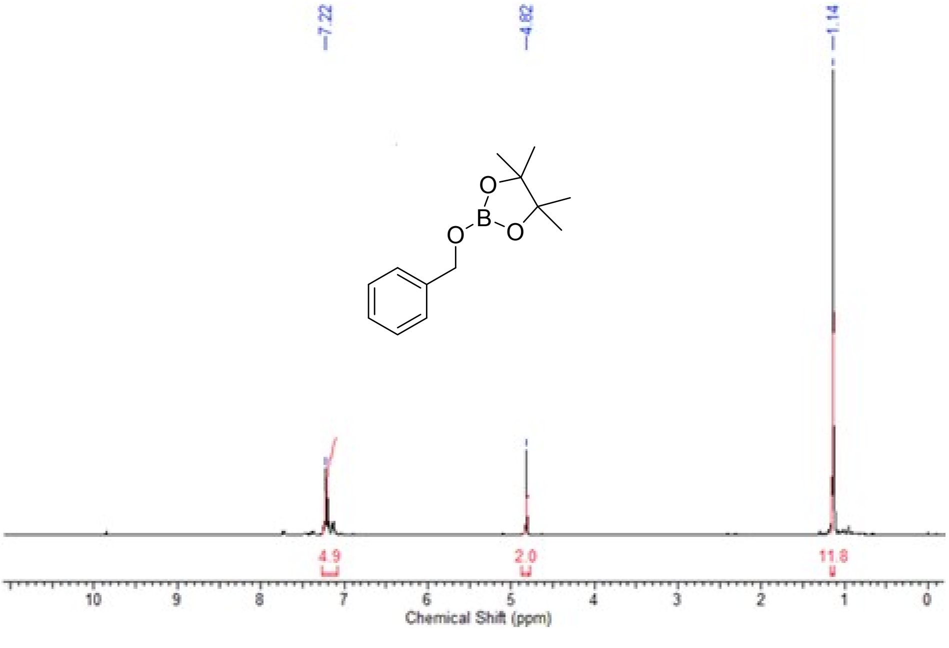

Figure FS15. ^{1}H NMR spectrum (400 MHz, 25°C, $CDCl_3$) of 2-(benzyloxy)-4,4,5,5-tetramethyl-1,3,2-dioxaborolane.

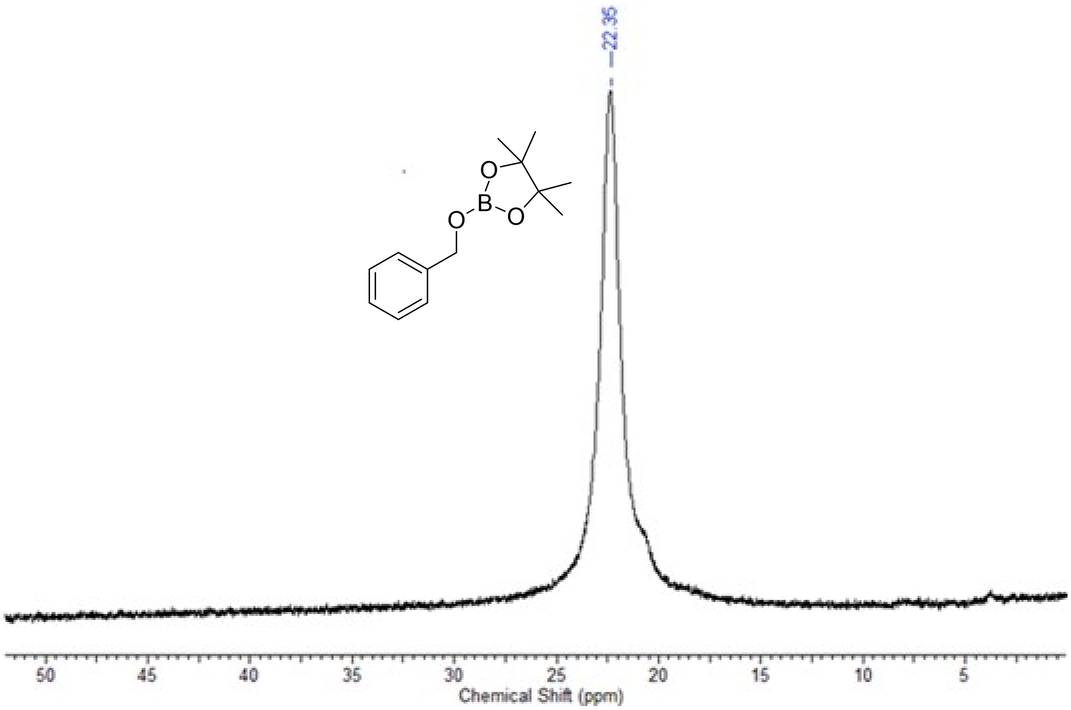

Figure S16. ^{11}B NMR spectrum (128.4 MHz, 25°C, $CDCl_3$) of 2-(benzyloxy)-4,4,5,5-tetramethyl-1,3,2-dioxaborolane.

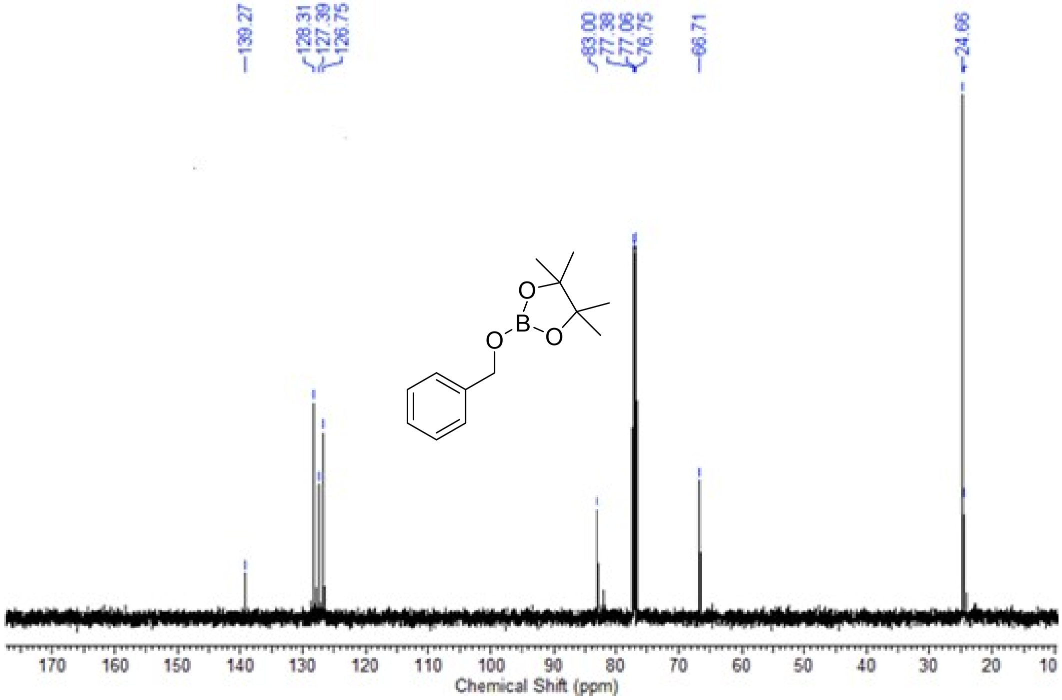

Figure FS17. ^{13}C NMR spectrum (100 MHz, 25°C, $CDCl_3$) of 2-(benzyloxy)-4,4,5,5-tetramethyl-1,3,2-dioxaborolane.

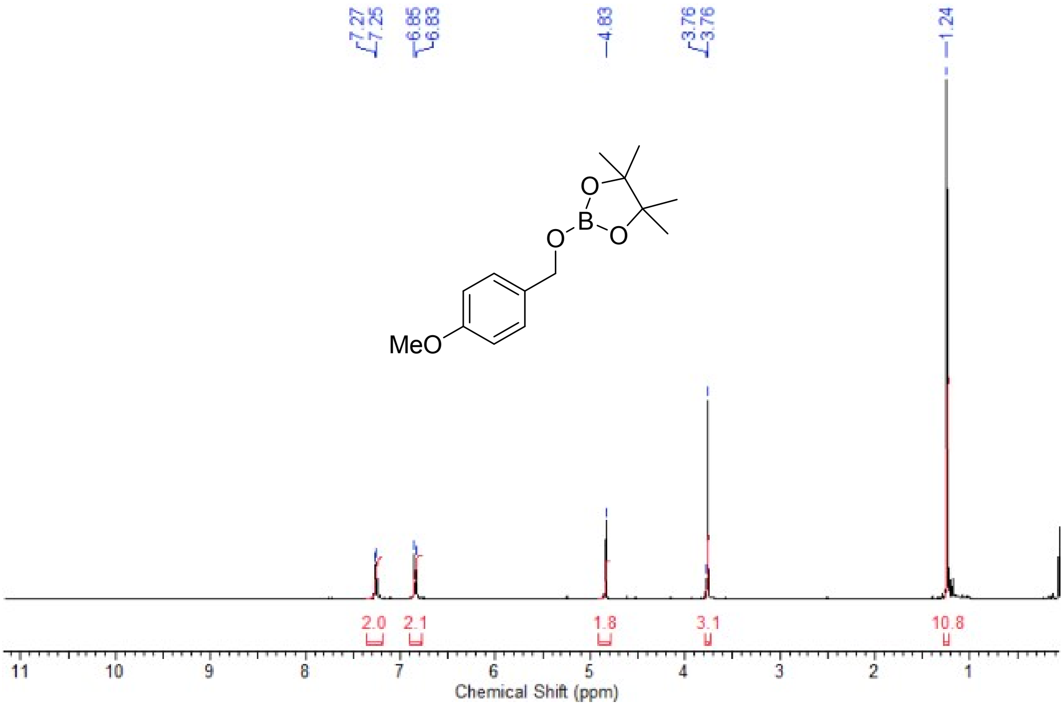

Figure FS18. ^{1}H NMR spectrum (400 MHz, 25°C, $CDCl_3$) of 2-((4-methoxybenzyl)oxy)-4,4,5,5-tetramethyl-1,3,2-dioxaborolane.

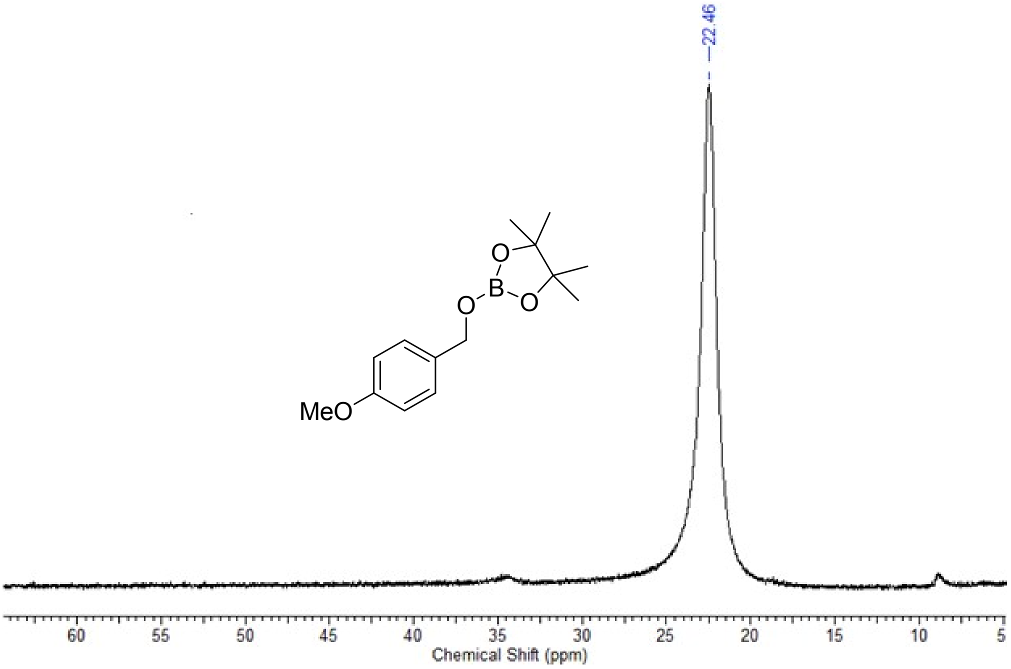

Figure S19. ^{11}B NMR spectrum (128.4 MHz, 25°C, $CDCl_3$) of 2-((4-methoxybenzyl)oxy)-4,4,5,5-tetramethyl-1,3,2-dioxaborolane.

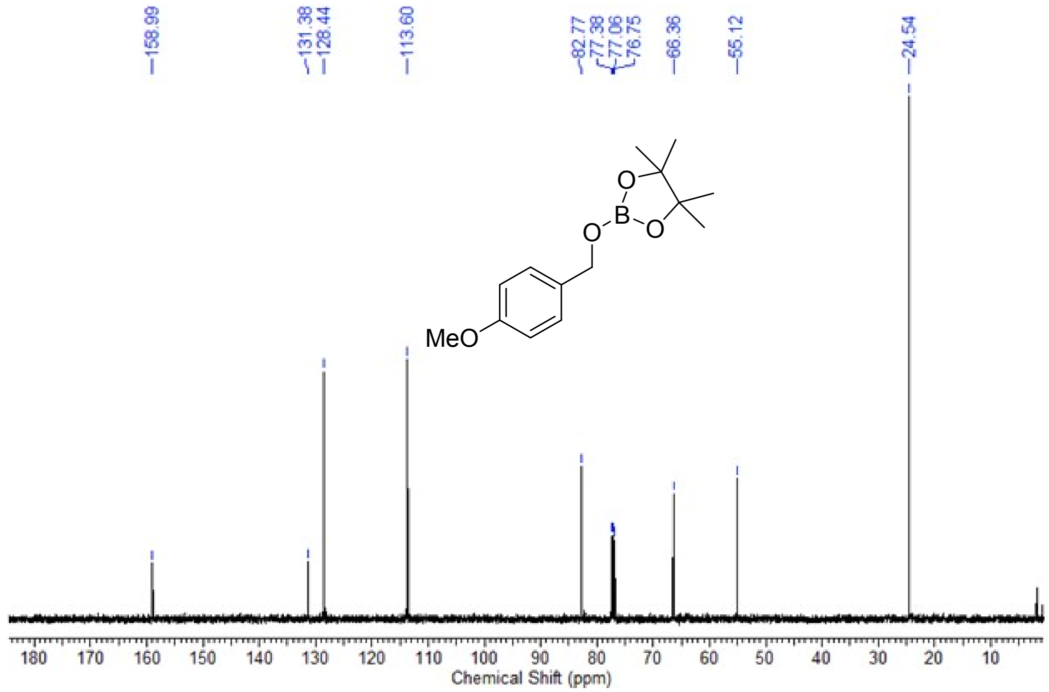

Figure FS20. ^{13}C NMR spectrum (100 MHz, 25°C, $CDCl_3$) of 2-((4-methoxybenzyl)oxy)-4,4,5,5-tetramethyl-1,3,2-dioxaborolane.

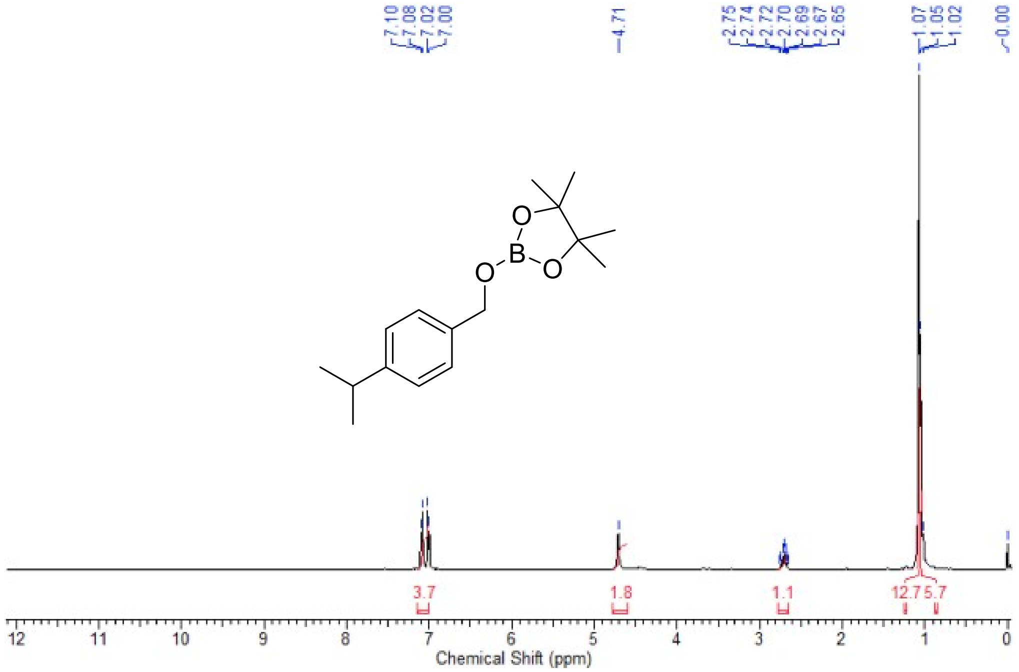

Figure FS21. ^{1}H NMR spectrum (400 MHz, 25°C, $CDCl_3$) of 2-((4-isopropylbenzyl)oxy)-4,4,5,5-tetramethyl-1,3,2-dioxaborolane.

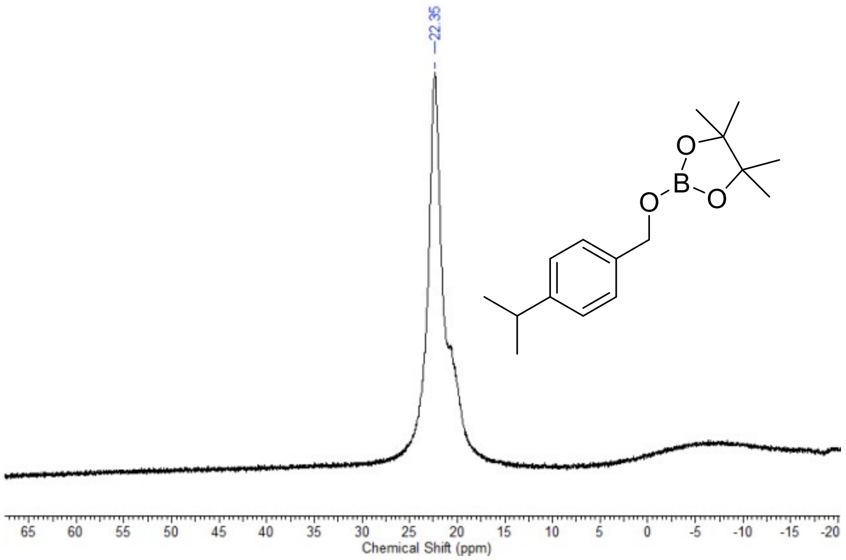

Figure S22. ^{11}B NMR spectrum (128.4 MHz, 25°C, $CDCl_3$) of 2-((4-isopropylbenzyl)oxy)-4,4,5,5-tetramethyl-1,3,2-dioxaborolane.

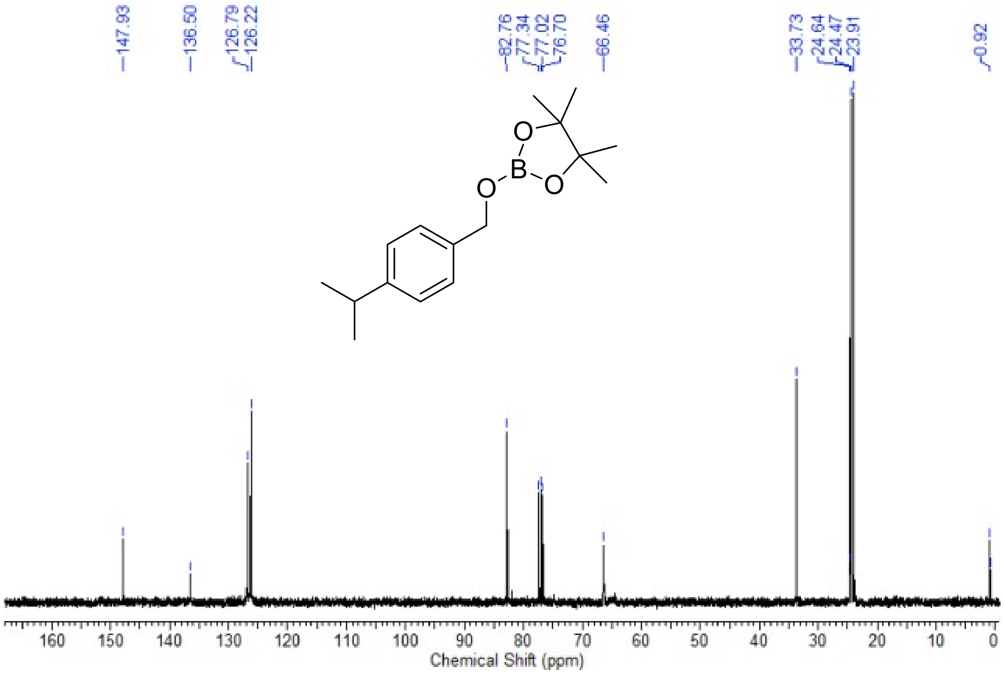

Figure FS23. ^{13}C NMR spectrum (100 MHz, 25°C, $CDCl_3$) of 2-((4-isopropylbenzyl)oxy)-4,4,5,5-tetramethyl-1,3,2-dioxaborolane.

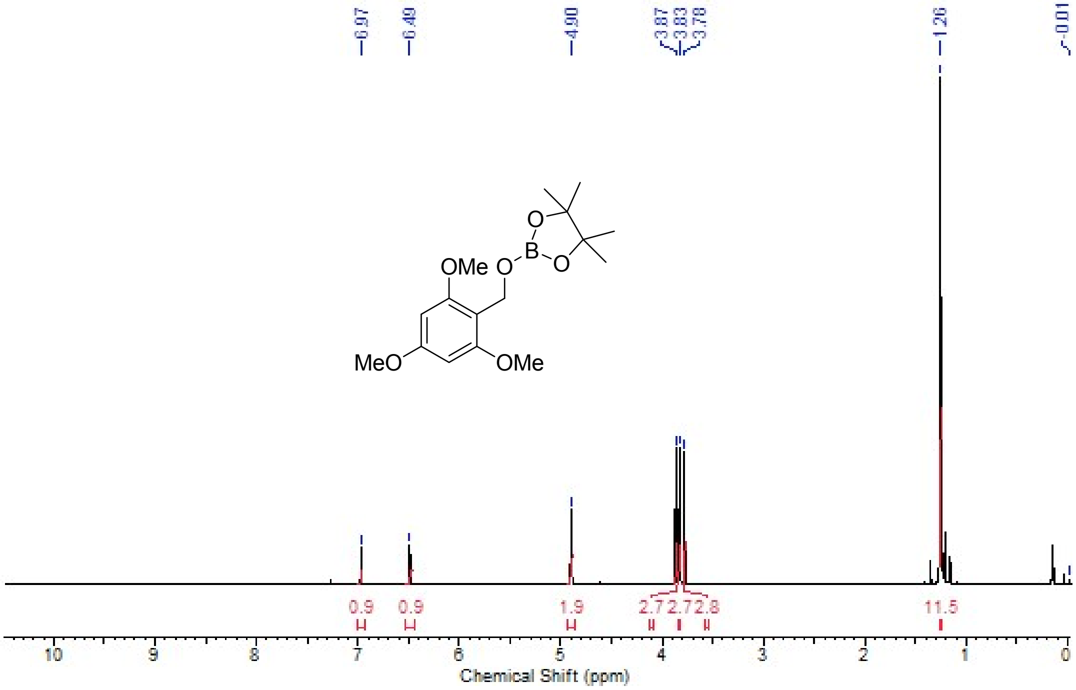

Figure FS24. ^{1}H NMR spectrum (400 MHz, 25°C, $CDCl_3$) of 4,4,5,5-tetramethyl-2-((2,4,6-trimethoxybenzyl)oxy)-1,3,2-dioxaborolane.

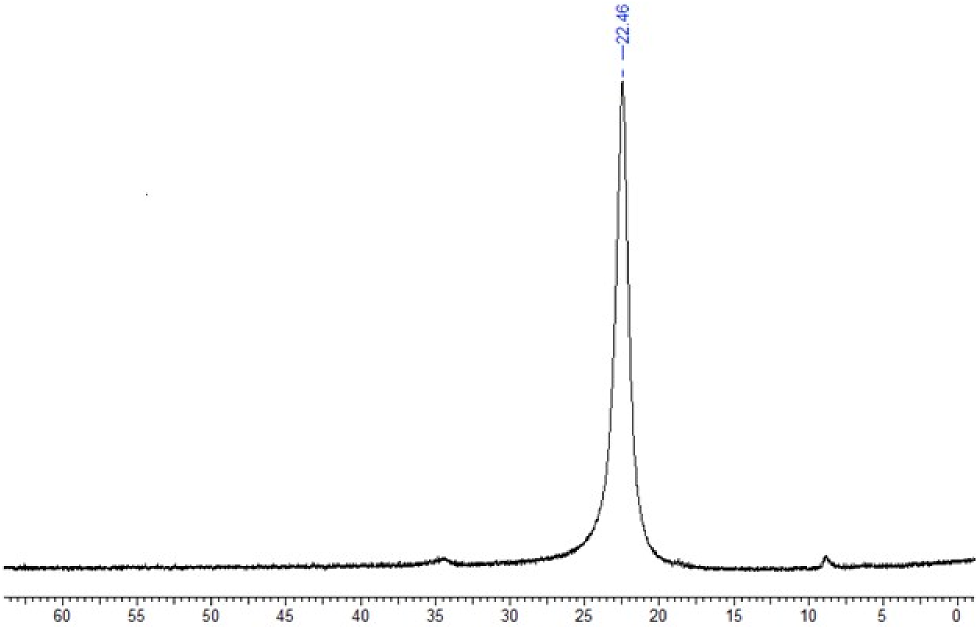

Figure S25. ^{11}B NMR spectrum (128.4 MHz, 25°C, $CDCl_3$) of 4,4,5,5-tetramethyl-2-((2,4,6-trimethoxybenzyl)oxy)-1,3,2-dioxaborolane.

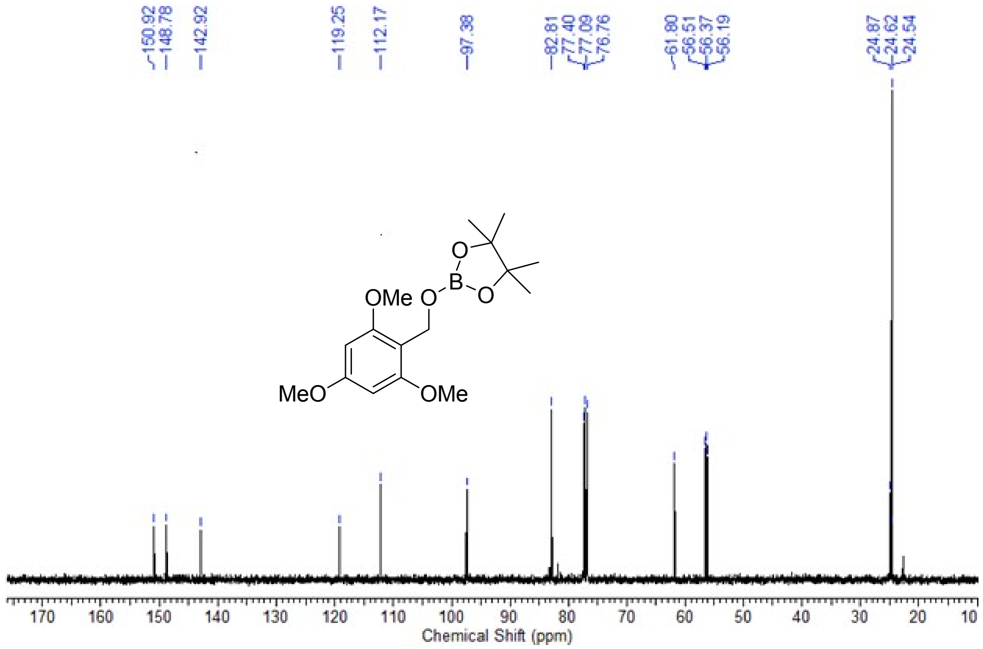

Figure FS26. ^{13}C NMR spectrum (100 MHz, 25°C, $CDCl_3$) of 4,4,5,5-tetramethyl-2-((2,4,6-trimethoxybenzyl)oxy)-1,3,2-dioxaborolane.

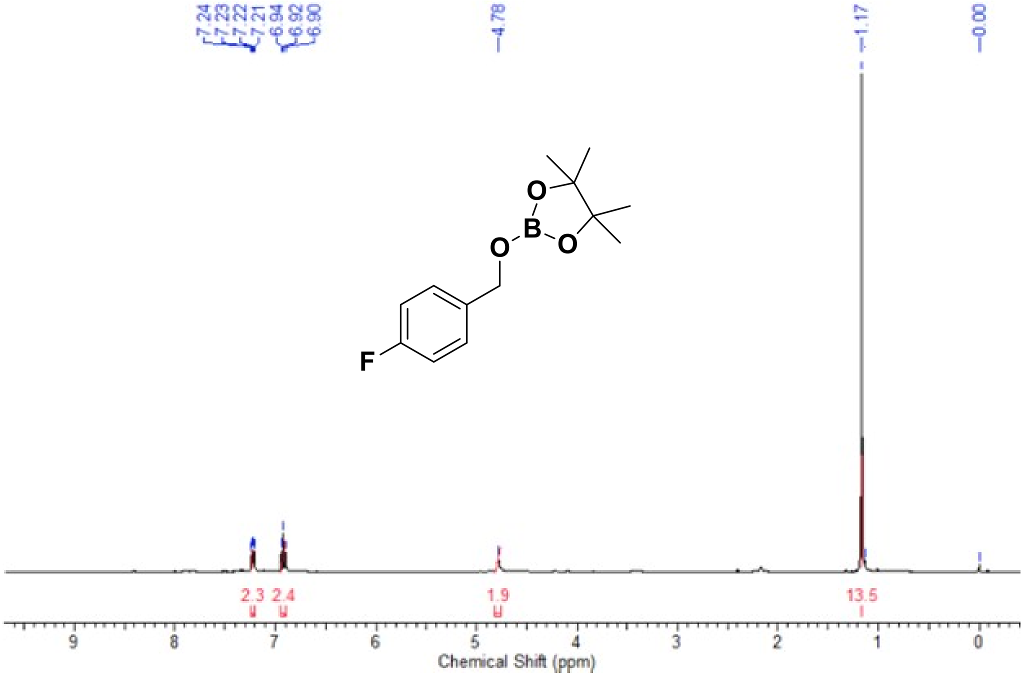

Figure FS27. ^{1}H NMR spectrum (400 MHz, 25°C, $CDCl_3$) of 2-((4-fluorobenzyl)oxy)-4,4,5,5-tetramethyl-1,3,2-dioxaborolane.

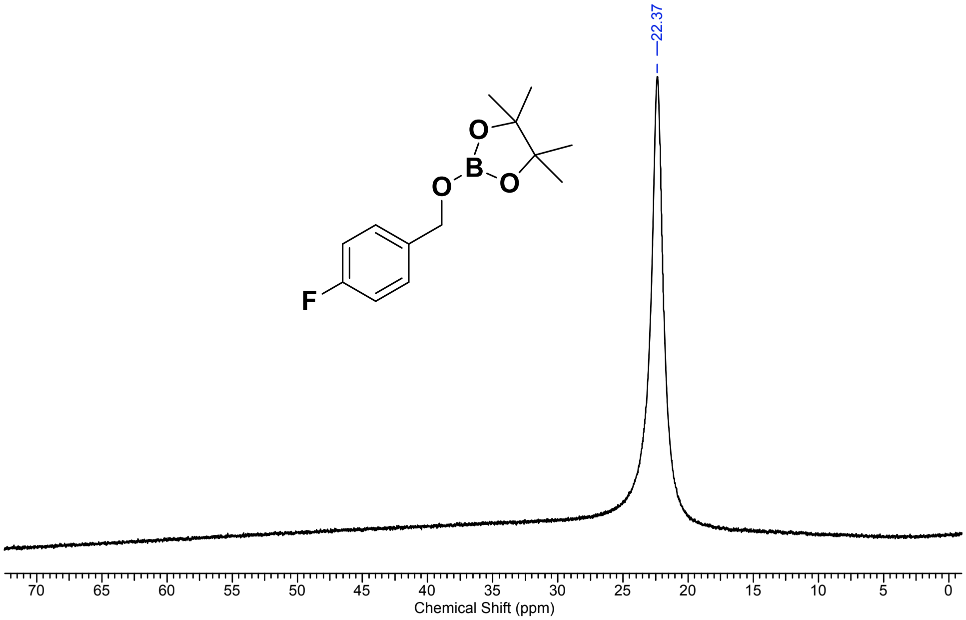

Figure S28. ^{11}B NMR spectrum (128.4 MHz, 25°C, $CDCl_3$) of 2-((4-fluorobenzyl)oxy)-4,4,5,5-tetramethyl-1,3,2-dioxaborolane

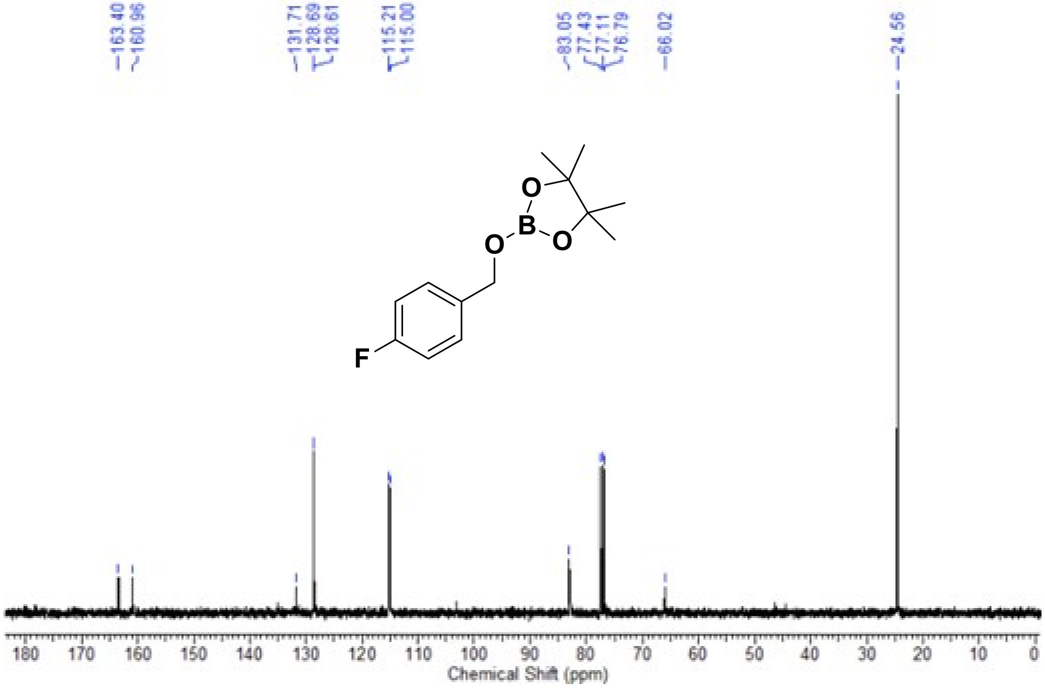

Figure FS29. ^{13}C NMR spectrum (100 MHz, 25°C, $CDCl_3$) of 2-((4-fluorobenzyl)oxy)-4,4,5,5-tetramethyl-1,3,2-dioxaborolane.

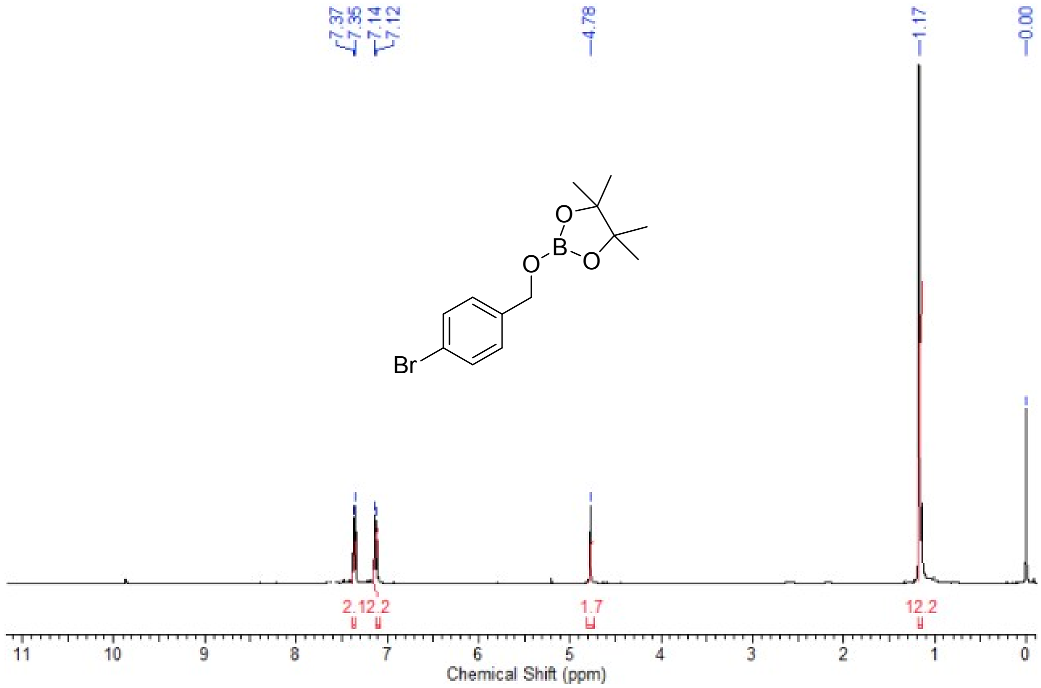

Figure FS30. ^{1}H NMR spectrum (400 MHz, 25°C, $CDCl_3$) of 2-((4-bromobenzyl)oxy)-4,4,5,5-tetramethyl-1,3,2-dioxaborolane.

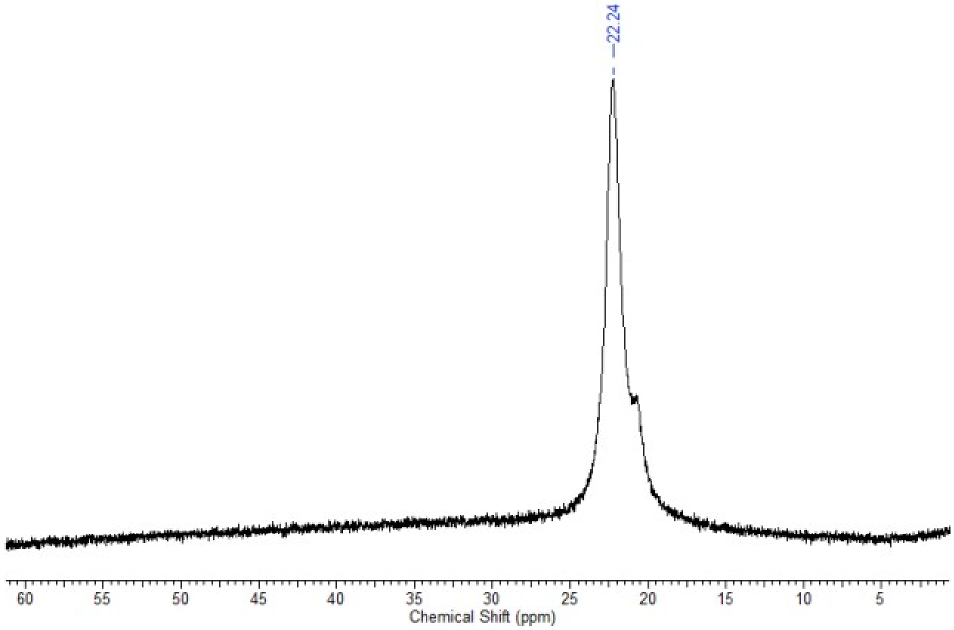

Figure S31. ^{11}B NMR spectrum (128.4 MHz, 25°C, $CDCl_3$) of 2-((4-bromobenzyl)oxy)-4,4,5,5-tetramethyl-1,3,2-dioxaborolane.

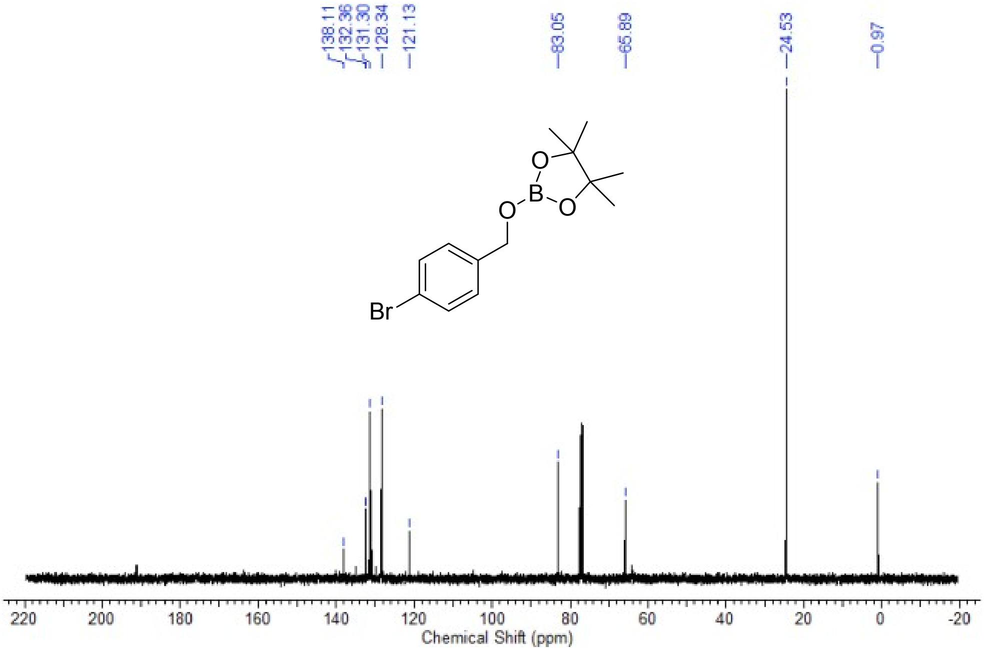

Figure FS32. ^{13}C NMR spectrum (100 MHz, 25°C, $CDCl_3$) of 2-((4-bromobenzyl)oxy)-4,4,5,5-tetramethyl-1,3,2-dioxaborolane.

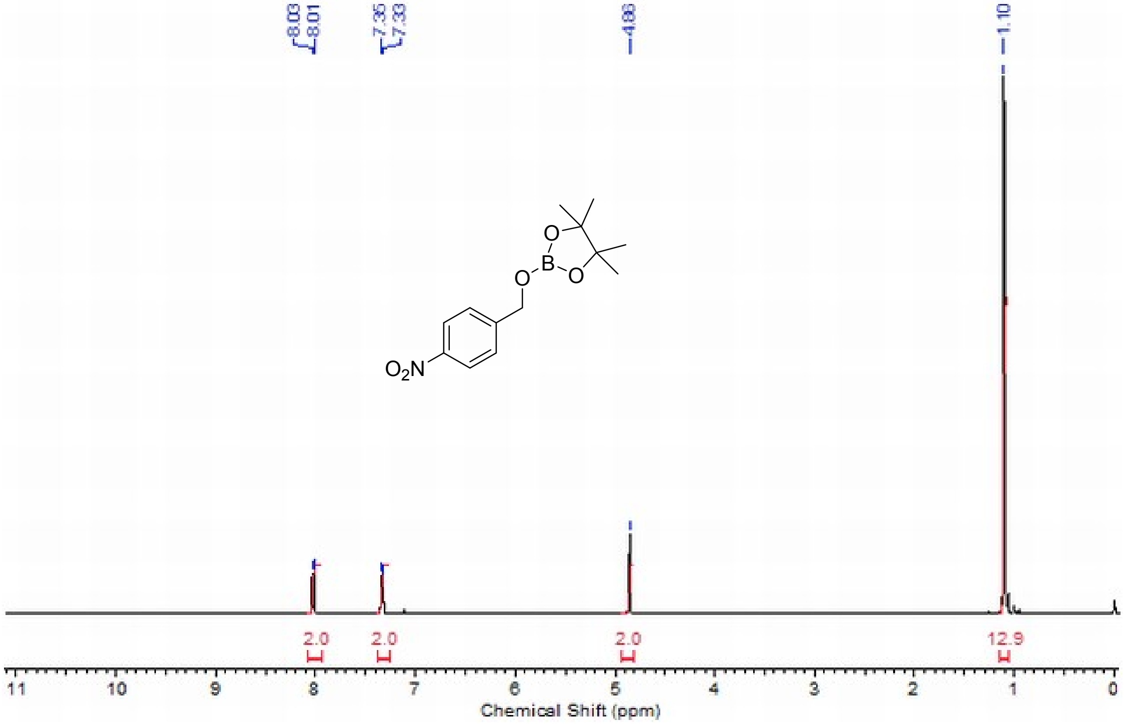

Figure FS33. ^{1}H NMR spectrum (400 MHz, 25°C, $CDCl_3$) of 4,4,5,5-tetramethyl-2-((4-nitrobenzyl)oxy)-1,3,2-dioxaborolane.

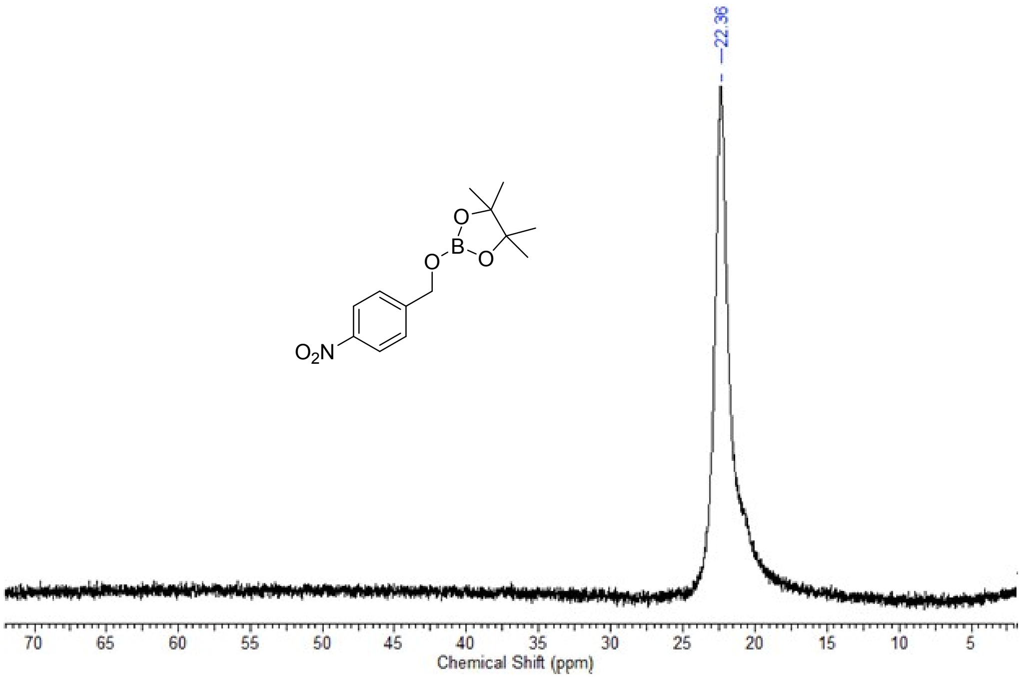

Figure S34. ^{11}B NMR spectrum (128.4 MHz, 25°C, $CDCl_3$) of 4,4,5,5-tetramethyl-2-((4-nitrobenzyl)oxy)-1,3,2-dioxaborolane.

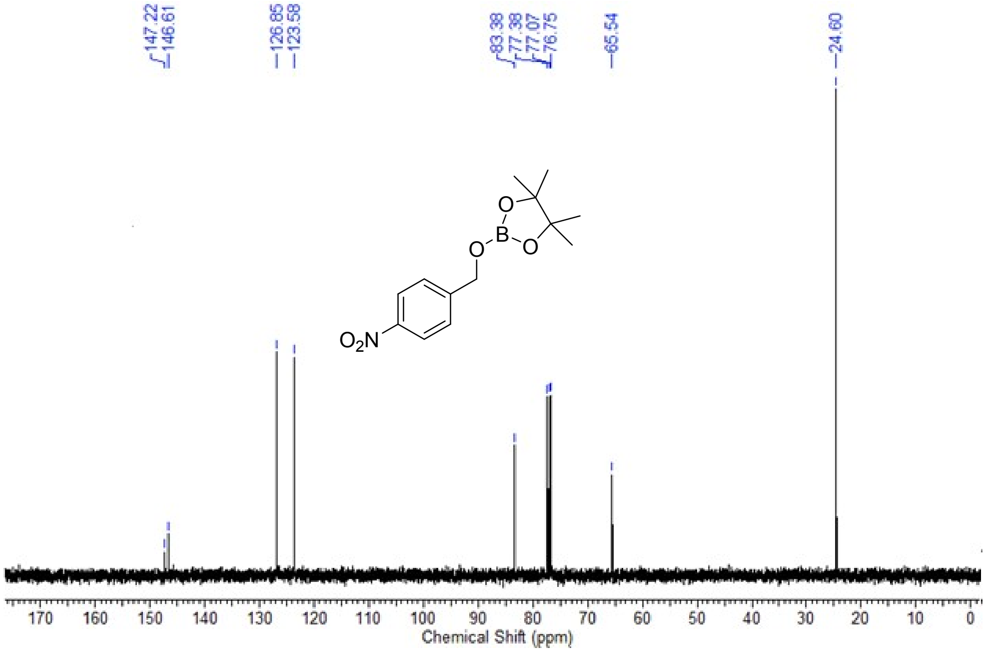

Figure FS35. ^{13}C NMR spectrum (100 MHz, 25°C, $CDCl_3$) of 4,4,5,5-tetramethyl-2-((4-nitrobenzyl)oxy)-1,3,2-dioxaborolane.

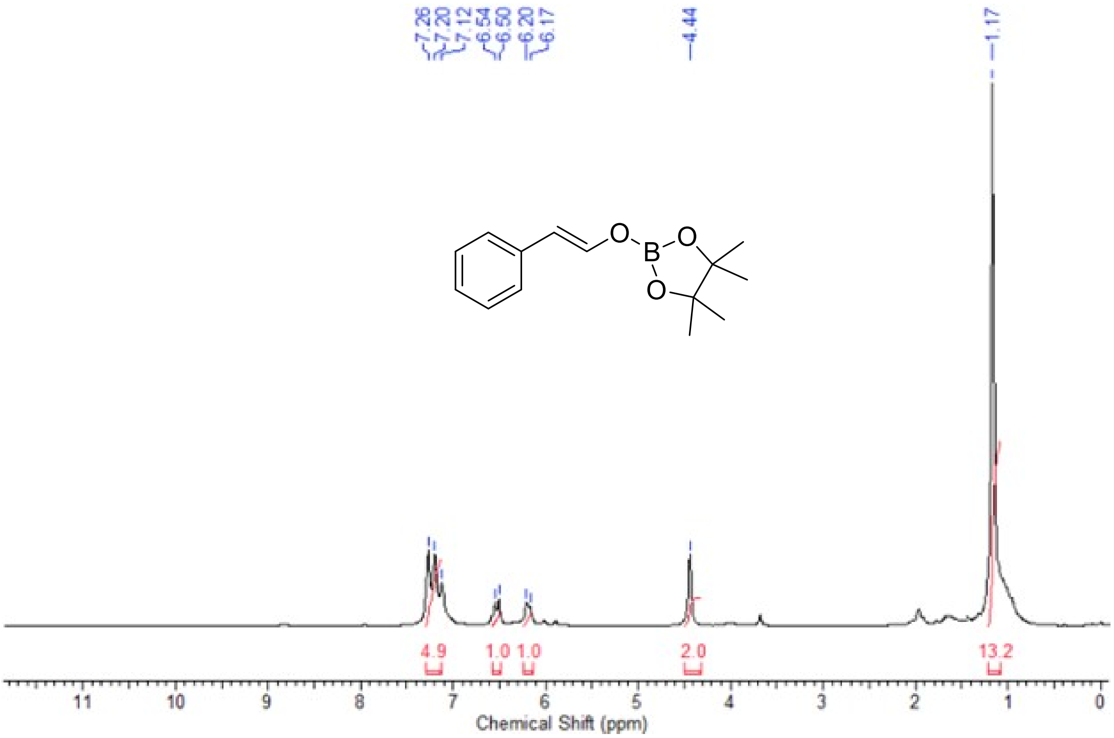

Figure FS36. ^{1}H NMR spectrum (400 MHz, 25°C, $CDCl_3$) of (E)-4,4,5,5-tetramethyl-2-(styryloxy)-1,3,2-dioxaborolane.

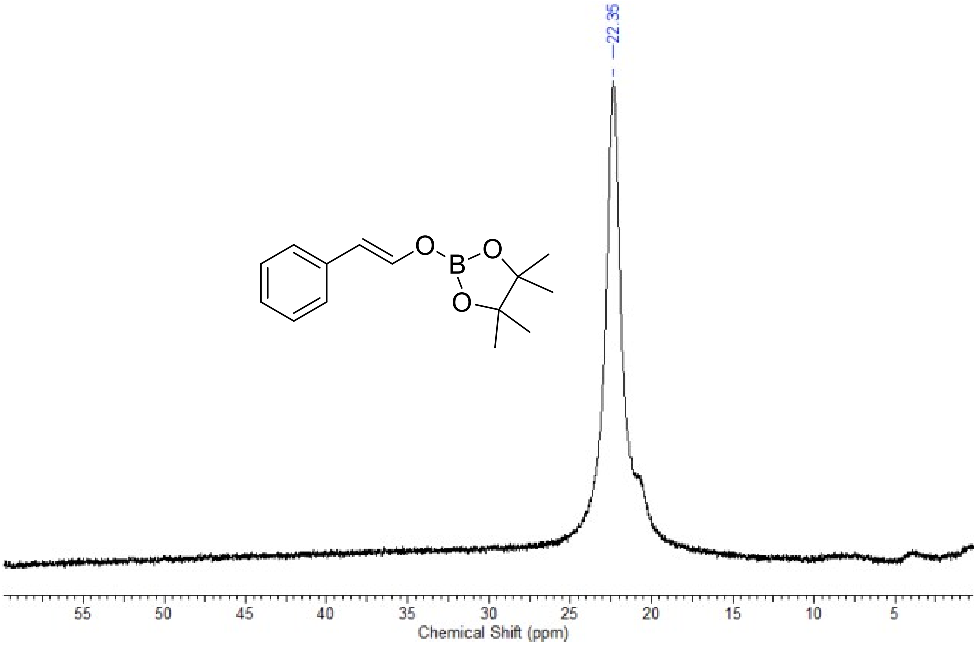

Figure S37. ^{11}B NMR spectrum (128.4 MHz, 25°C, $CDCl_3$) of (E)-4,4,5,5-tetramethyl-2-(styryloxy)-1,3,2-dioxaborolane.

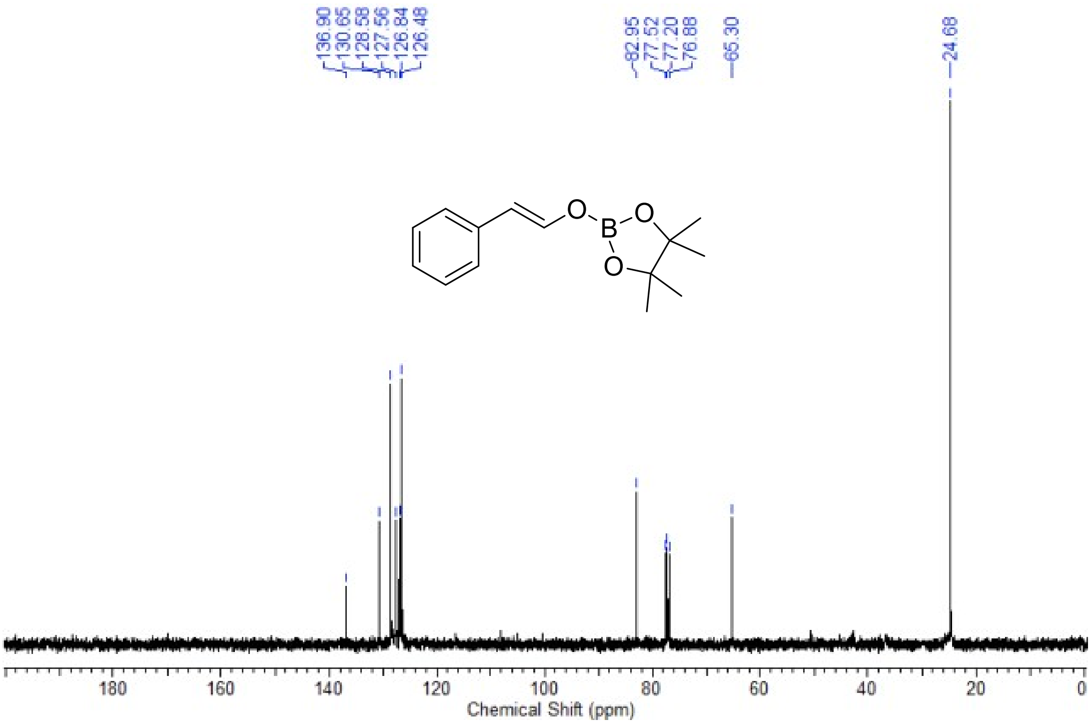

Figure FS38. ^{13}C NMR spectrum (100 MHz, 25°C, $CDCl_3$) of (E)-4,4,5,5-tetramethyl-2-(styryloxy)-1,3,2-dioxaborolane.

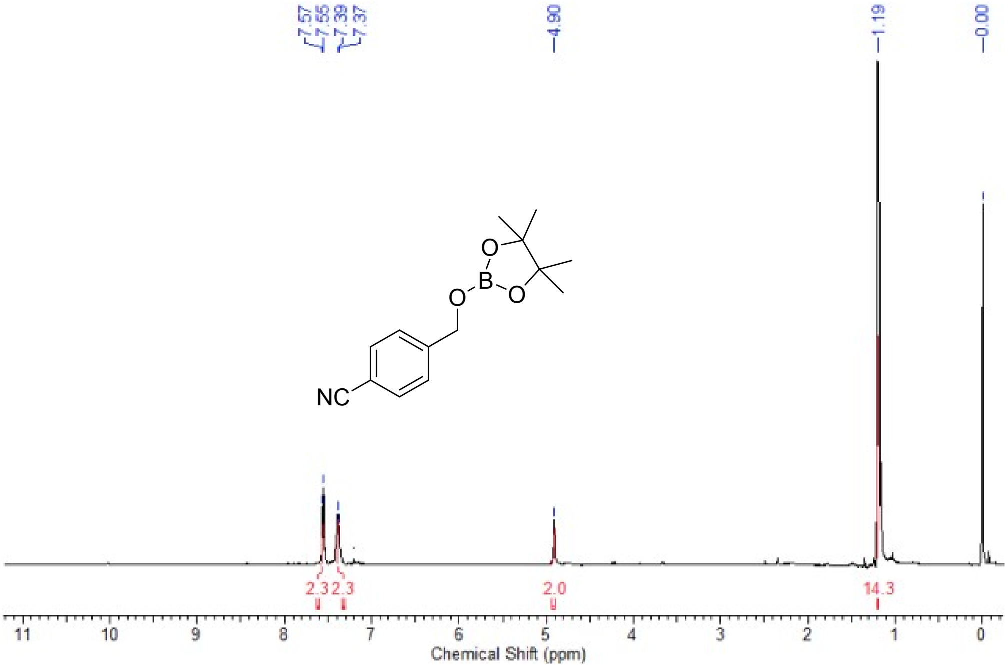

Figure FS39. ^{1}H NMR spectrum (400 MHz, 25°C, $CDCl_3$) of 4-(((4,4,5,5-tetramethyl-1,3,2-dioxaborolan-2-yl)oxy)methyl)benzonitrile.

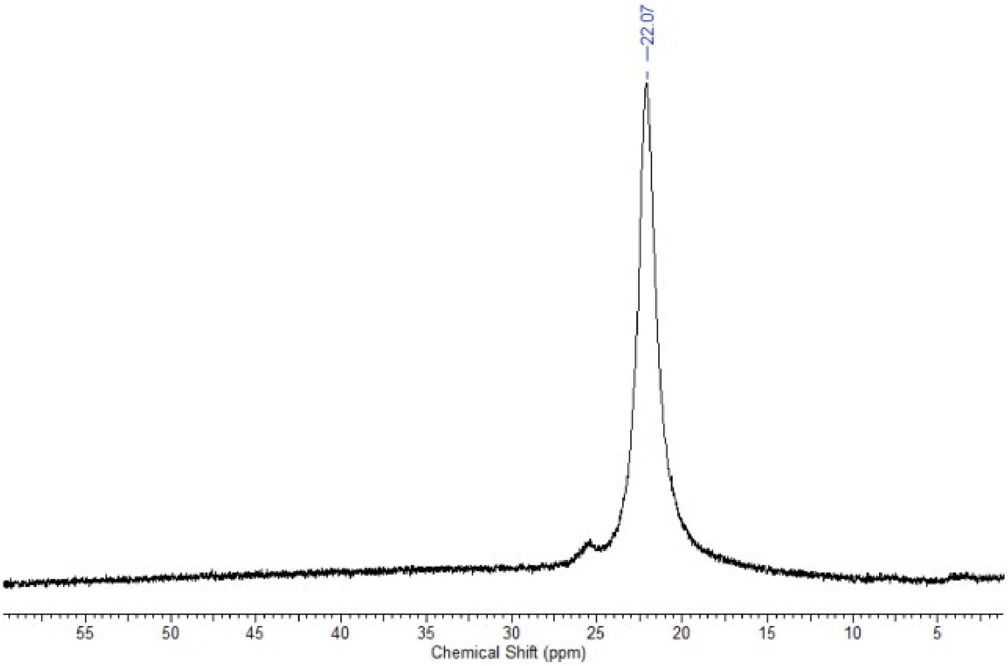

Figure S40. ^{11}B NMR spectrum (128.4 MHz, 25°C, $CDCl_3$) of 4-(((4,4,5,5-tetramethyl-1,3,2-dioxaborolan-2-yl)oxy)methyl)benzonitrile.

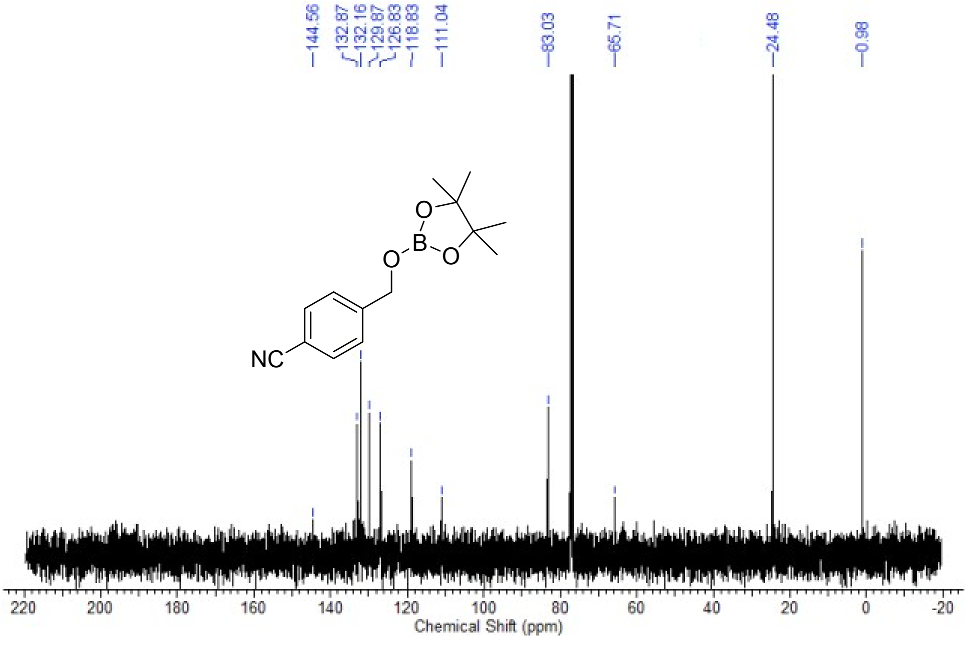

Figure FS41. ^{13}C NMR spectrum (100 MHz, 25°C, $CDCl_3$) of 4-(((4,4,5,5-tetramethyl-1,3,2-dioxaborolan-2-yl)oxy)methyl)benzonitrile.

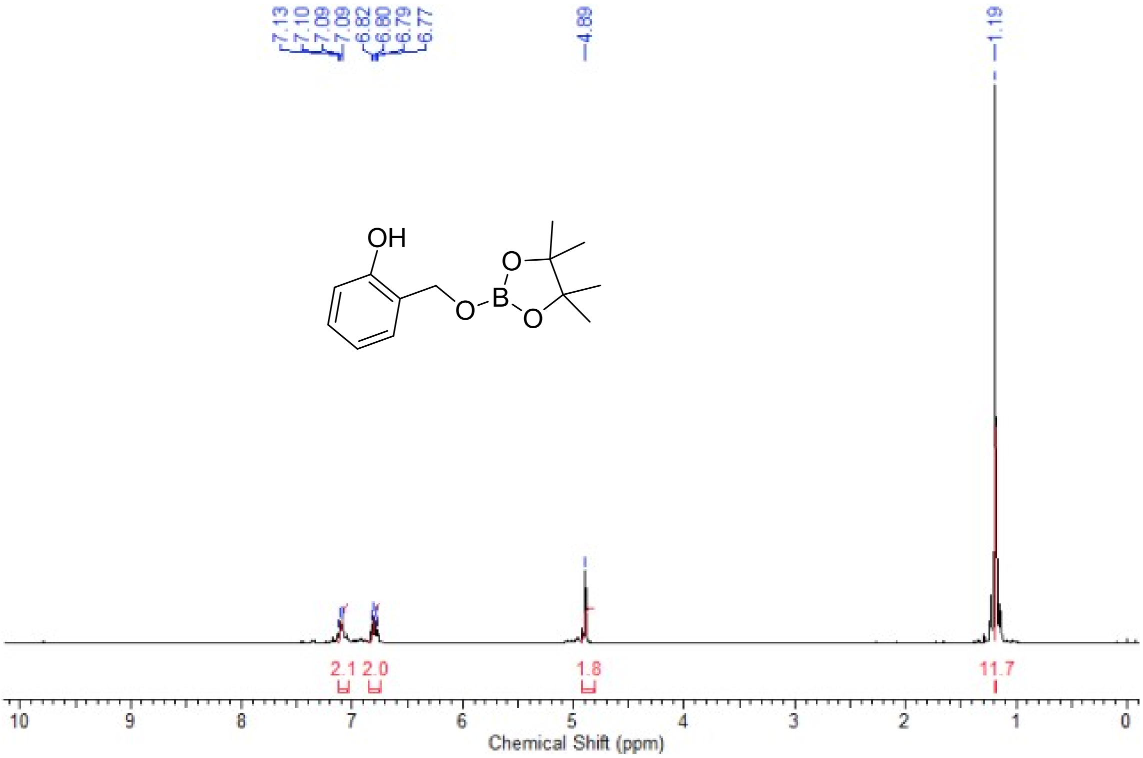

Figure FS42. ^{1}H NMR spectrum (400 MHz, 25°C, $CDCl_3$) of 4-(((4,4,5,5-tetramethyl-1,3,2-dioxaborolan-2-yl)oxy)methyl)phenol.

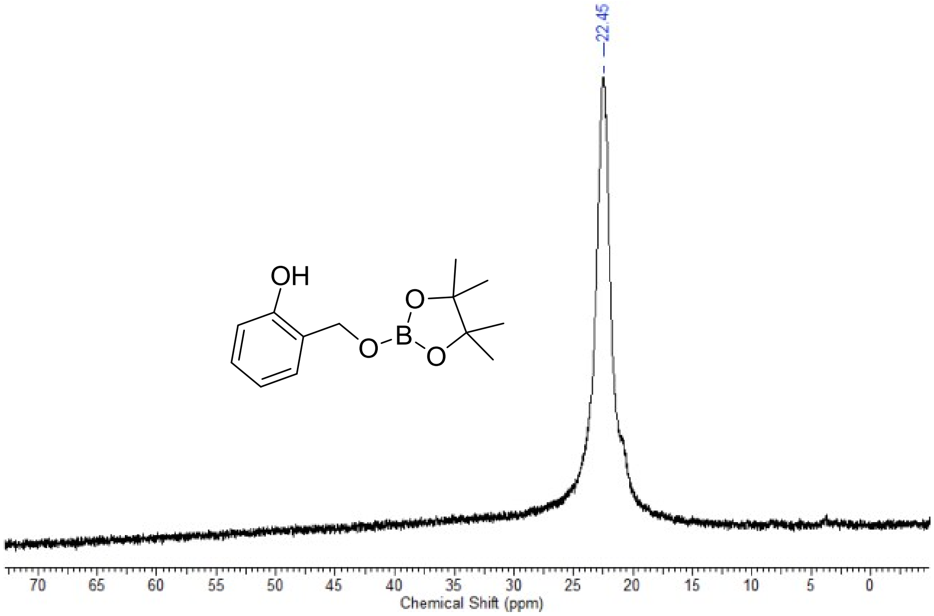

Figure S43. ^{11}B NMR spectrum (128.4 MHz, 25°C, $CDCl_3$) of 4-(((4,4,5,5-tetramethyl-1,3,2-dioxaborolan-2-yl)oxy)methyl)phenol.

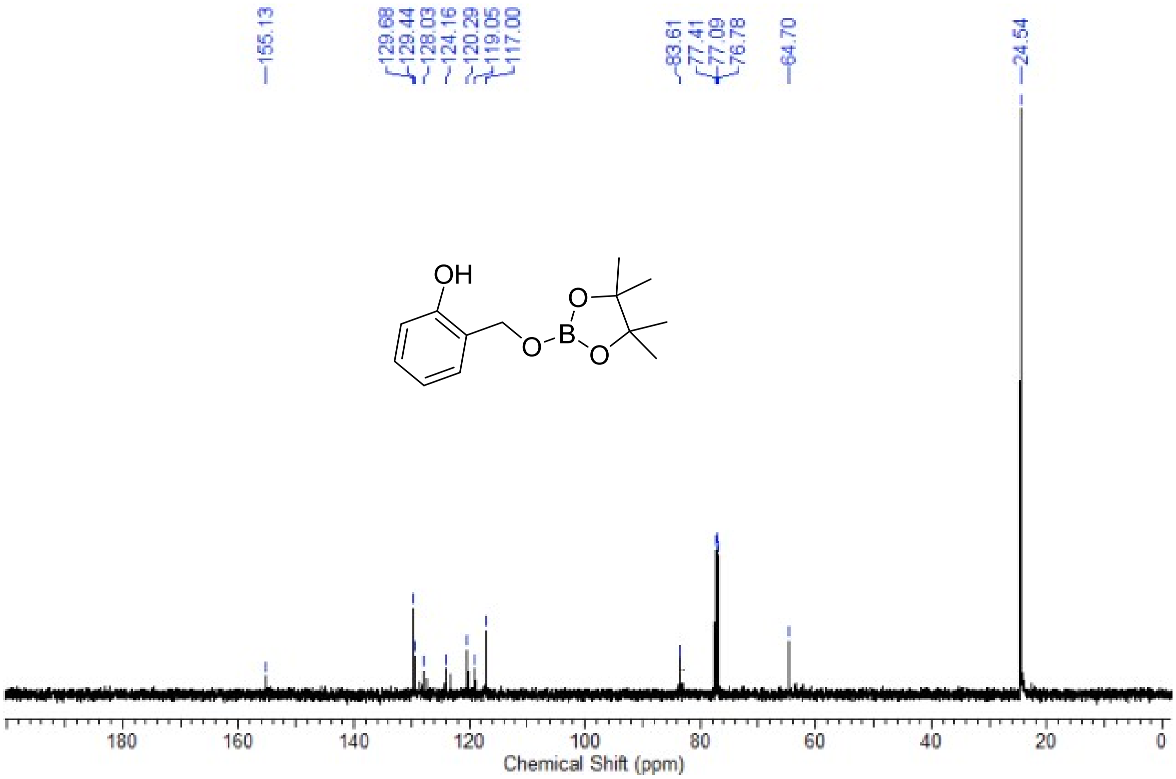

Figure S44. ^{13}C NMR spectrum (128.4 MHz, 25°C, $CDCl_3$) of 2-(((4,4,5,5-tetramethyl-1,3,2-dioxaborolan-2-yl)oxy)methyl)phenol.

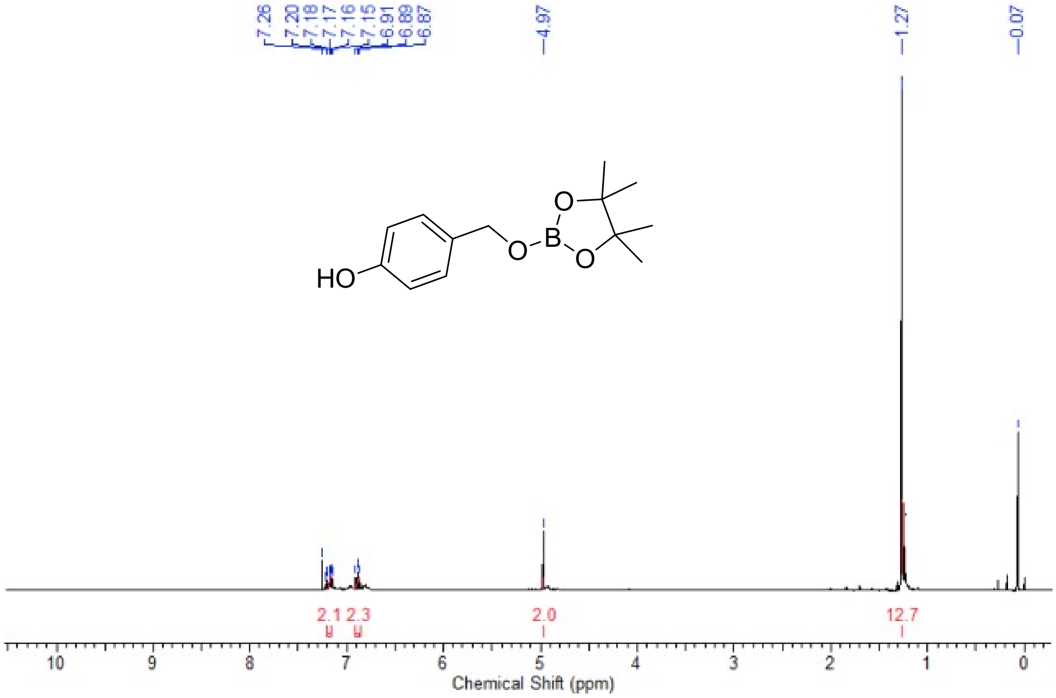

Figure FS45. ^{1}H NMR spectrum (400 MHz, 25°C, $CDCl_3$) of 4-(((4,4,5,5-tetramethyl-1,3,2-dioxaborolan-2-yl)oxy)methyl)phenol.

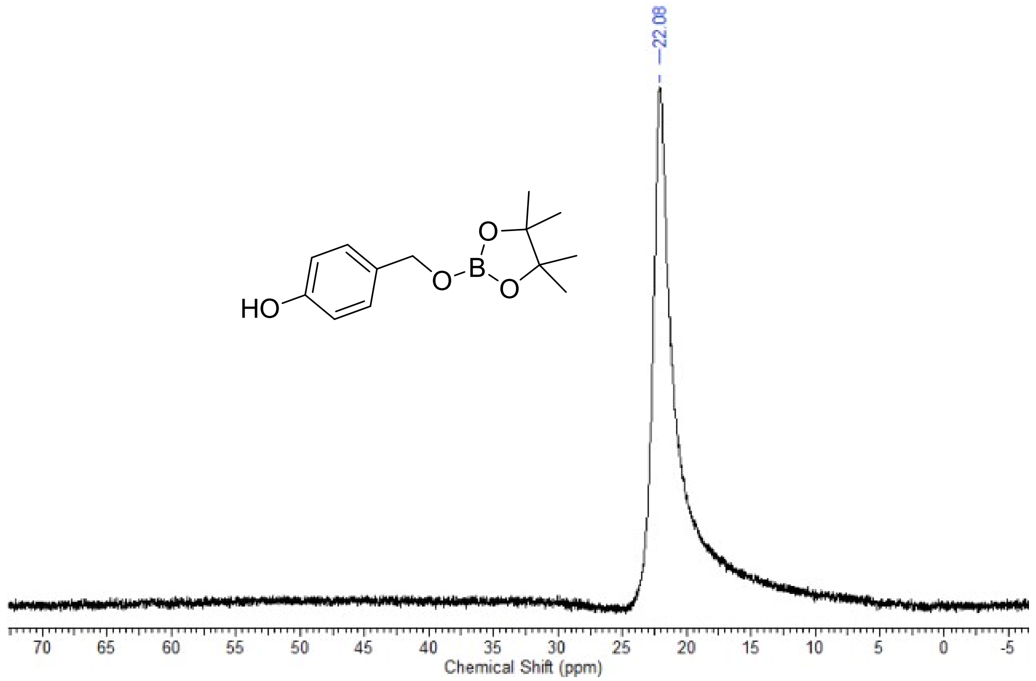

Figure S46. ^{11}B NMR spectrum (128.4 MHz, 25°C, $CDCl_3$) of 4-(((4,4,5,5-tetramethyl-1,3,2-dioxaborolan-2-yl)oxy)methyl)phenol.

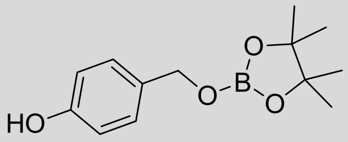

Figure S47. ^{13}C NMR spectrum (128.4 MHz, 25°C, $CDCl_3$) of 4-(((4,4,5,5-tetramethyl-1,3,2-dioxaborolan-2-yl)oxy)methyl)phenol.

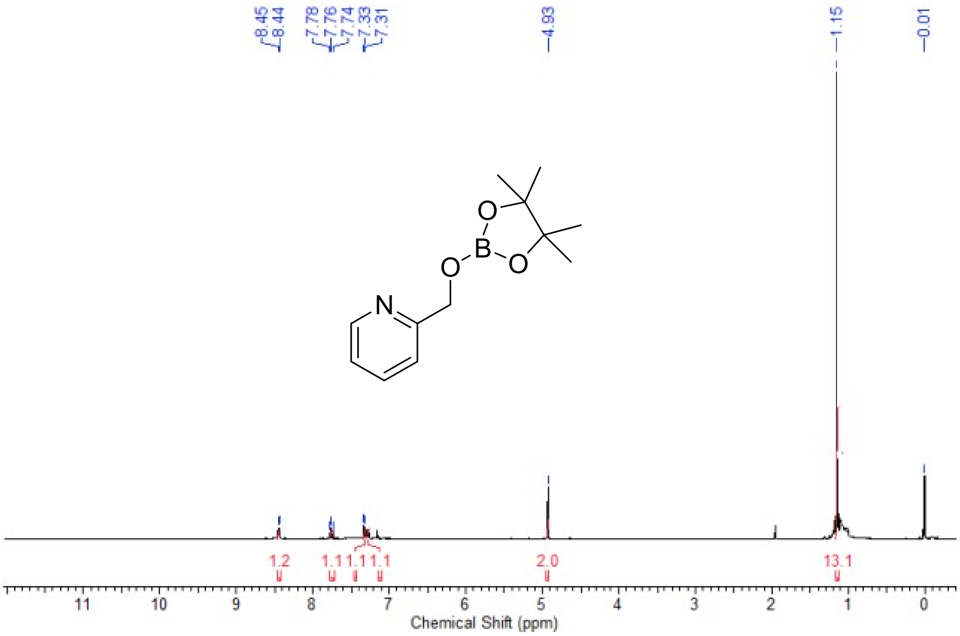

Figure FS48. ^1H NMR spectrum (400 MHz, 25°C, $CDCl_3$) of 2-(((4,4,5,5-tetramethyl-1,3,2-dioxaborolan-2-yl)oxy)methyl)pyridine.

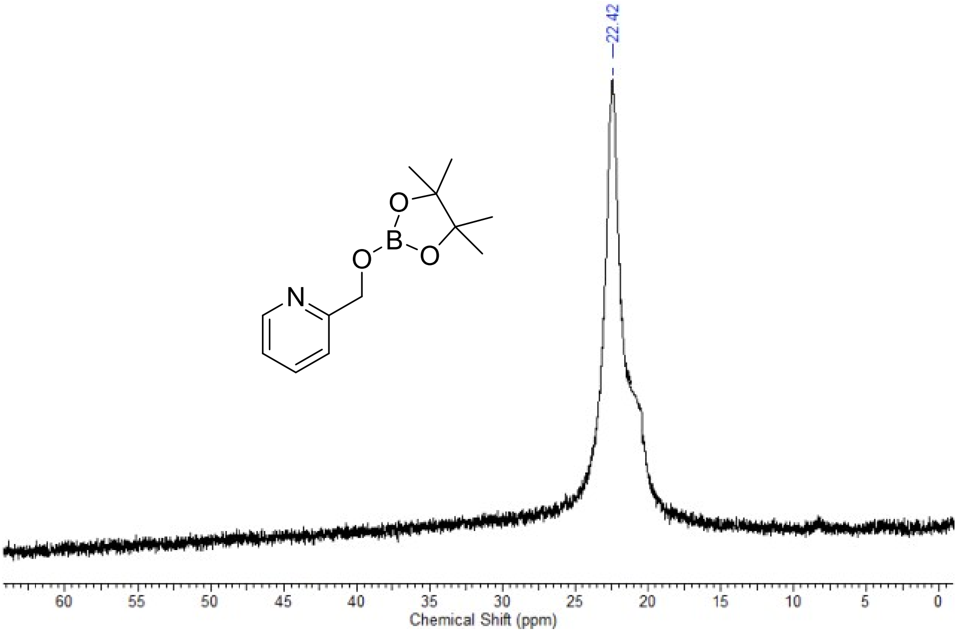

Figure S49. ^{11}B NMR spectrum (128.4 MHz, 25°C, $CDCl_3$) of 2-(((4,4,5,5-tetramethyl-1,3,2-dioxaborolan-2-yl)oxy)methyl)pyridine.

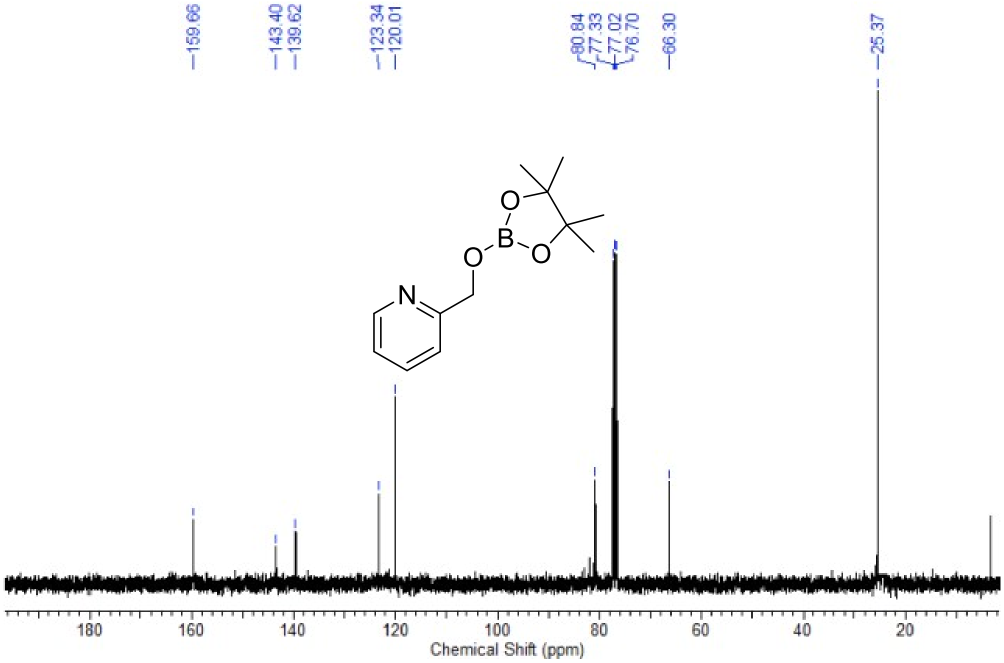

Figure FS50. ^{13}C NMR spectrum (100 MHz, 25°C, $CDCl_3$) of 2-(((4,4,5,5-tetramethyl-1,3,2-dioxaborolan-2-yl)oxy)methyl)pyridine.

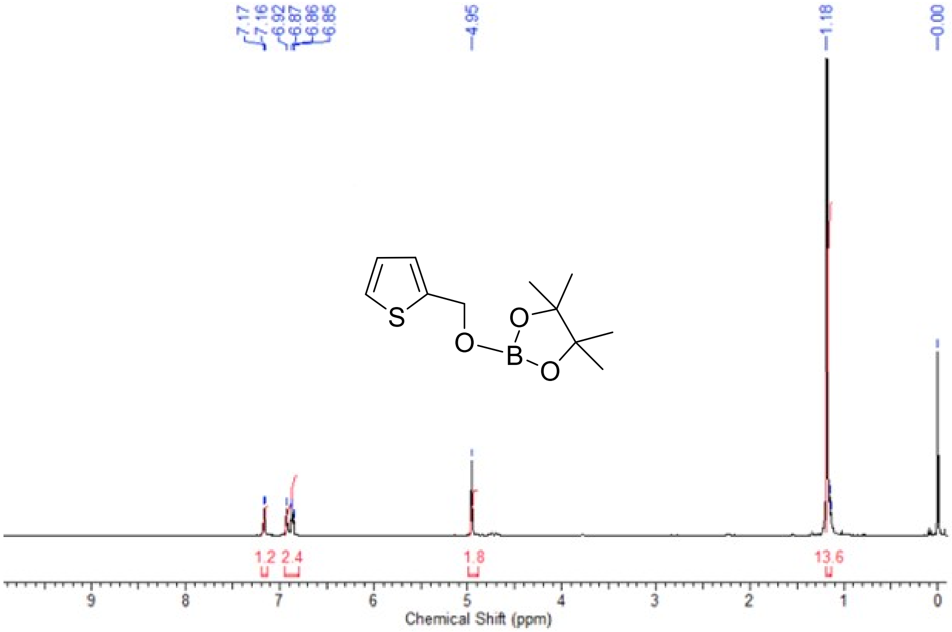

Figure FS51. ^{1}H NMR spectrum (400 MHz, 25°C, $CDCl_3$) of 4,4,5,5-tetramethyl-2-(thiophen-2-ylmethoxy)-1,3,2-dioxaborolane.

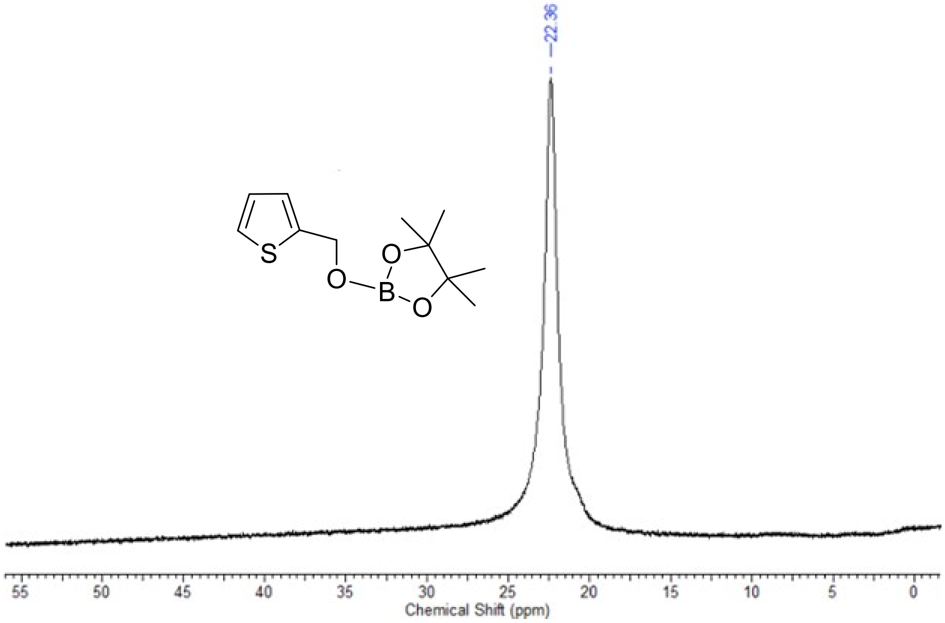

Figure S52. ^{11}B NMR spectrum (128.4 MHz, 25°C, $CDCl_3$) of 4,4,5,5-tetramethyl-2-(thiophen-2-ylmethoxy)-1,3,2-dioxaborolane.

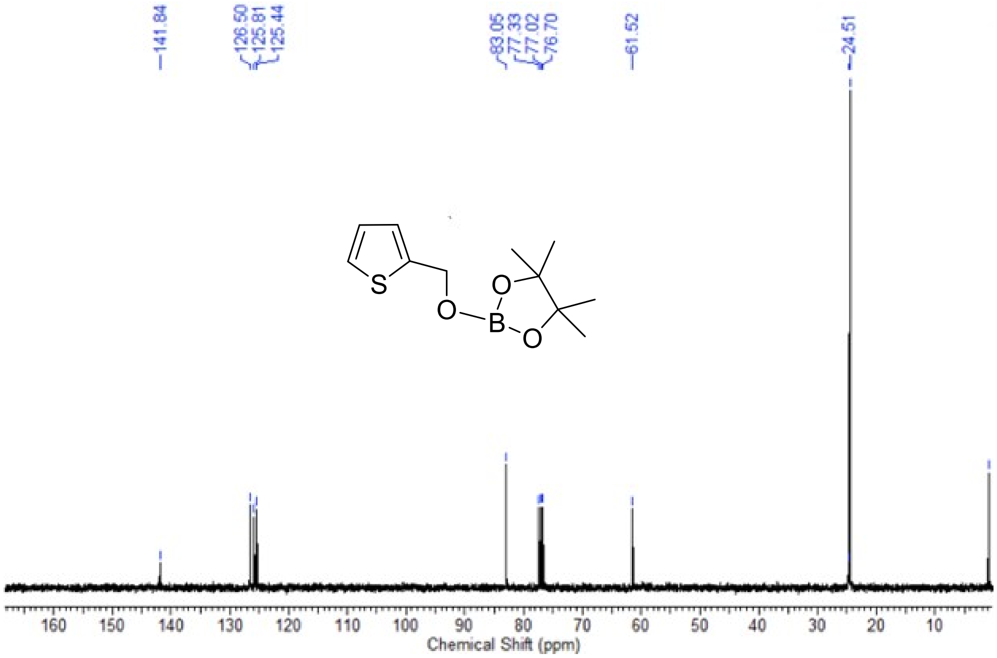

Figure FS53. ^{13}C NMR spectrum (100 MHz, 25°C, $CDCl_3$) of 4,4,5,5-tetramethyl-2-(thiophen-2-ylmethoxy)-1,3,2-dioxaborolane.

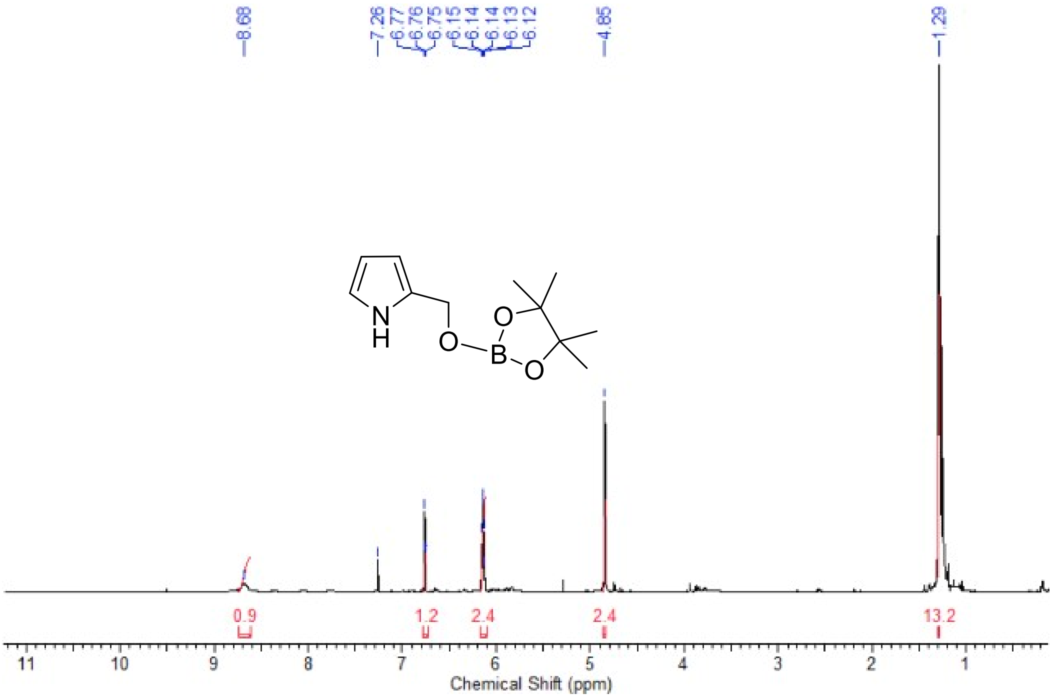

Figure FS54. ^{1}H NMR spectrum (400 MHz, 25°C, $CDCl_3$) of 2-(((4,4,5,5-tetramethyl-1,3,2-dioxaborolan-2-yl)oxy)methyl)-1H-pyrrole.

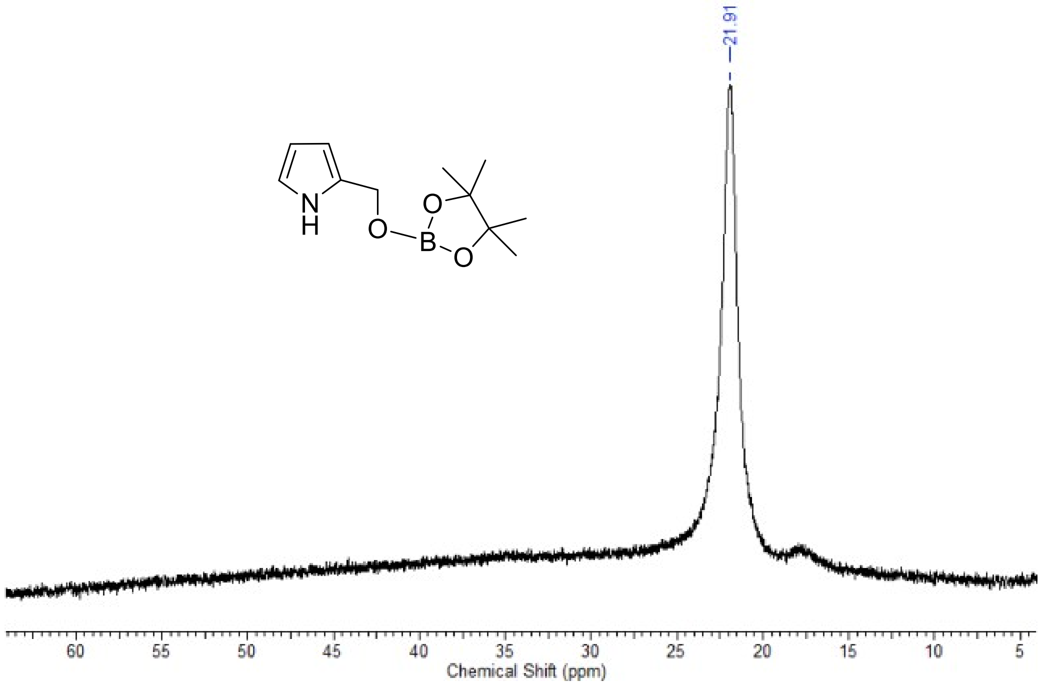

Figure S55. ^{11}B NMR spectrum (128.4 MHz, 25°C, $CDCl_3$) of 2-(((4,4,5,5-tetramethyl-1,3,2-dioxaborolan-2-yl)oxy)methyl)-1H-pyrrole.

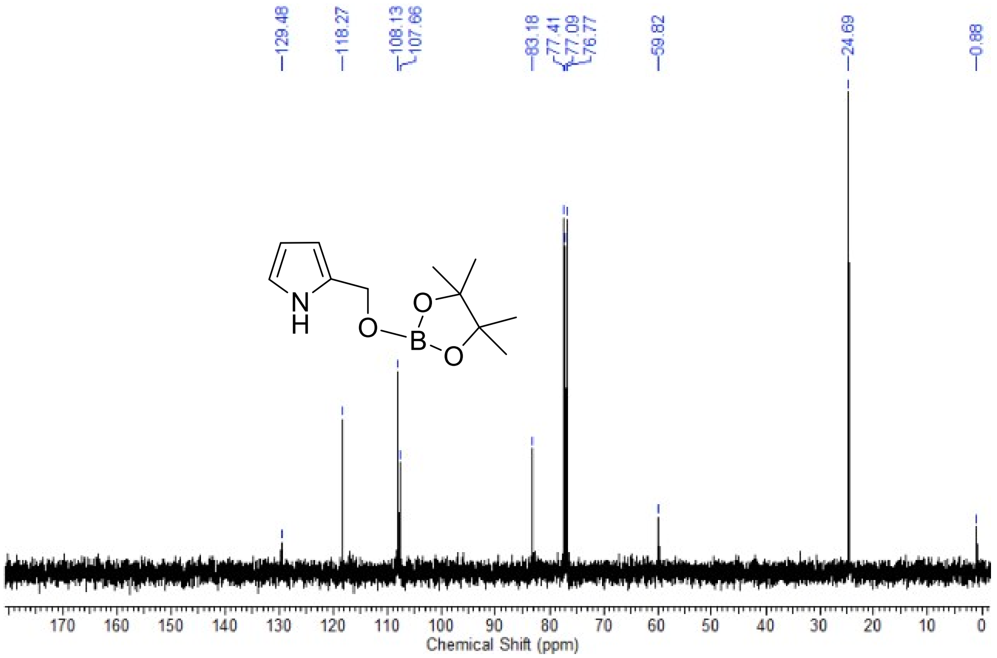

Figure FS56. ^{13}C NMR spectrum (100 MHz, 25°C, $CDCl_3$) of 2-(((4,4,5,5-tetramethyl-1,3,2-dioxaborolan-2-yl)oxy)methyl)-1H-pyrrole.

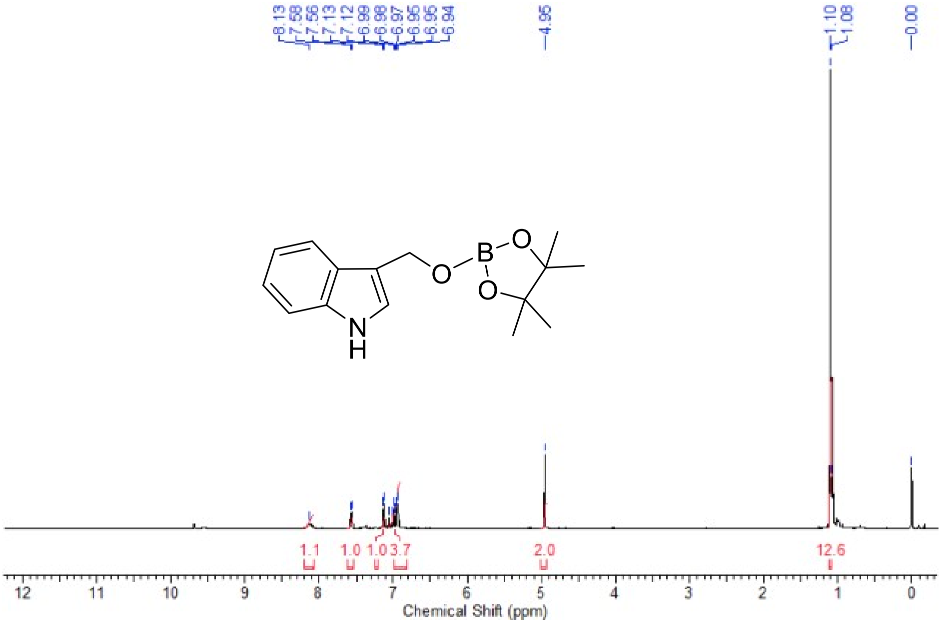

Figure FS57. ^{1}H NMR spectrum (400 MHz, 25°C, $CDCl_3$) of 3-(((4,4,5,5-tetramethyl-1,3,2-dioxaborolan-2-yl)oxy)methyl)-1H-indole.

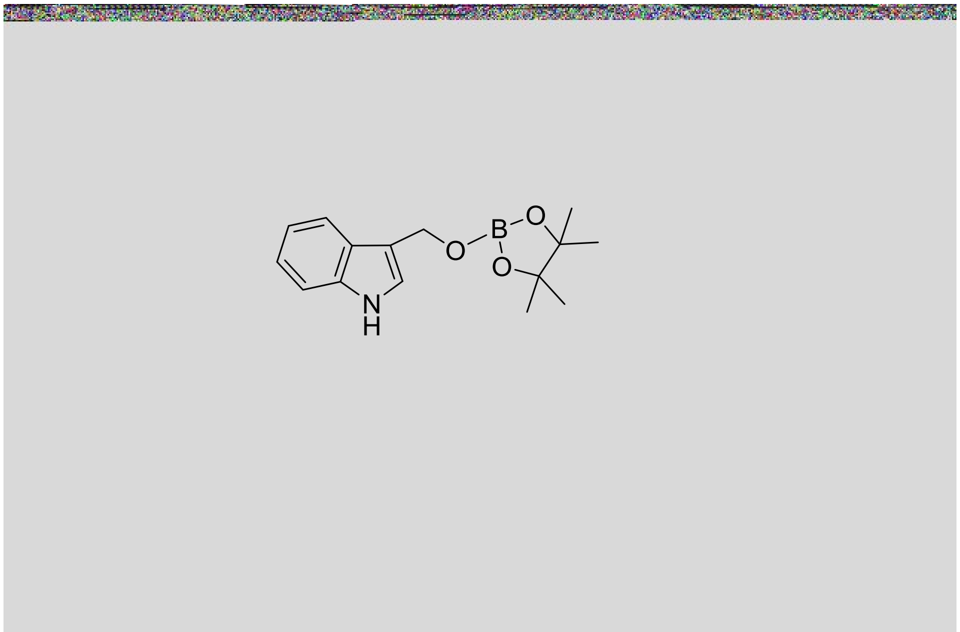

Figure S58. ^{11}B NMR spectrum (128.4 MHz, 25°C, $CDCl_3$) of 3-(((4,4,5,5-tetramethyl-1,3,2-dioxaborolan-2-yl)oxy)methyl)-1H-indole.

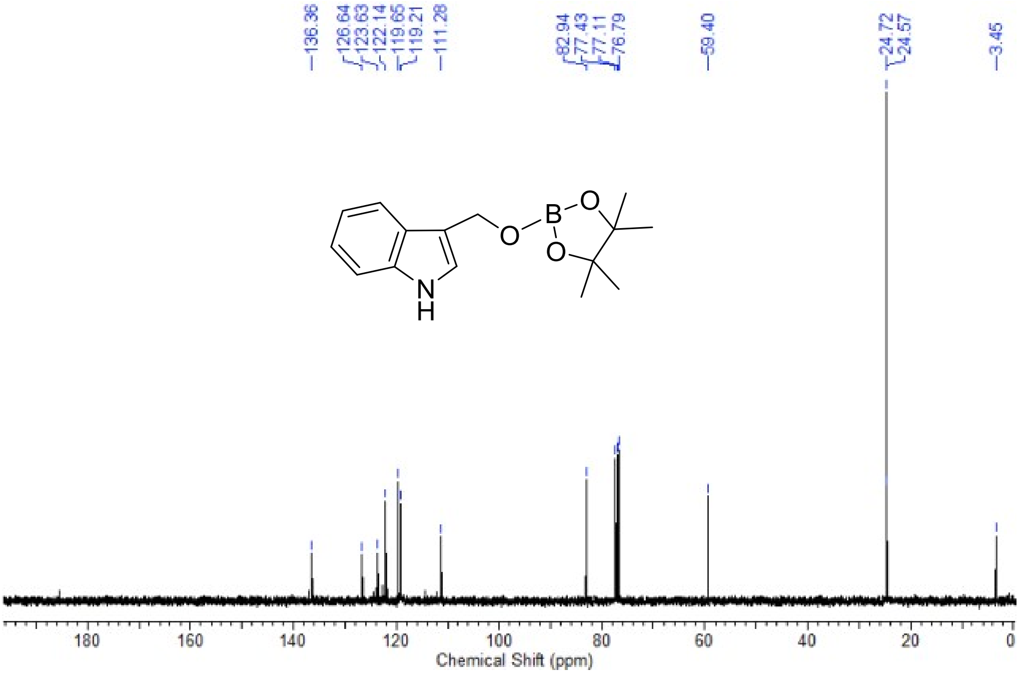

Figure FS59. ^{13}C NMR spectrum (100 MHz, 25°C, $CDCl_3$) of 3-(((4,4,5,5-tetramethyl-1,3,2-dioxaborolan-2-yl)oxy)methyl)-1H-indole.

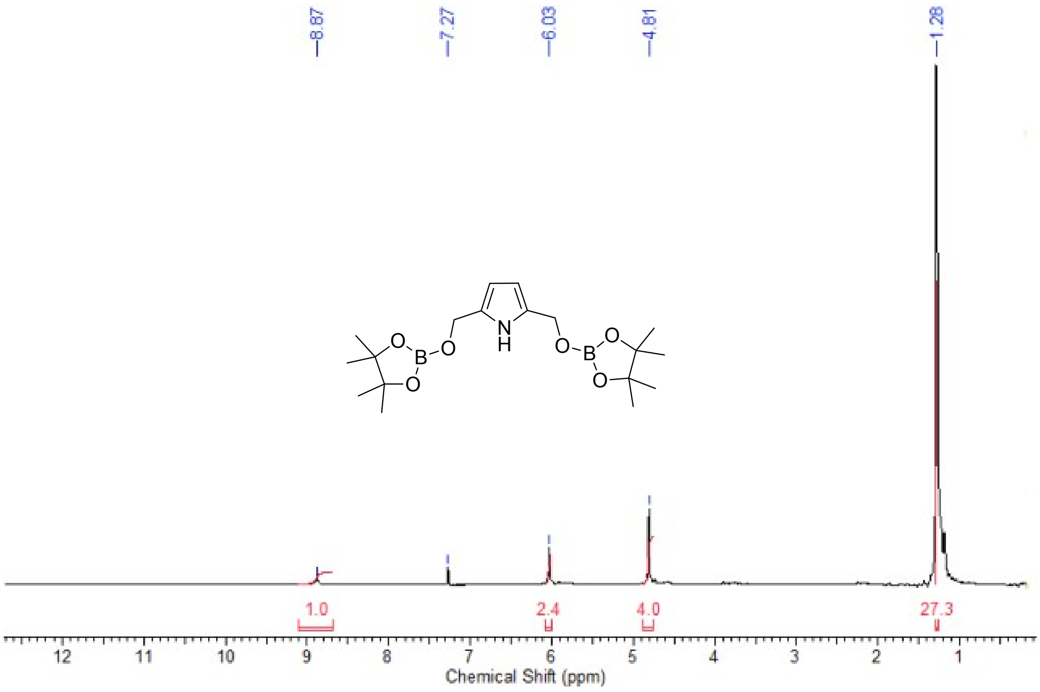

Figure FS60. ^{1}H NMR spectrum (400 MHz, 25°C, $CDCl_3$) of 2,5-bis(((4,4,5,5-tetramethyl-1,3,2-dioxaborolan-2-yl)oxy)methyl)-1H-pyrrole.

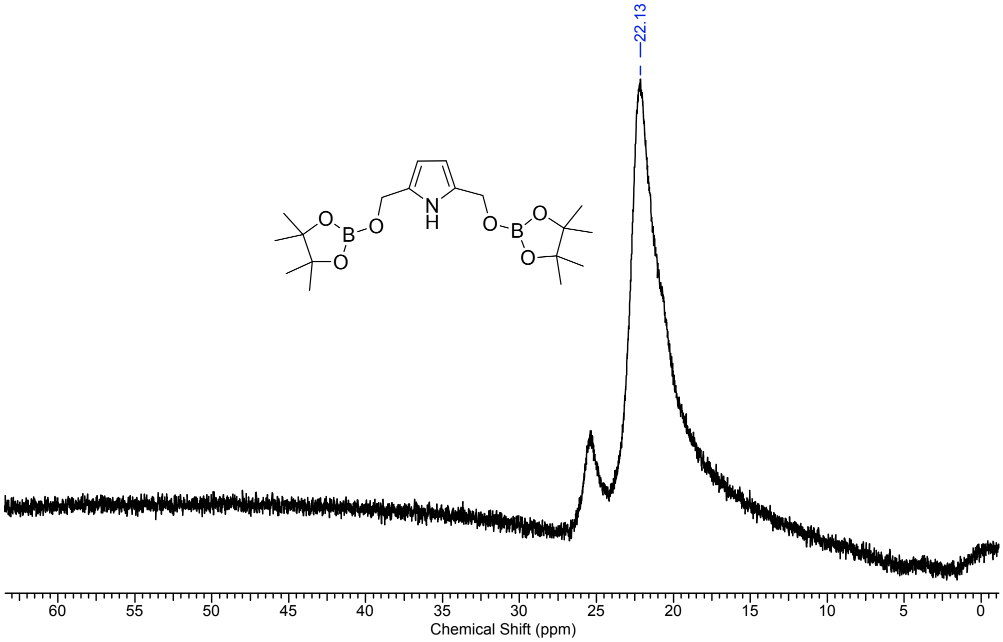

Figure S61. ^{11}B NMR spectrum (128.4 MHz, 25°C, $CDCl_3$) of 2,5-bis(((4,4,5,5-tetramethyl-1,3,2-dioxaborolan-2-yl)oxy)methyl)-1H-pyrrole.

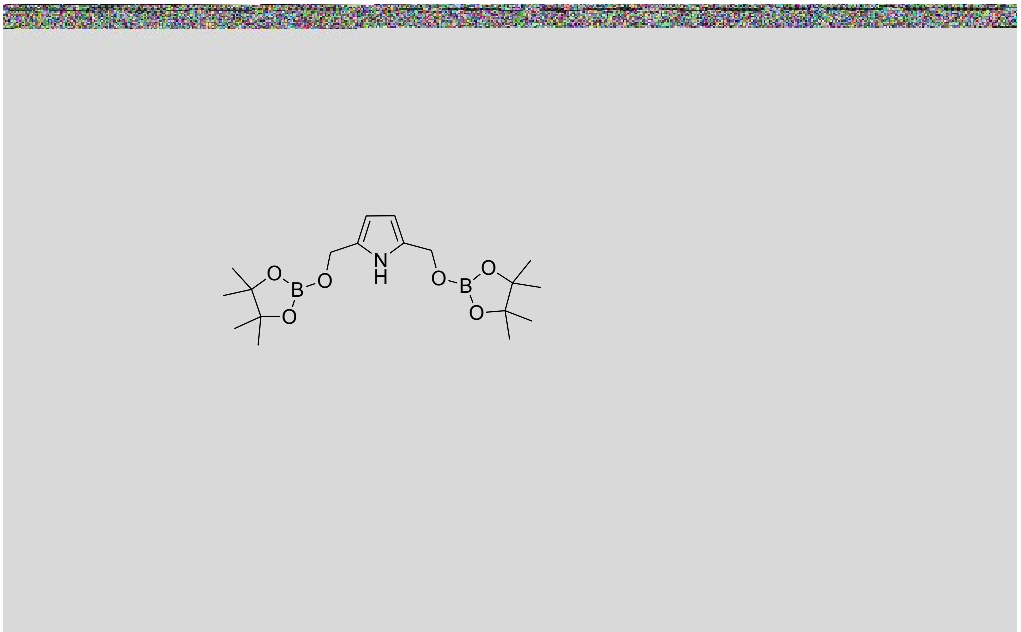

Figure FS62. ^{13}C NMR spectrum (100 MHz, 25°C, $CDCl_3$) of 2,5-bis(((4,4,5,5-tetramethyl-1,3,2-dioxaborolan-2-yl)oxy)methyl)-1H-pyrrole.

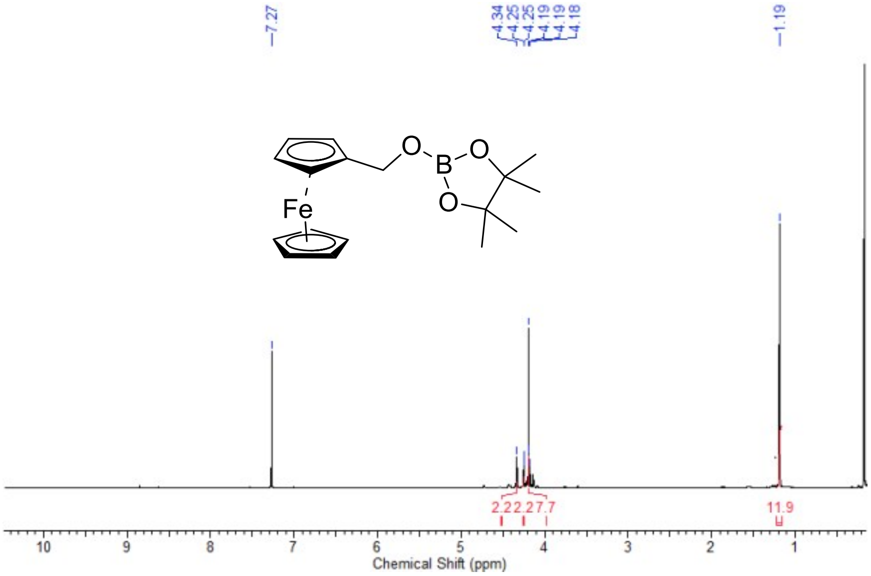

Figure FS63. ^{1}H NMR spectrum (400 MHz, 25°C, $CDCl_3$) of 2-ferrocenyl-4,4,5,5-tetramethyl-1,3,2-dioxaborolane.

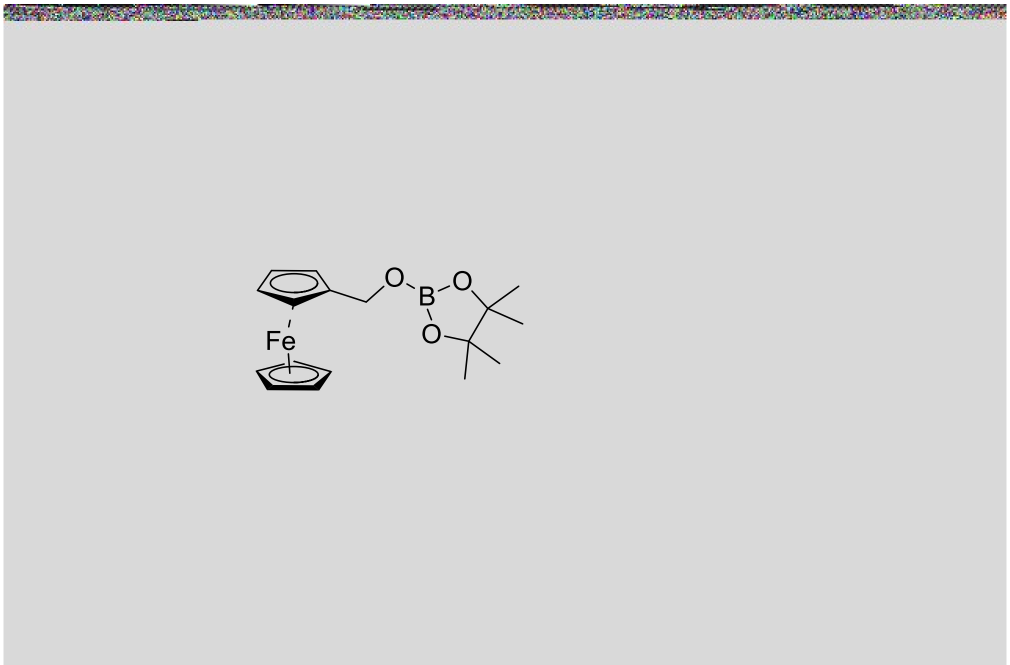

Figure S64. ^{11}B NMR spectrum (128.4 MHz, 25°C, $CDCl_3$) of 2-ferrocenyl-4,4,5,5-tetramethyl-1,3,2-dioxaborolane.

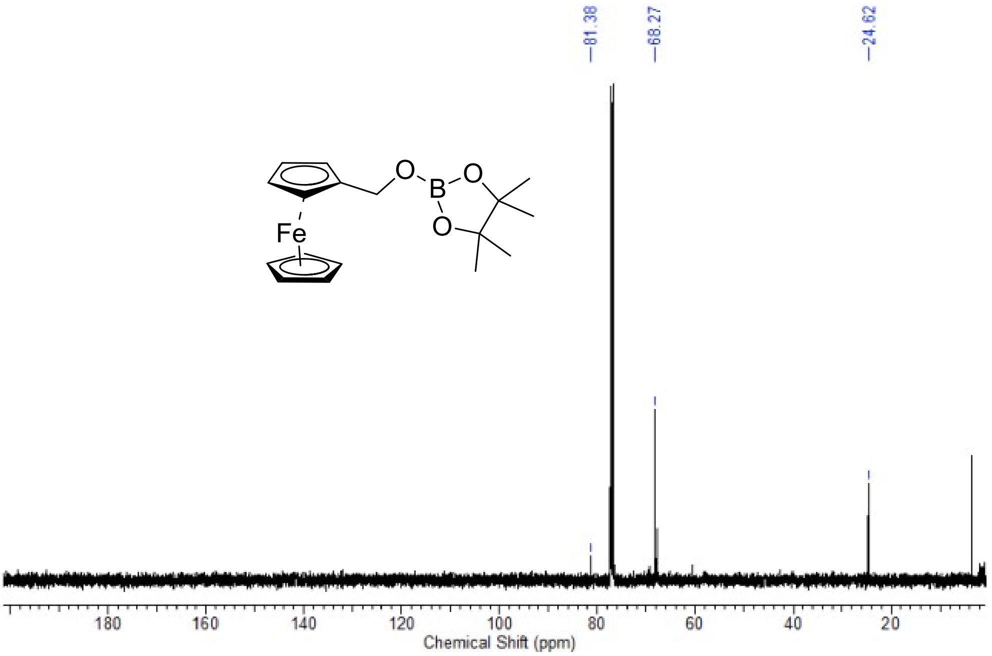

Figure FS65. ^{13}C NMR spectrum (100 MHz, 25°C, $CDCl_3$) of 2-ferrocenyl-4,4,5,5-tetramethyl-1,3,2-dioxaborolane.

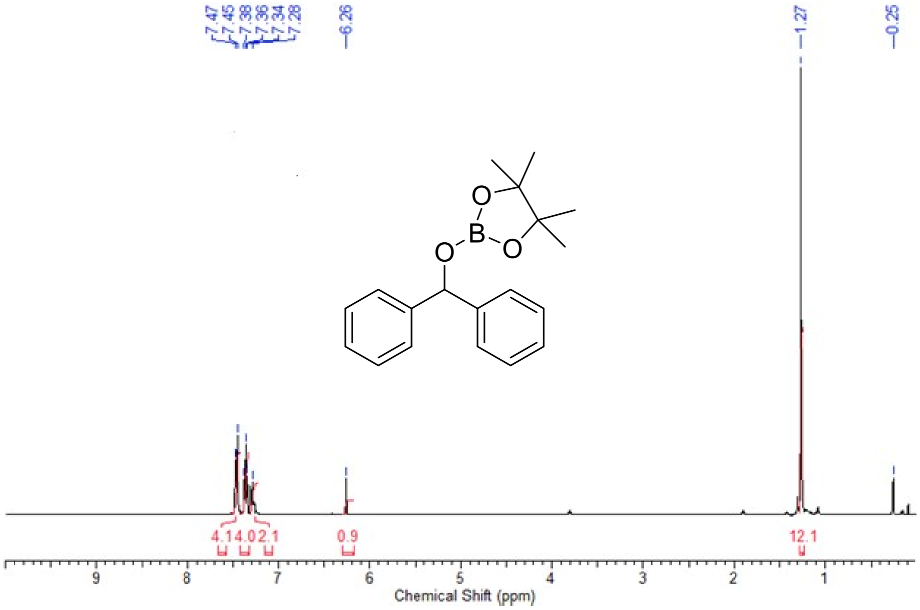

Figure FS66. ^{1}H NMR spectrum (400 MHz, 25°C, $CDCl_3$) of 2-(benzhydryloxy)-4,4,5,5-tetramethyl-1,3,2-dioxaborolane.

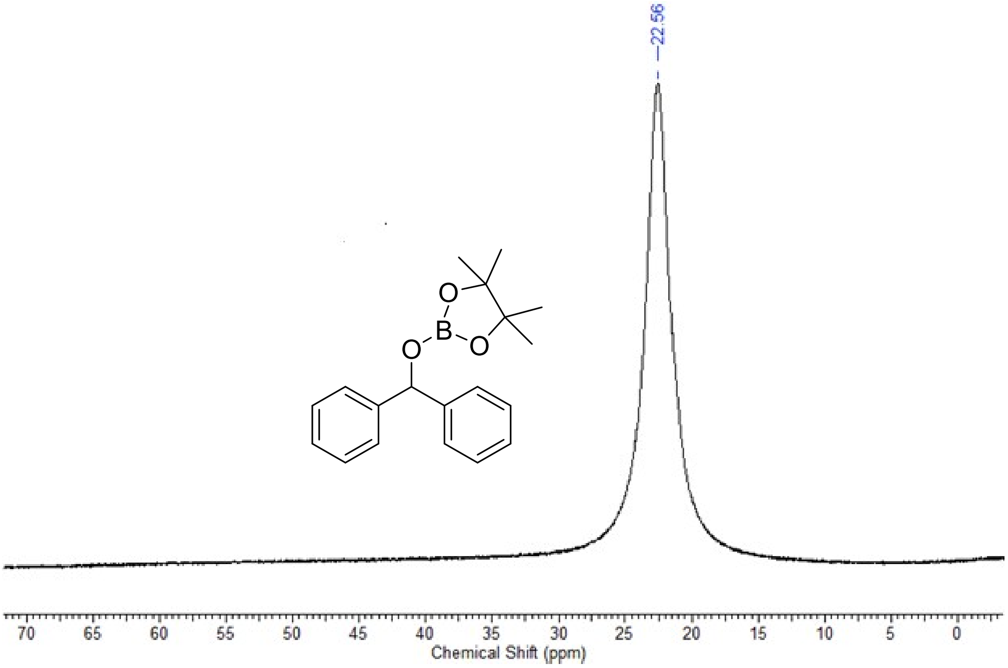

Figure S67. ^{11}B NMR spectrum (128.4 MHz, 25°C, $CDCl_3$) of 2-(benzhydryloxy)-4,4,5,5-tetramethyl-1,3,2-dioxaborolane.

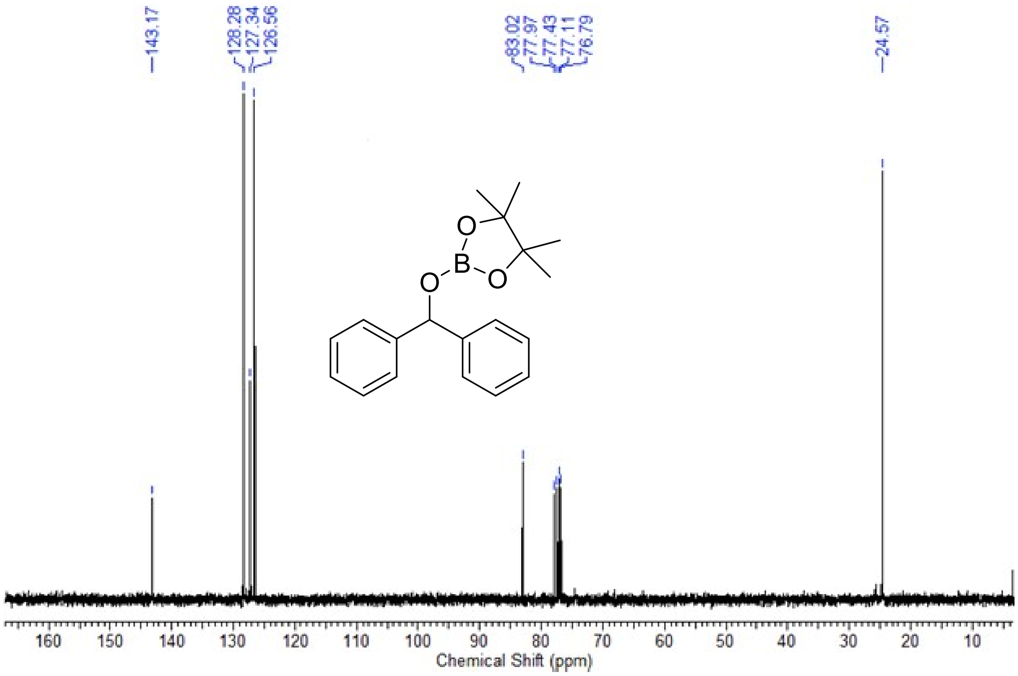

Figure FS68. ^{13}C NMR spectrum (100 MHz, 25°C, $CDCl_3$) of 2-(benzhydryloxy)-4,4,5,5-tetramethyl-1,3,2-dioxaborolane.

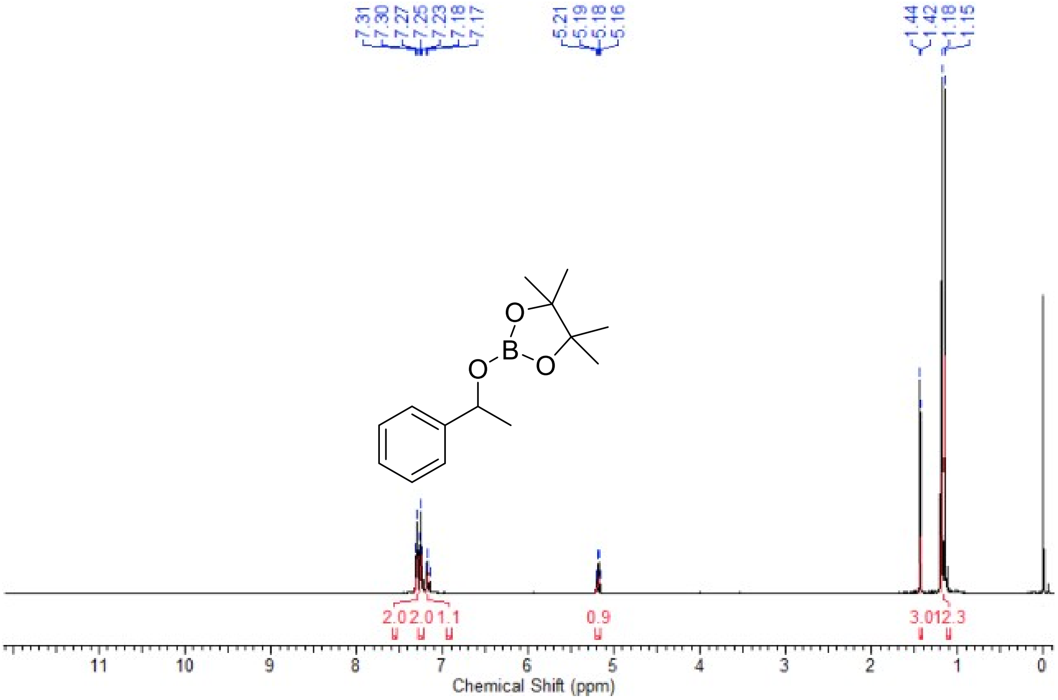

Figure FS69. ^{1}H NMR spectrum (400 MHz, 25°C, $CDCl_3$) of 4,4,5,5-tetramethyl-2-(1-phenylethoxy)-1,3,2-dioxaborolane.

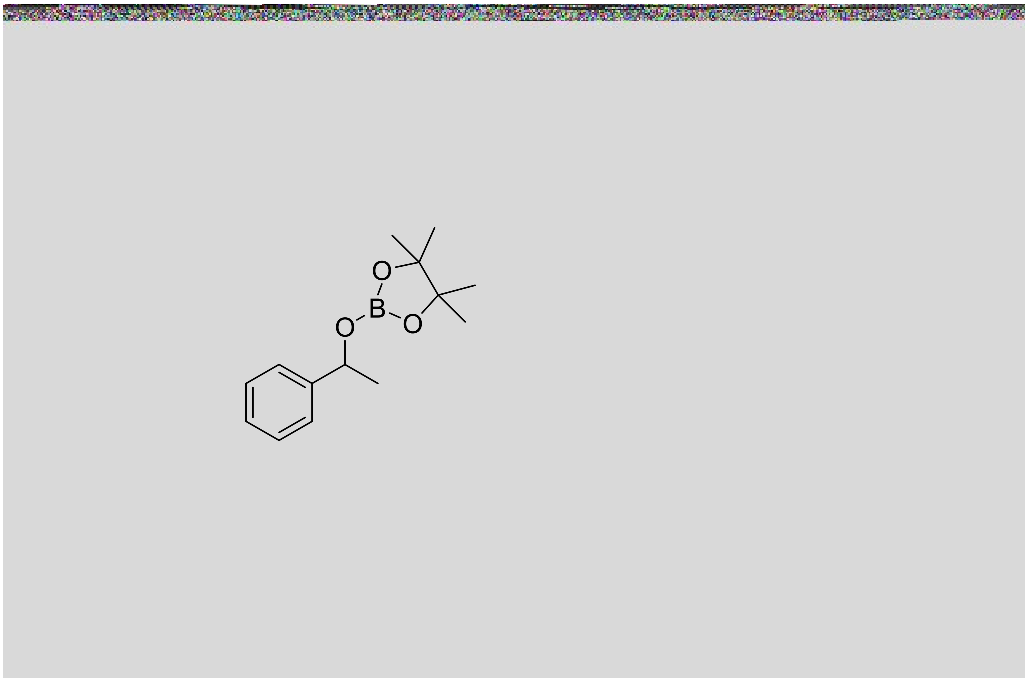

Figure S70. ^{11}B NMR spectrum (128.4 MHz, 25°C, $CDCl_3$) of 4,4,5,5-tetramethyl-2-(1-phenylethoxy)-1,3,2-dioxaborolane.

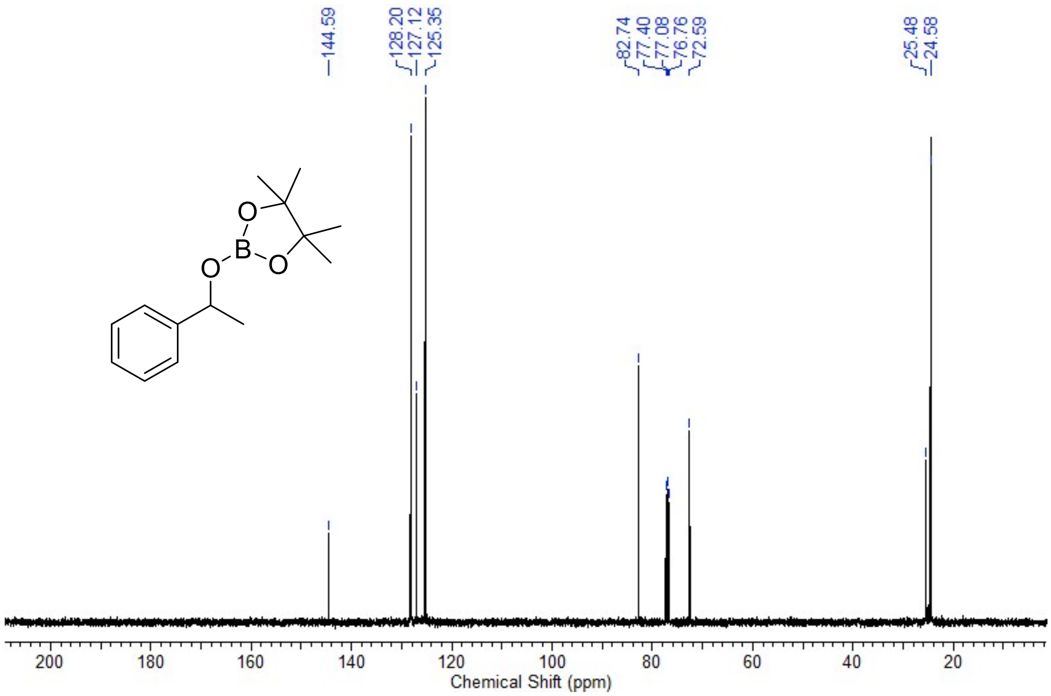

Figure FS71. ^{13}C NMR spectrum (100 MHz, 25°C, $CDCl_3$) of 4,4,5,5-tetramethyl-2-(1-phenylethoxy)-1,3,2-dioxaborolane.

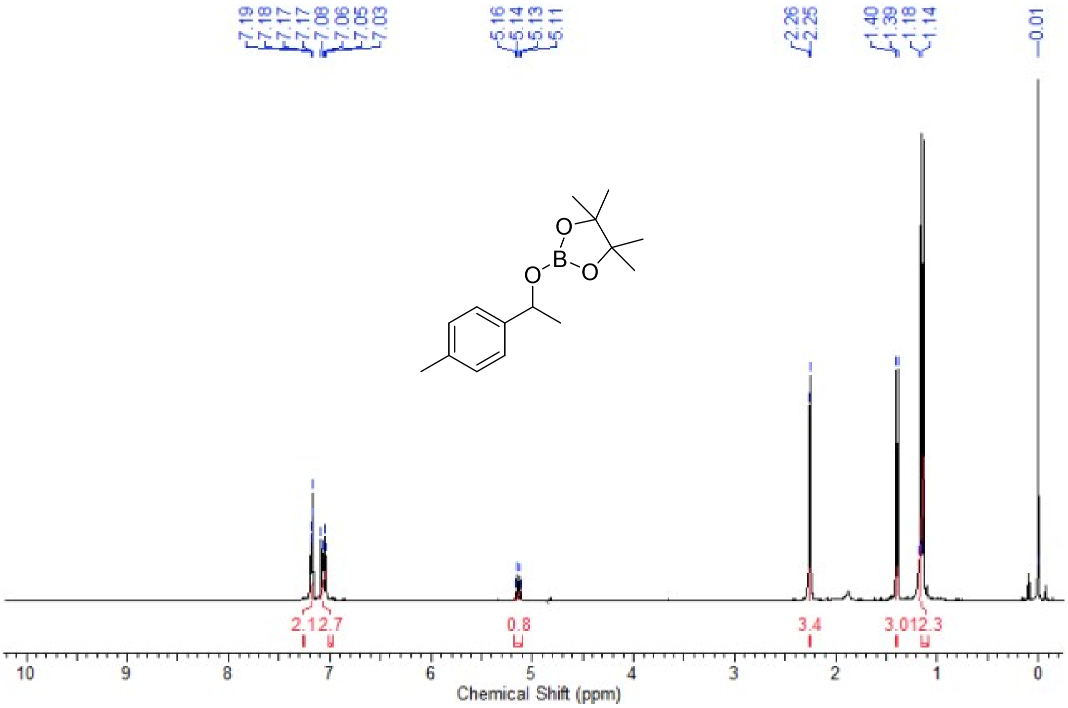

Figure FS72. ^1H NMR spectrum (400 MHz, 25°C, $CDCl_3$) of 4,4,5,5-tetramethyl-2-(1-(p-tolyl)ethoxy)-1,3,2-dioxaborolane.

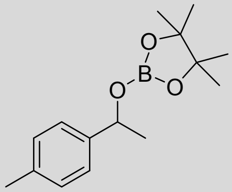

Figure S73. ^{11}B NMR spectrum (128.4 MHz, 25°C, $CDCl_3$) of 4,4,5,5-tetramethyl-2-(1-(p-tolyl)ethoxy)-1,3,2-dioxaborolane.

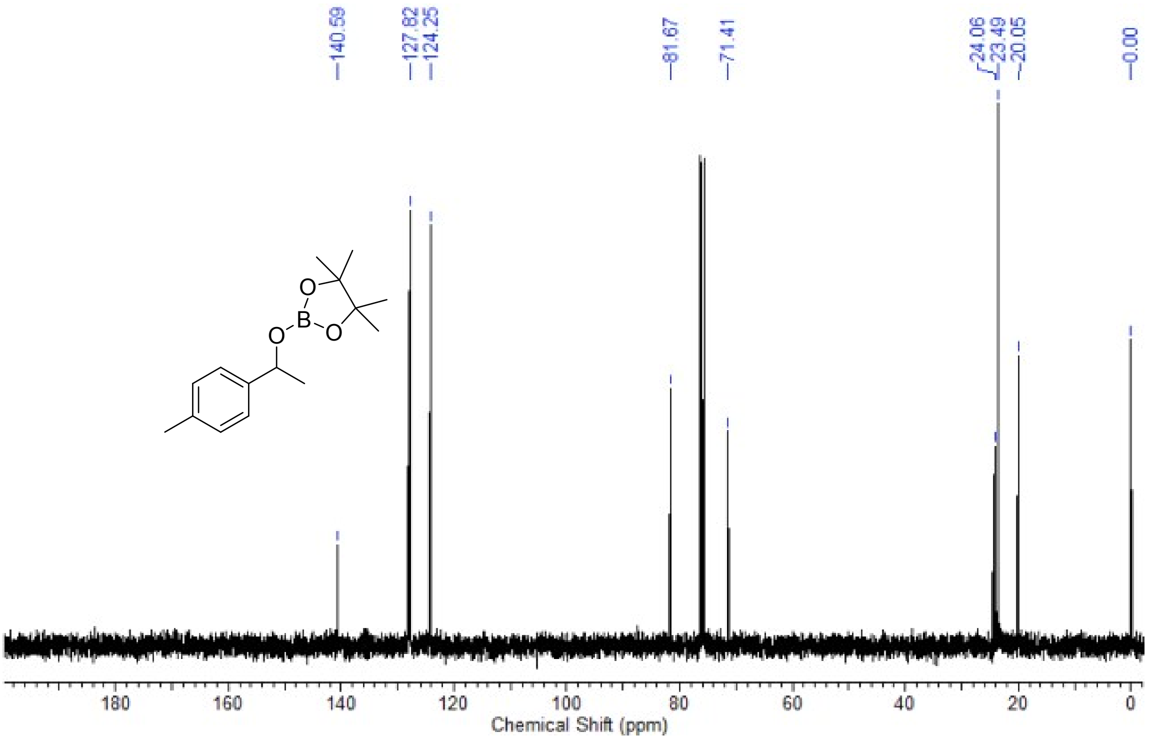

Figure FS74. ^{13}C NMR spectrum (100 MHz, 25°C, $CDCl_3$) of 4,4,5,5-tetramethyl-2-(1-(p-tolyl)ethoxy)-1,3,2-dioxaborolane.

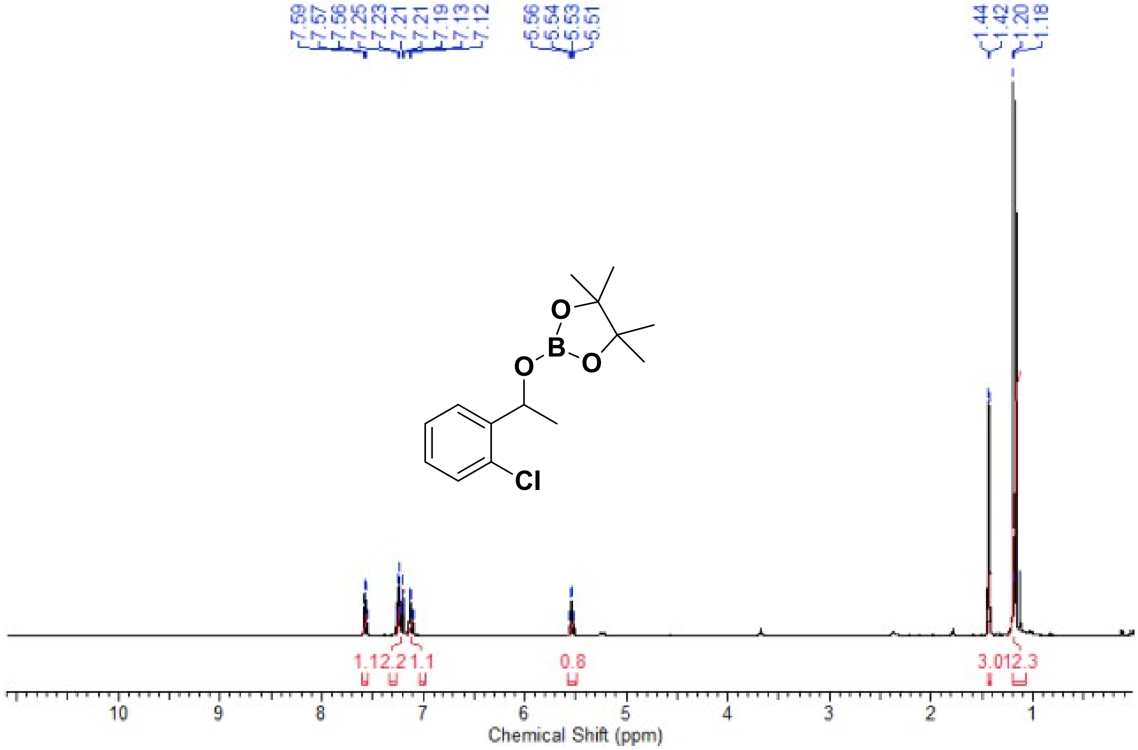

Figure FS75. ^{1}H NMR spectrum (400 MHz, 25°C, $CDCl_3$) of 2-(1-(2-chlorophenyl)ethoxy)-4,4,5,5-tetramethyl-1,3,2-dioxaborolane.

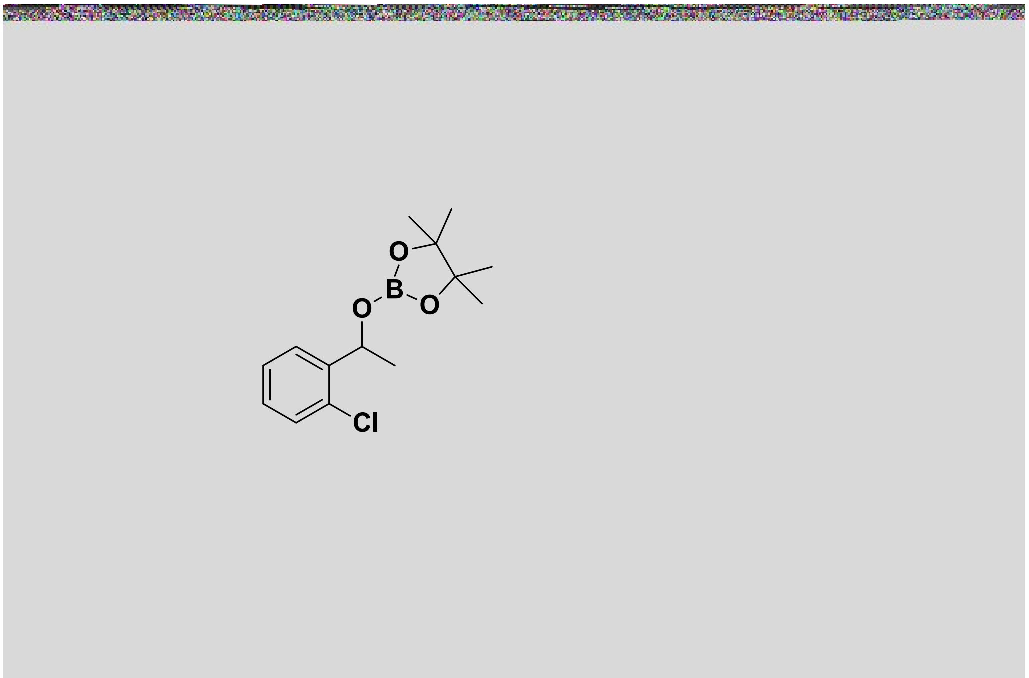

Figure S76. ^{11}B NMR spectrum (128.4 MHz, 25°C, $CDCl_3$) of 2-(1-(2-chlorophenyl)ethoxy)-4,4,5,5-tetramethyl-1,3,2-dioxaborolane.

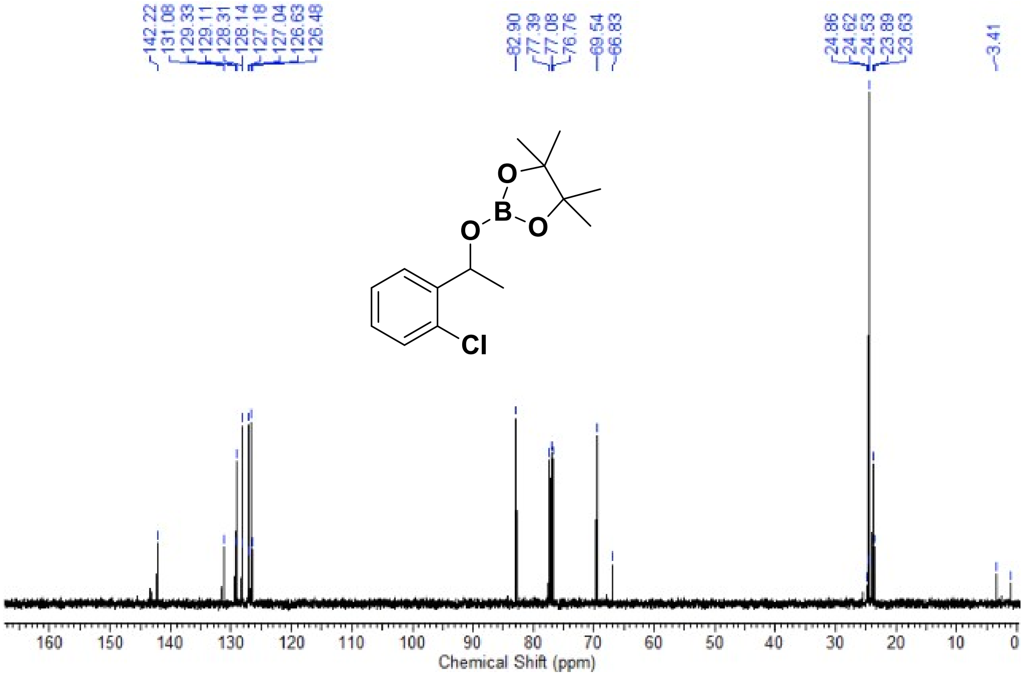

Figure FS77. ^{13}C NMR spectrum (100 MHz, 25°C, $CDCl_3$) of 2-(1-(2-chlorophenyl)ethoxy)-4,4,5,5-tetramethyl-1,3,2-dioxaborolane.

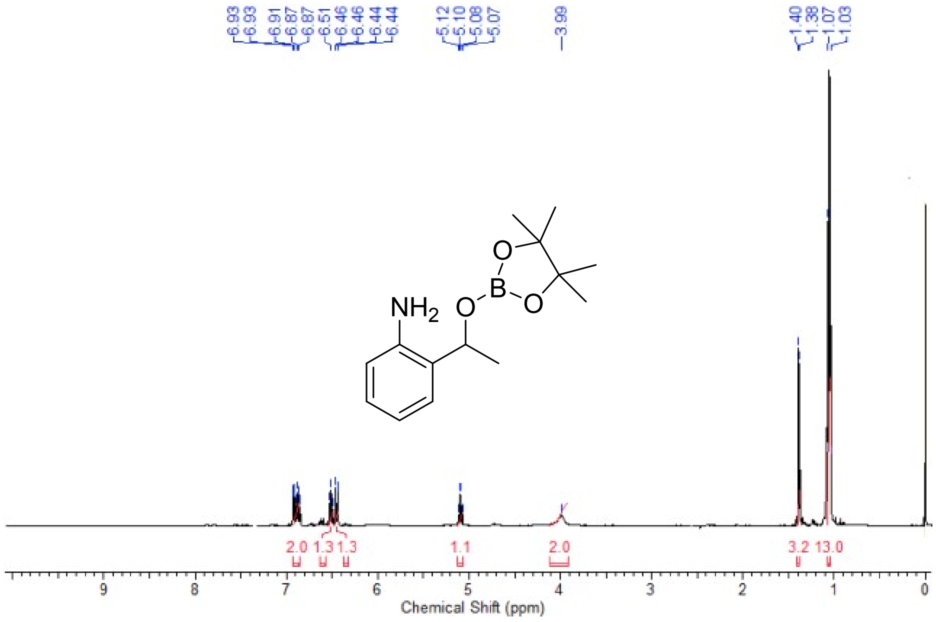

Figure FS78. ^{1}H NMR spectrum (400 MHz, 25°C, $CDCl_3$) of 2-(1-((4,4,5,5-tetramethyl-1,3,2-dioxaborolan-2-yl)oxy)ethyl)aniline.

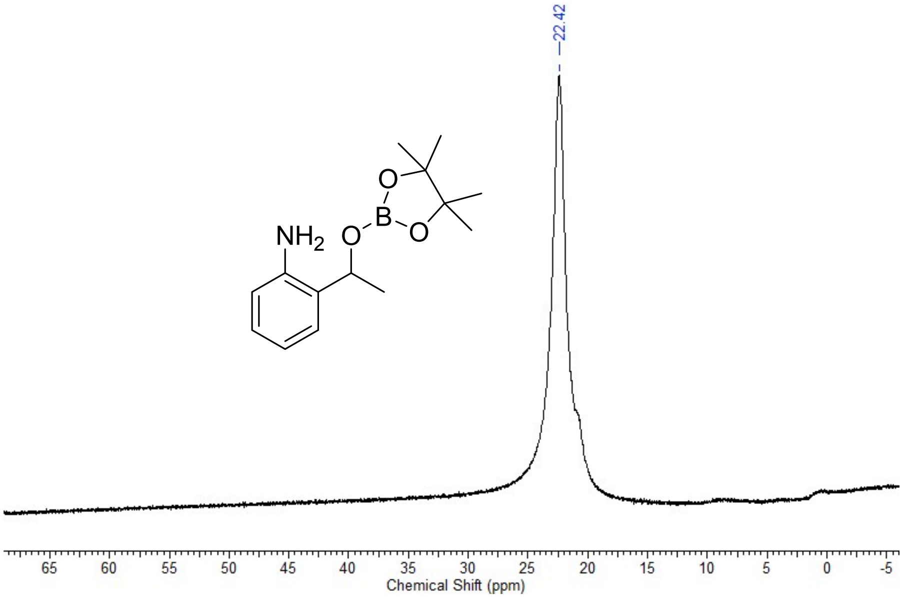

Figure S79. ^{11}B NMR spectrum (128.4 MHz, 25°C, $CDCl_3$) of 2-(1-((4,4,5,5-tetramethyl-1,3,2-dioxaborolan-2-yl)oxy)ethyl)aniline.

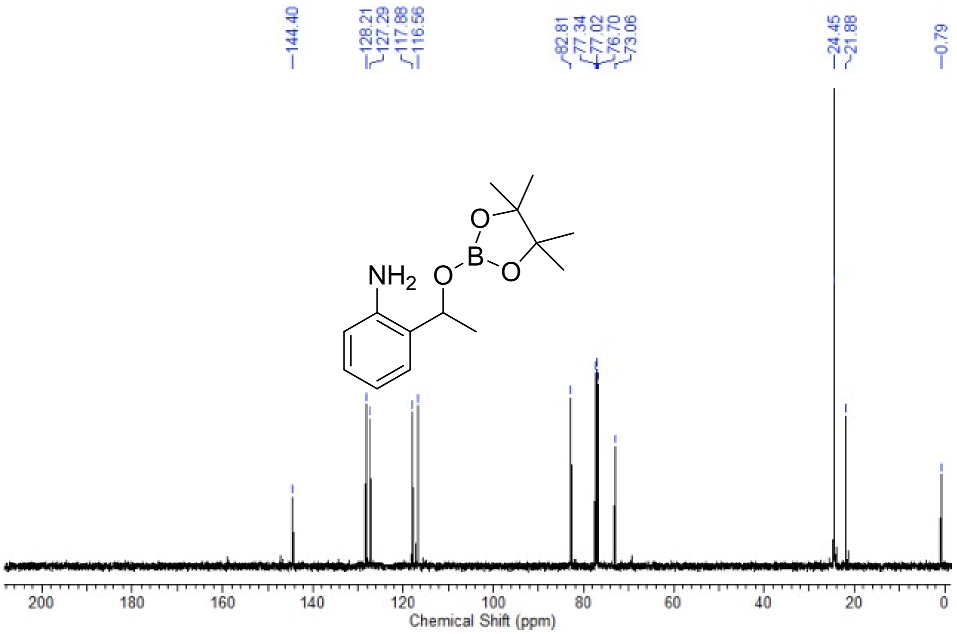

Figure FS80. ^{13}C NMR spectrum (100 MHz, 25°C, $CDCl_3$) of 2-(1-((4,4,5,5-tetramethyl-1,3,2-dioxaborolan-2-yl)oxy)ethyl)aniline.

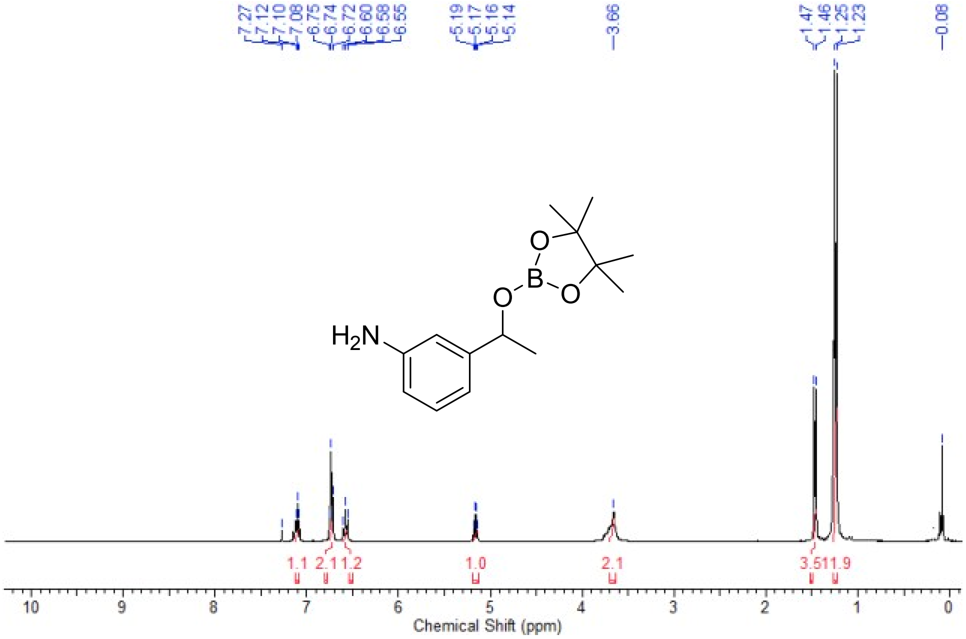

Figure FS81. ^{1}H NMR spectrum (400 MHz, 25°C, $CDCl_3$) of 3-(1-((4,4,5,5-tetramethyl-1,3,2-dioxaborolan-2-yl)oxy)ethyl)aniline.

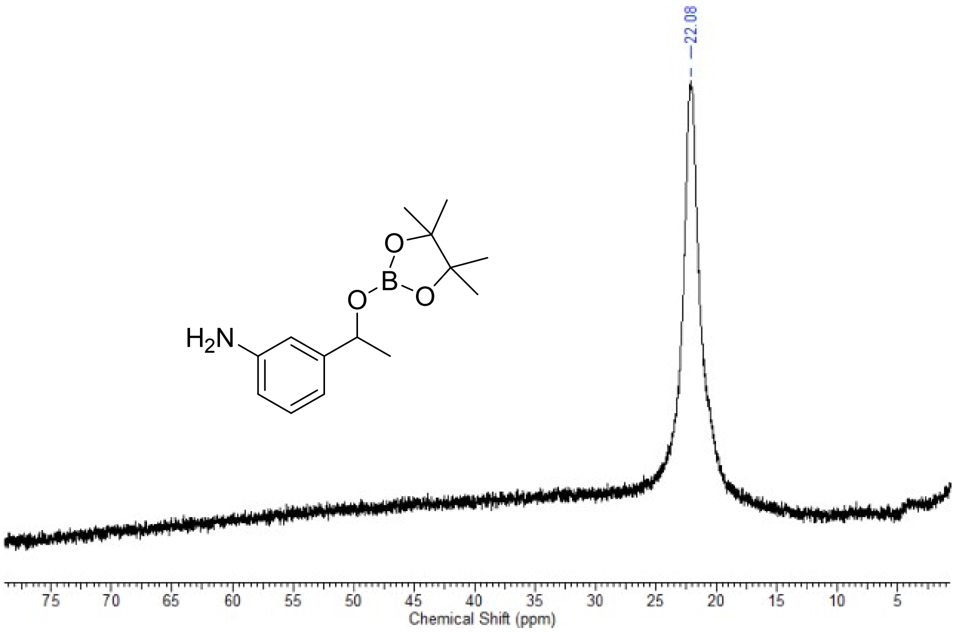

Figure S82. ^{11}B NMR spectrum (128.4 MHz, 25°C, $CDCl_3$) of 3-(1-((4,4,5,5-tetramethyl-1,3,2-dioxaborolan-2-yl)oxy)ethyl)aniline.

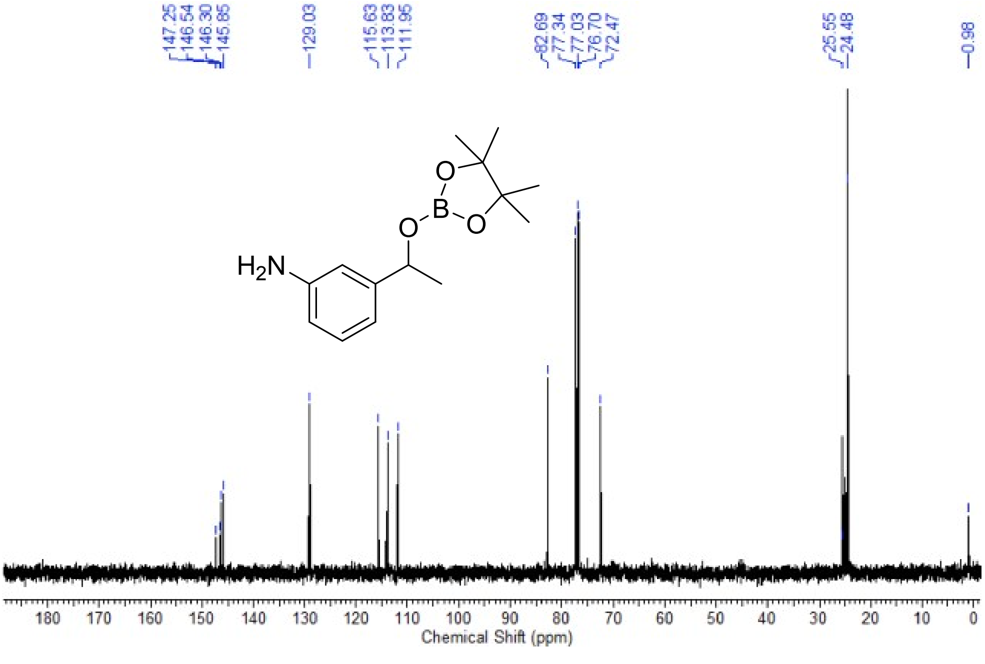

Figure FS83. ^{13}C NMR spectrum (100 MHz, 25°C, $CDCl_3$) of 3-(1-((4,4,5,5-tetramethyl-1,3,2-dioxaborolan-2-yl)oxy)ethyl)aniline.

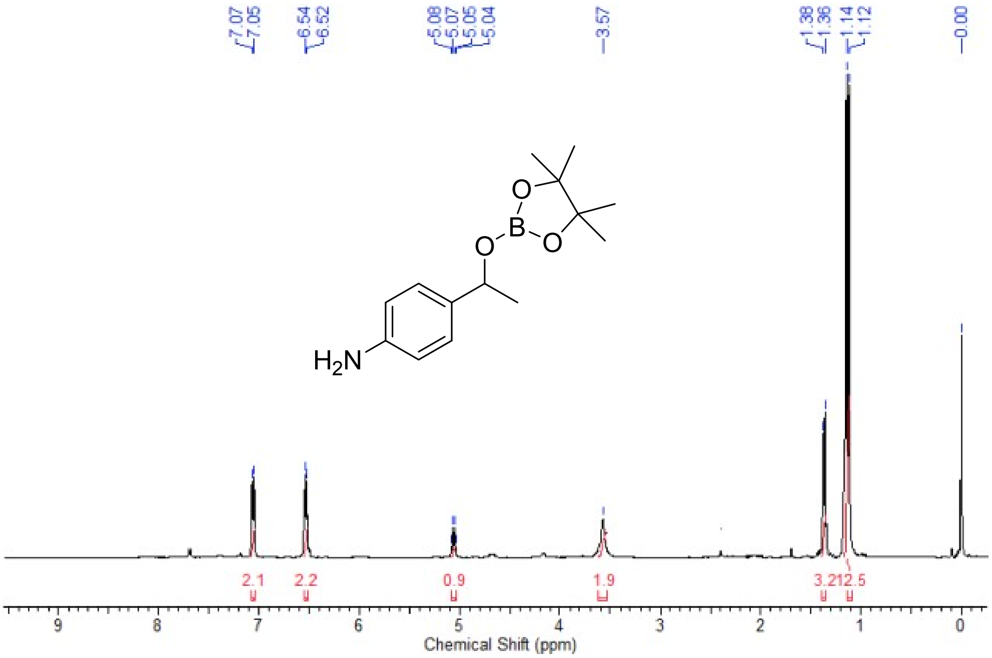

Figure FS84. ^{1}H NMR spectrum (400 MHz, 25°C, $CDCl_3$) of 4-(1-((4,4,5,5-tetramethyl-1,3,2-dioxaborolan-2-yl)oxy)ethyl)aniline.

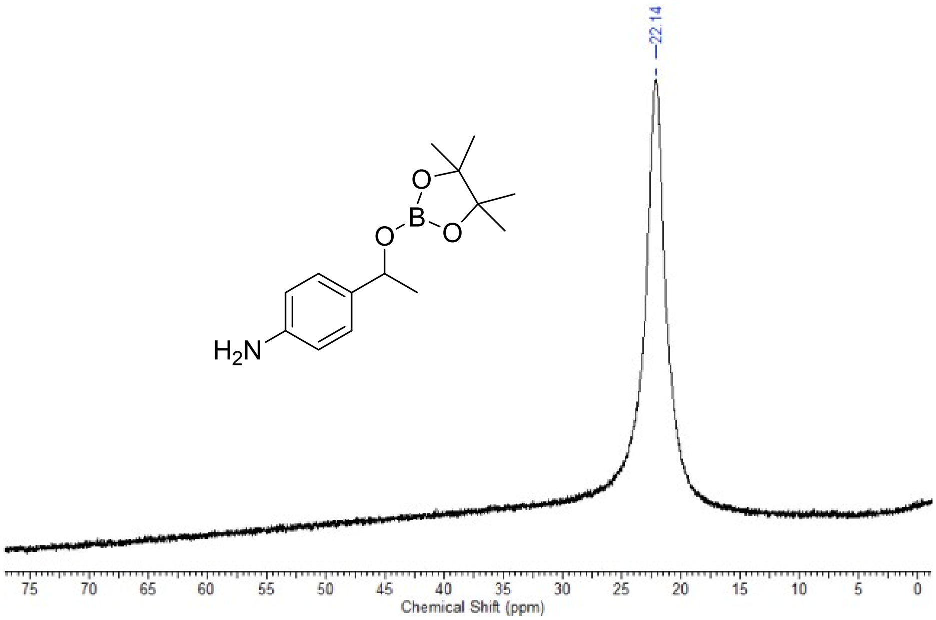

Figure S85. ^{11}B NMR spectrum (128.4 MHz, 25°C, $CDCl_3$) of 4-(1-((4,4,5,5-tetramethyl-1,3,2-dioxaborolan-2-yl)oxy)ethyl)aniline.

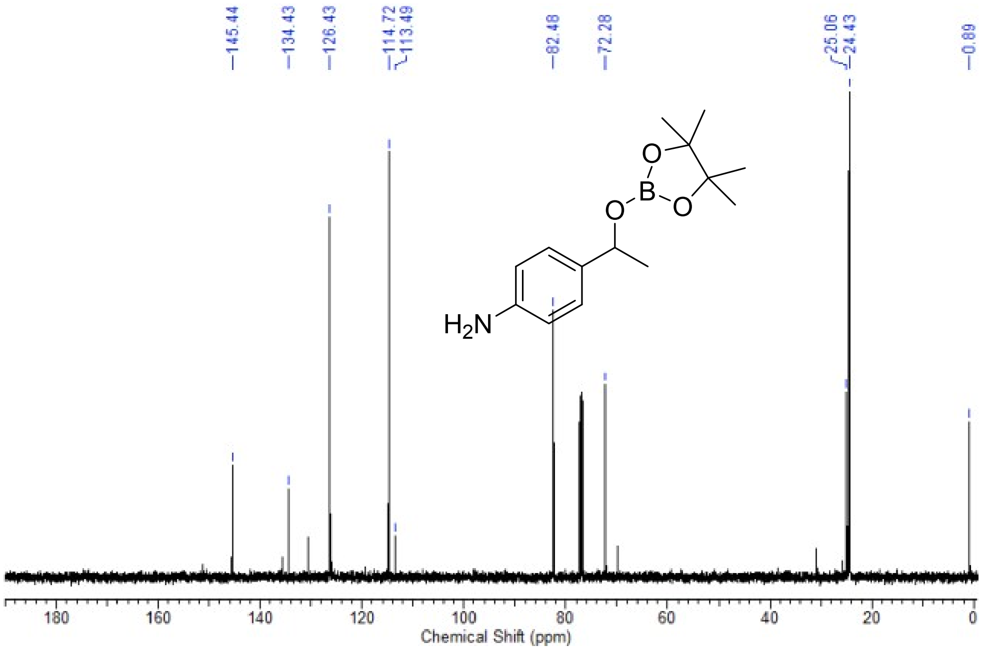

Figure FS86. ^{13}C NMR spectrum (100 MHz, 25°C, $CDCl_3$) of 4-(1-((4,4,5,5-tetramethyl-1,3,2-dioxaborolan-2-yl)oxy)ethyl)aniline.

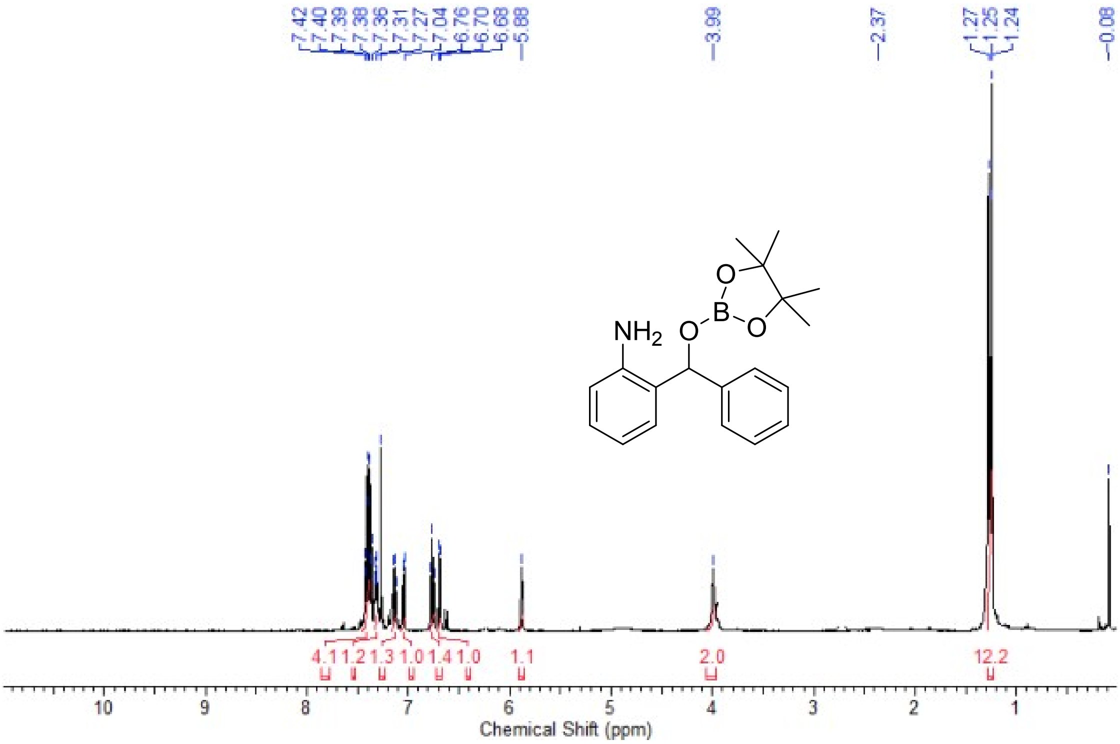

Figure FS87. ^{1}H NMR spectrum (400 MHz, 25°C, $CDCl_3$) of 2-(phenyl((4,4,5,5-tetramethyl-1,3,2-dioxaborolan-2-yl)oxy)methyl)aniline.

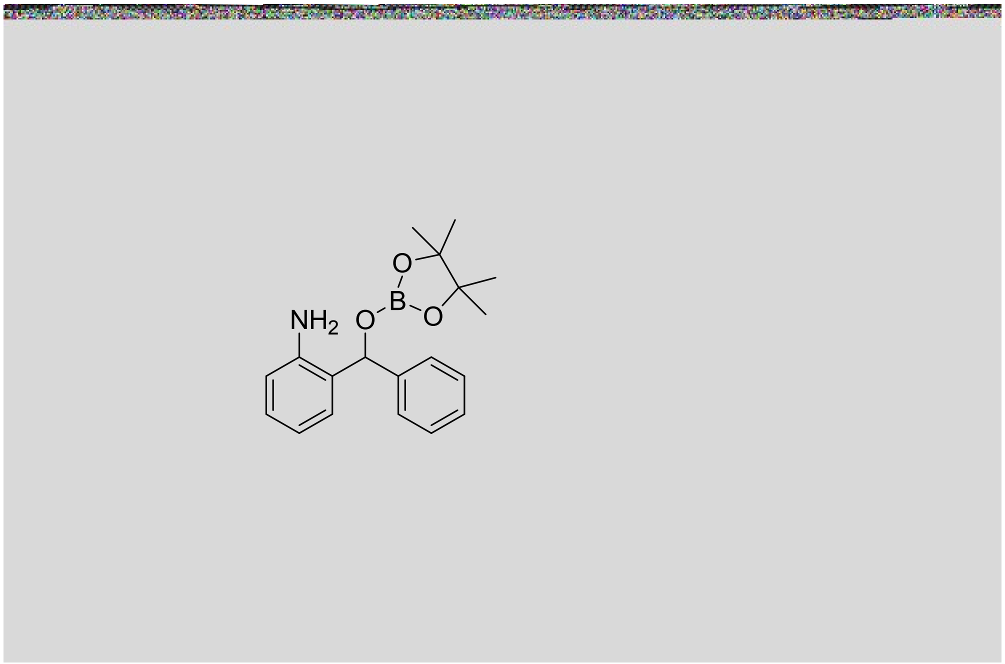

Figure S88. ^{11}B NMR spectrum (128.4 MHz, 25°C, CDCl$_3$) of 2-(phenyl((4,4,5,5-tetramethyl-1,3,2-dioxaborolan-2-yl)oxy)methyl)aniline.

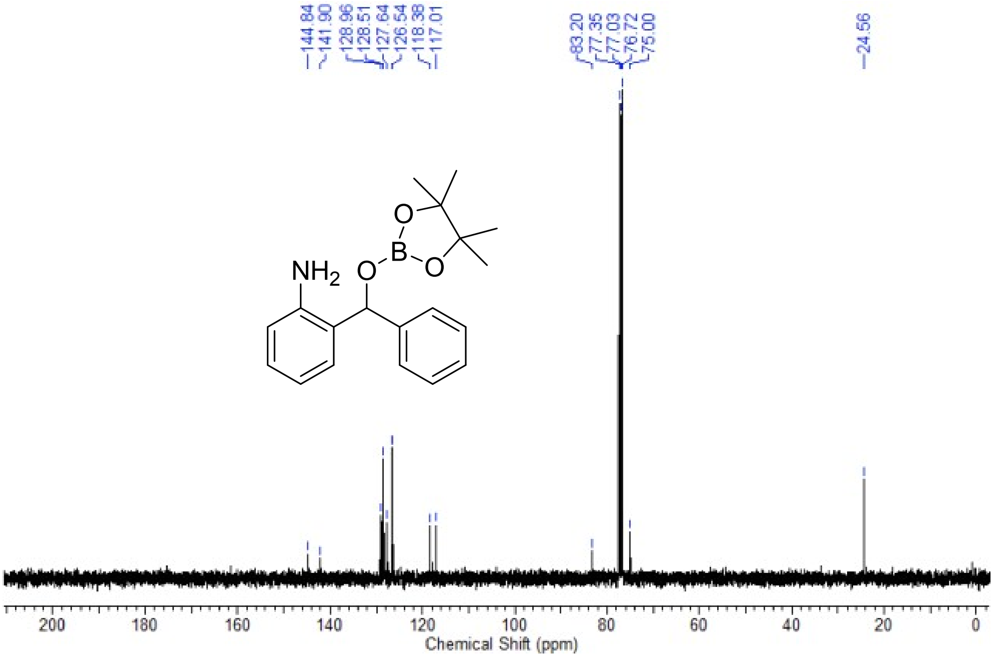

Figure FS89. ^{13}C NMR spectrum (100 MHz, 25°C, CDCl$_3$) of 2-(phenyl((4,4,5,5-tetramethyl-1,3,2-dioxaborolan-2-yl)oxy)methyl)aniline.

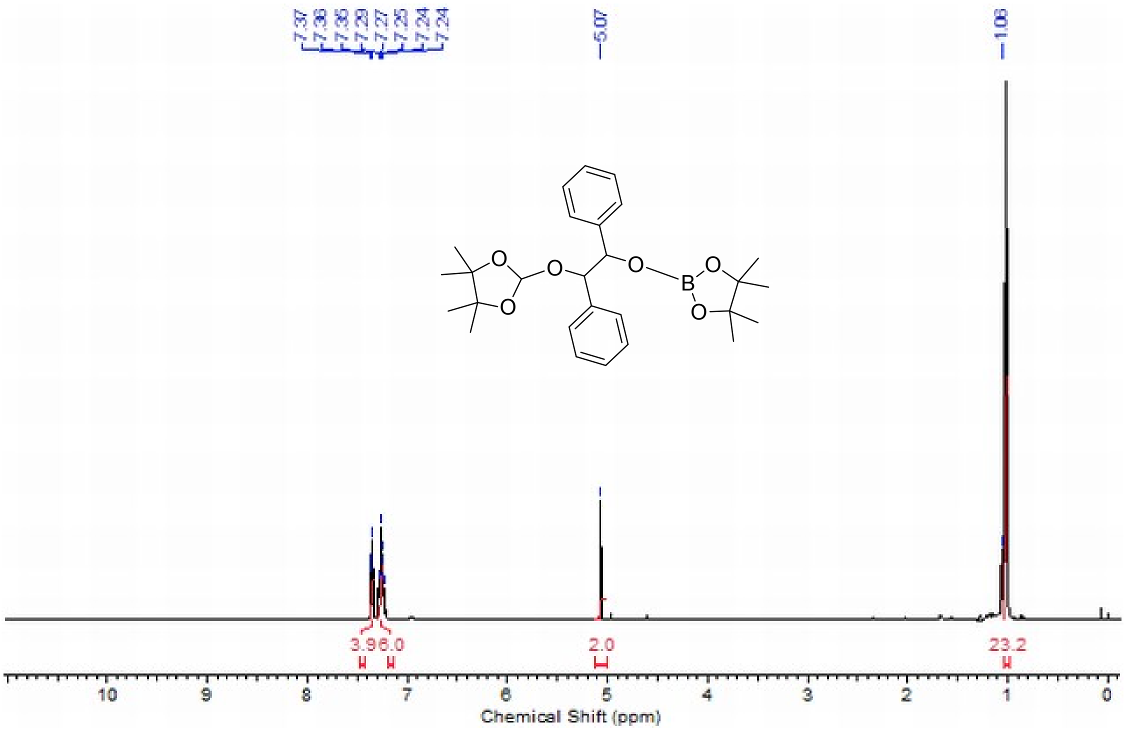

Figure FS90. ^{1}H NMR spectrum (400 MHz, 25°C, $CDCl_3$) of 1,2-bis((4,4,5,5-tetramethyl-1,3,2-dioxaborolan-2-yl)oxy)-1,2-dihydroacenaphthylene.

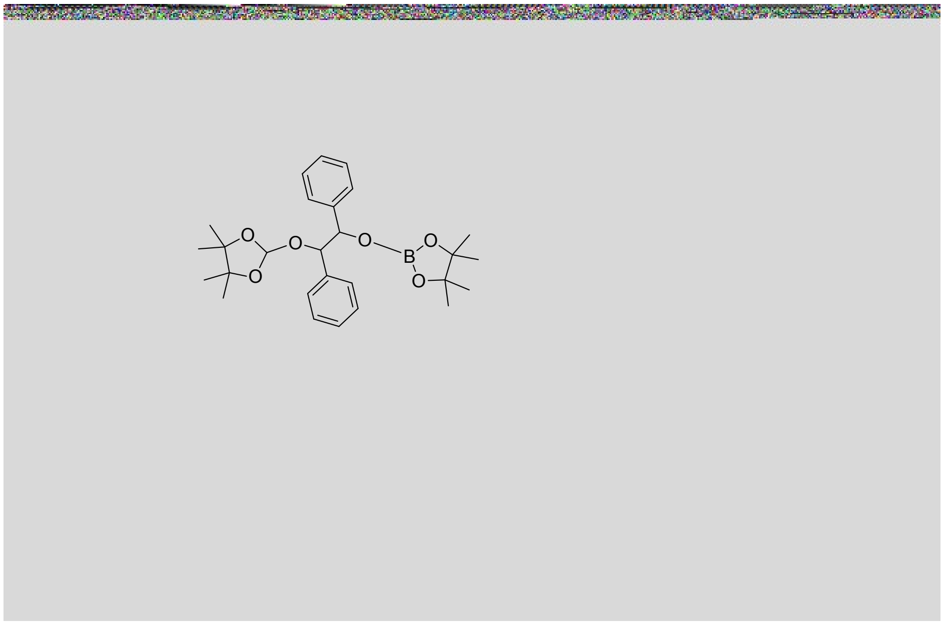

Figure S91. ^{11}B NMR spectrum (128.4 MHz, 25°C, $CDCl_3$) of 1,2-bis((4,4,5,5-tetramethyl-1,3,2-dioxaborolan-2-yl)oxy)-1,2-dihydroacenaphthylene.

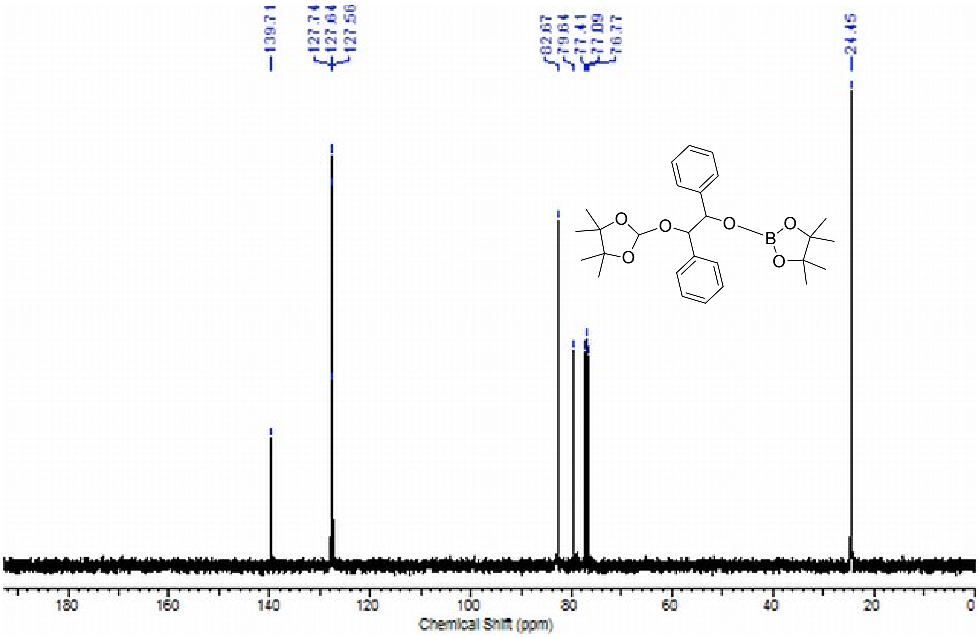

Figure FS92. ^{13}C NMR spectrum (100 MHz, 25°C, $CDCl_3$) of 1,2-bis((4,4,5,5-tetramethyl-1,3,2-dioxaborolan-2-yl)oxy)-1,2-dihydroacenaphthylene.

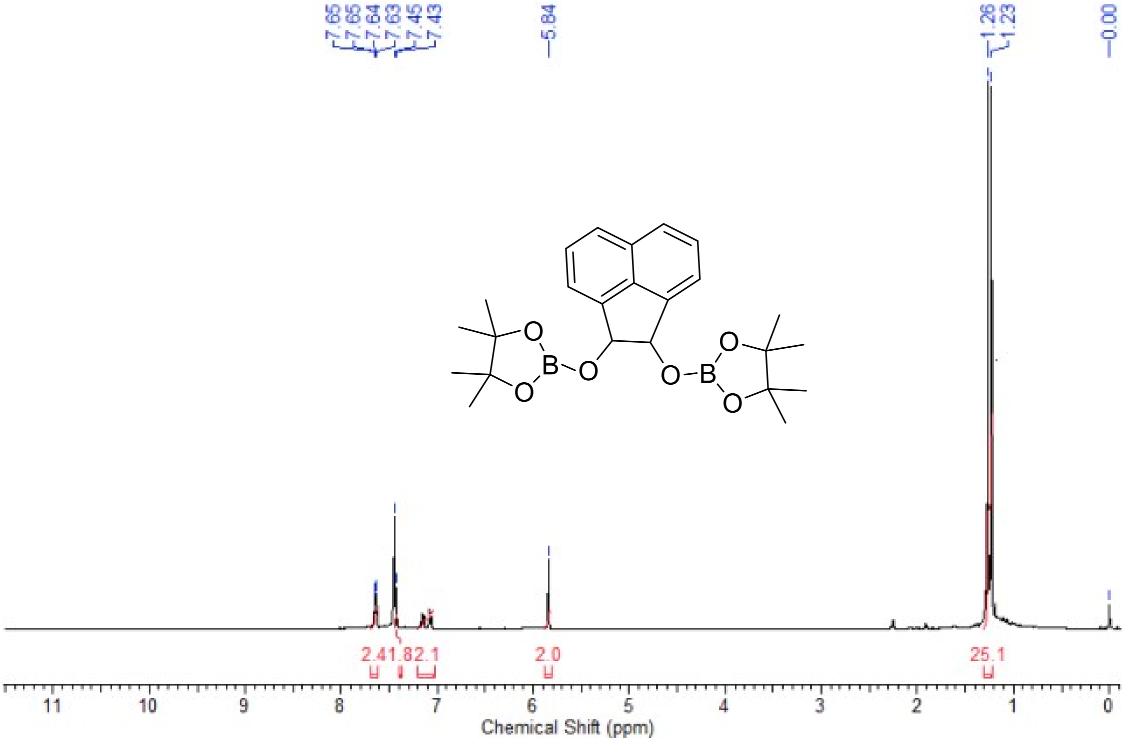

Figure FS93. ^{1}H NMR spectrum (400 MHz, 25°C, $CDCl_3$) of 1,2-bis((4,4,5,5-tetramethyl-1,3,2-dioxaborolan-2-yl)oxy)-1,2-dihydroacenaphthylene.

Figure S94. ^{11}B NMR spectrum (128.4 MHz, 25°C, $CDCl_3$) of 1,2-bis((4,4,5,5-tetramethyl-1,3,2-dioxaborolan-2-yl)oxy)-1,2-dihydroacenaphthylene.

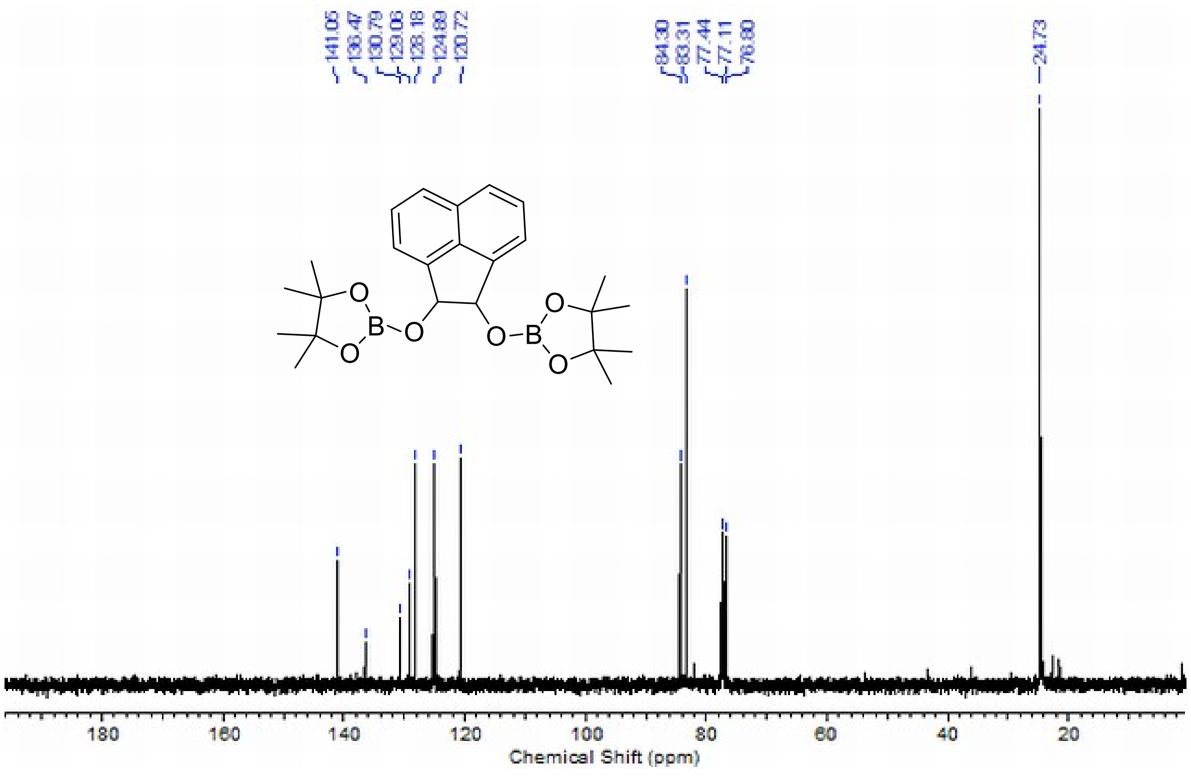

Figure FS95. ^{13}C NMR spectrum (100 MHz, 25°C, $CDCl_3$) of 1,2-bis((4,4,5,5-tetramethyl-1,3,2-dioxaborolan-2-yl)oxy)-1,2-dihydroacenaphthylene.

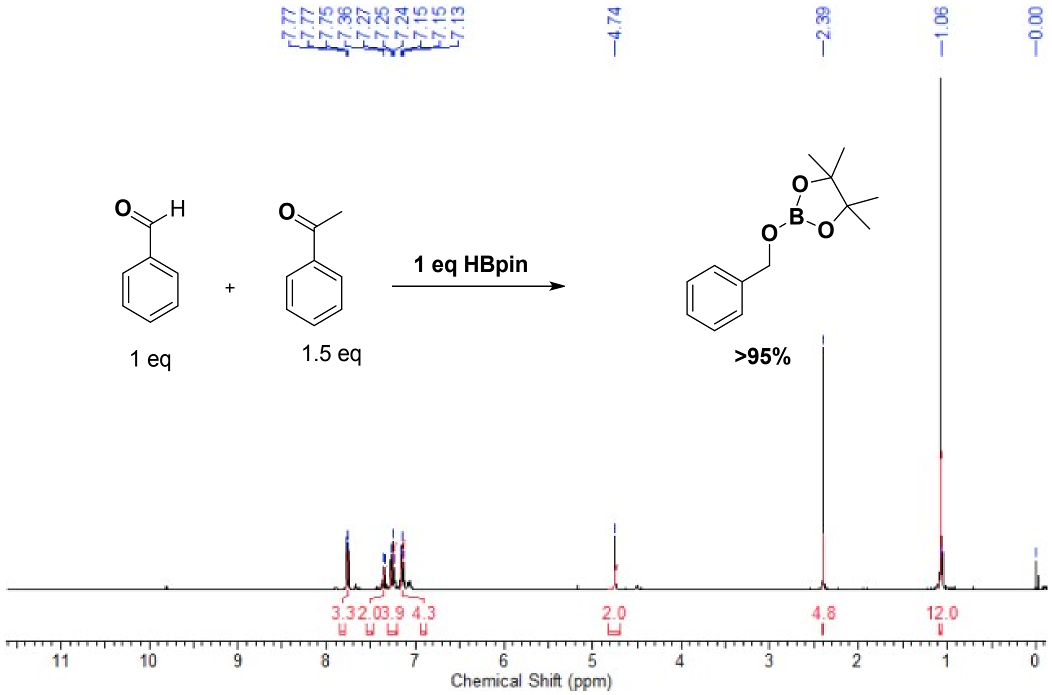

Figure FS96. ^{1}H NMR spectrum (128.4 MHz, 25°C, CDCl$_3$) of chemo selective reduction of aldehydes.

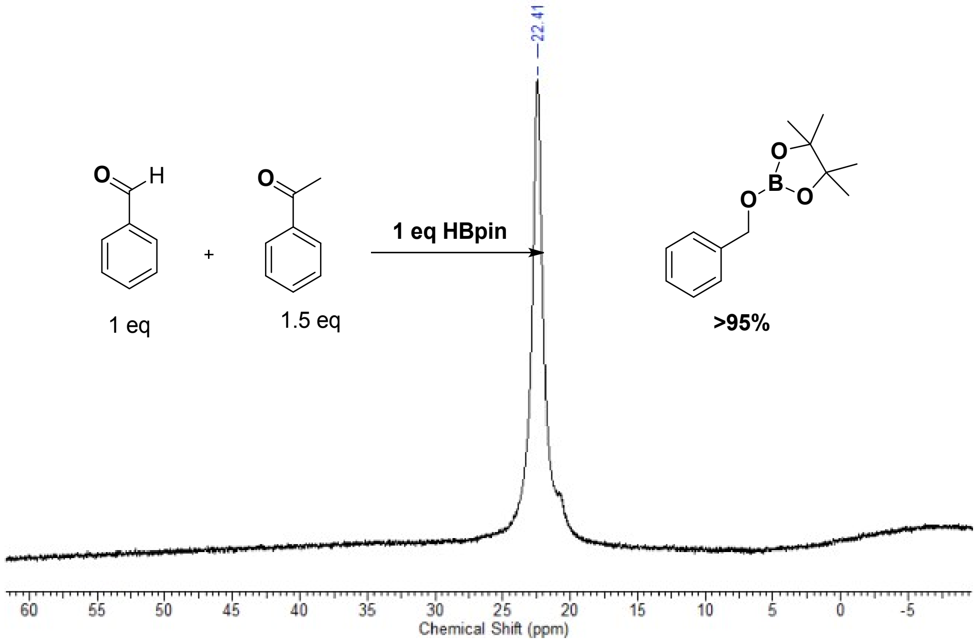

Figure FS97. ^{11}B NMR spectrum (128.4 MHz, 25°C, CDCl$_3$) of Chemo selective reduction of aldehydes**.**

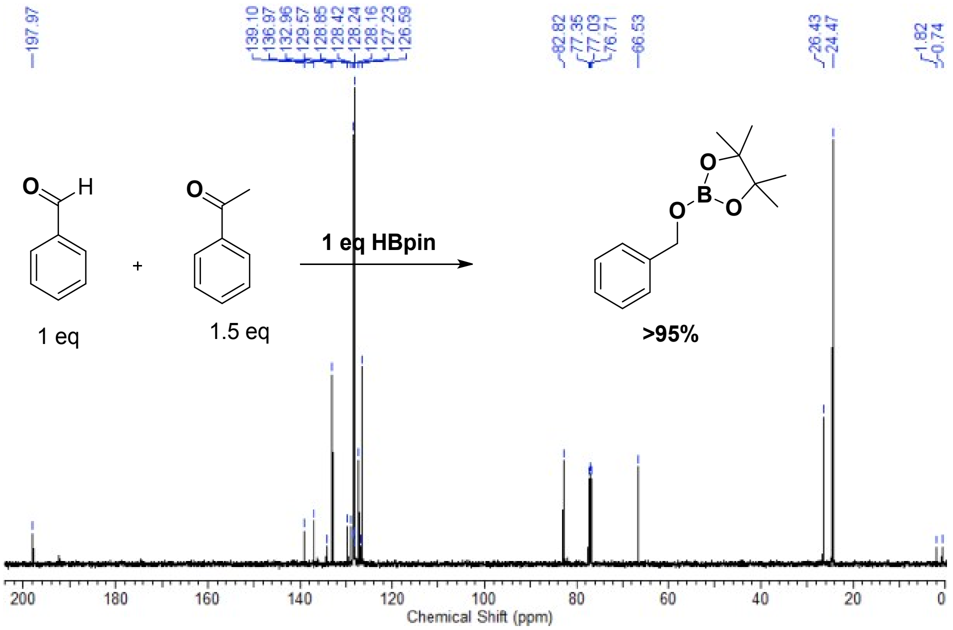

Figure FS98. ^{13}C NMR spectrum (100 MHz, 25°C, $CDCl_3$) Chemo selective reduction of aldehyde.

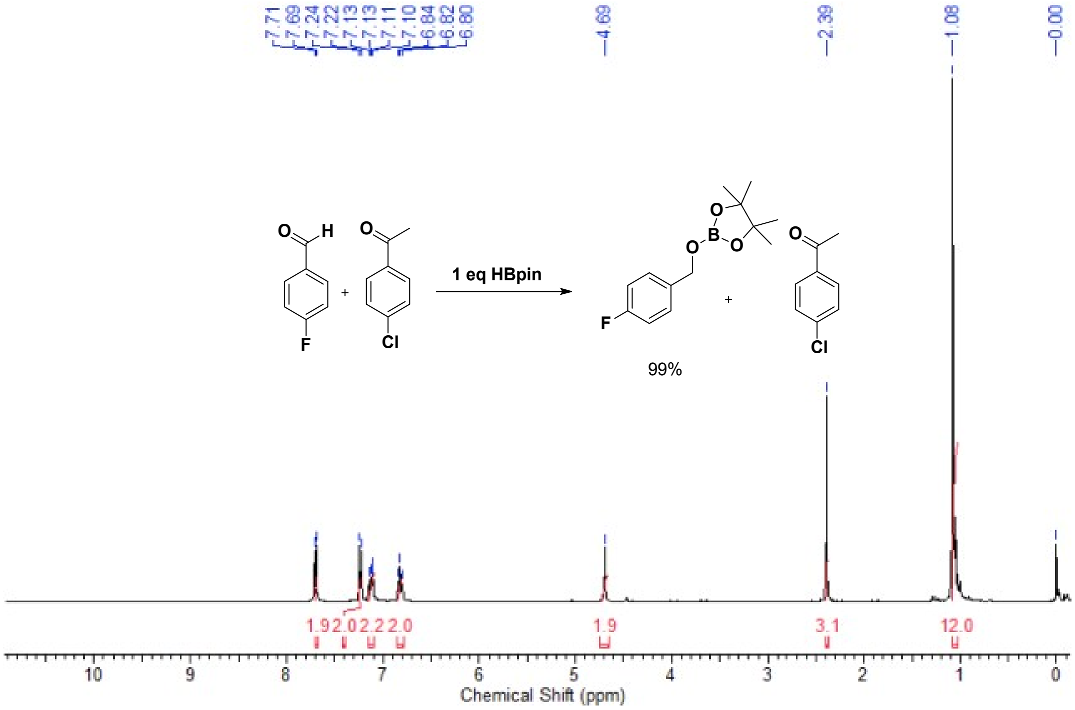

Figure FS99. ^{1}H NMR spectrum (128.4 MHz, 25°C, $CDCl_3$) of chemo selective reduction of aldehydes.

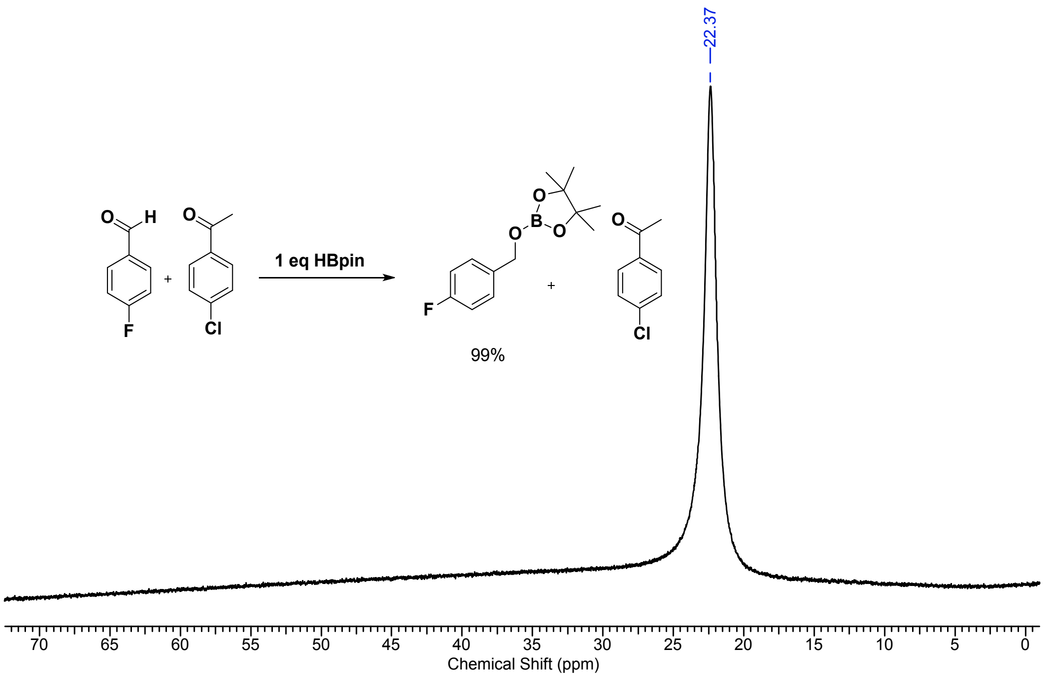

Figure FS100. ^{11}B NMR spectrum (128.4 MHz, 25°C, $CDCl_3$) of Chemo selective reduction of aldehydes**.**

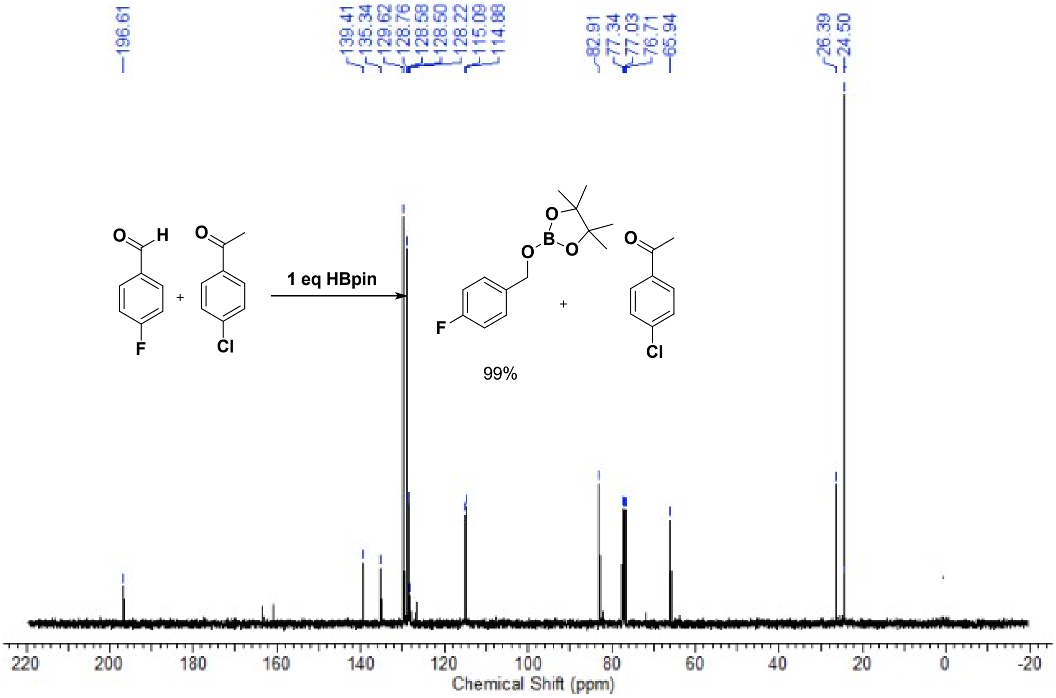

Figure FS101.^{13}C NMR spectrum (100 MHz, 25°C, $CDCl_3$) Chemo selective reduction of aldehyde**.**

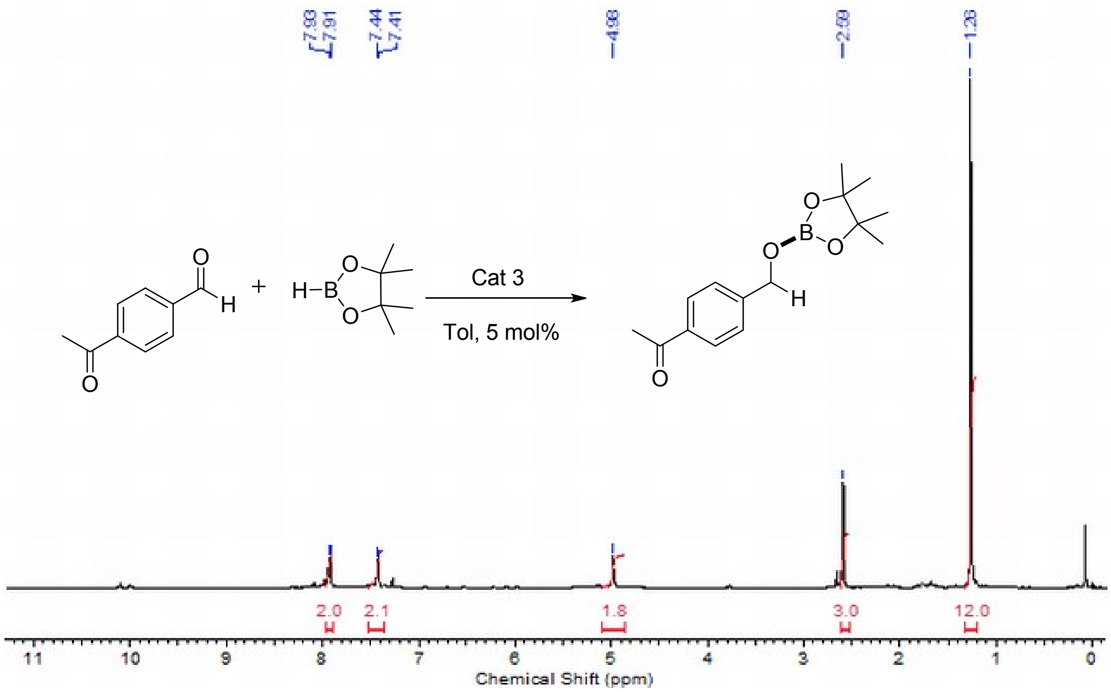

Figure FS102. ^{1}H NMR spectrum (128.4 MHz, 25°C, $CDCl_3$) of chemo selective reduction of aldehydes.

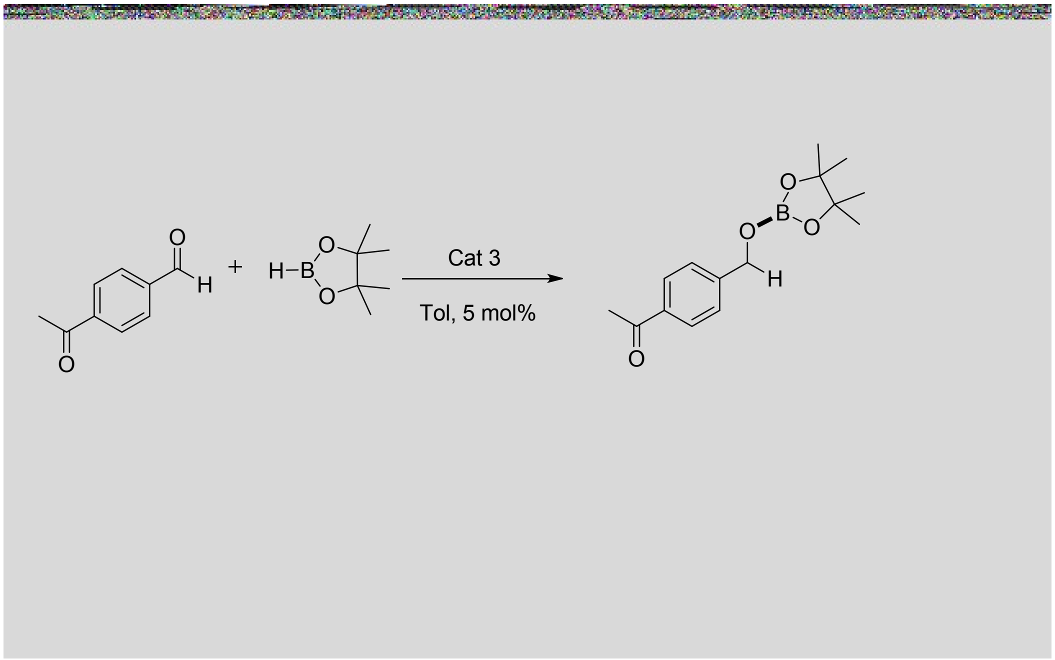

Figure FS103. ^{11}B NMR spectrum (128.4 MHz, 25°C, $CDCl_3$) of Chemo selective reduction of aldehydes**.**

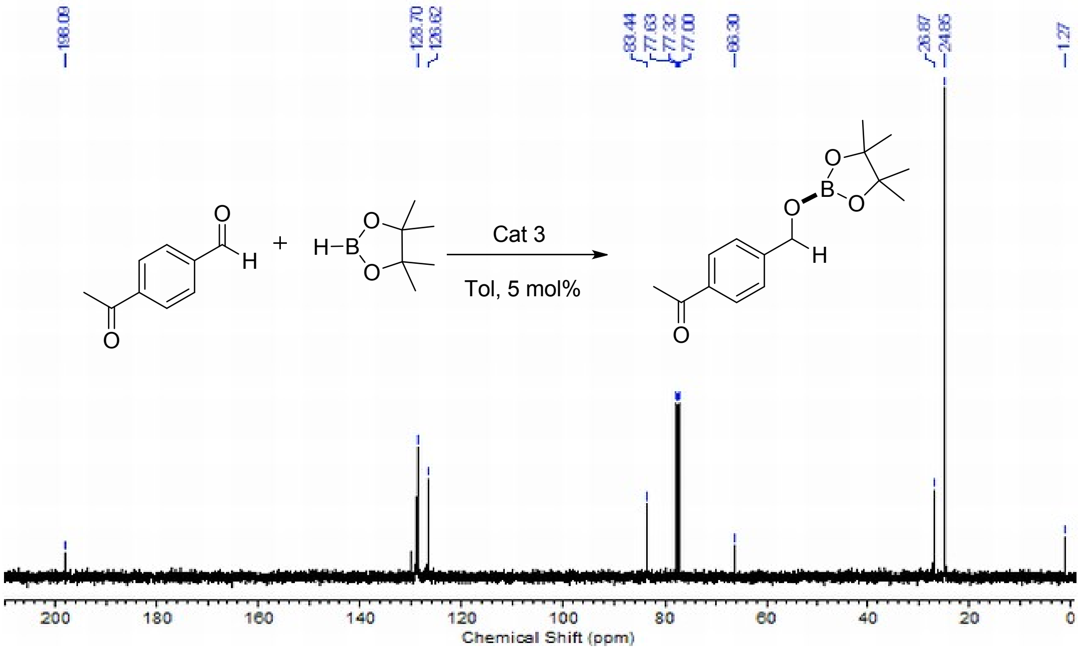

Figure FS104.^{13}C NMR spectrum (100 MHz, 25°C, $CDCl_3$) Chemo selective reduction of aldehyde**.**

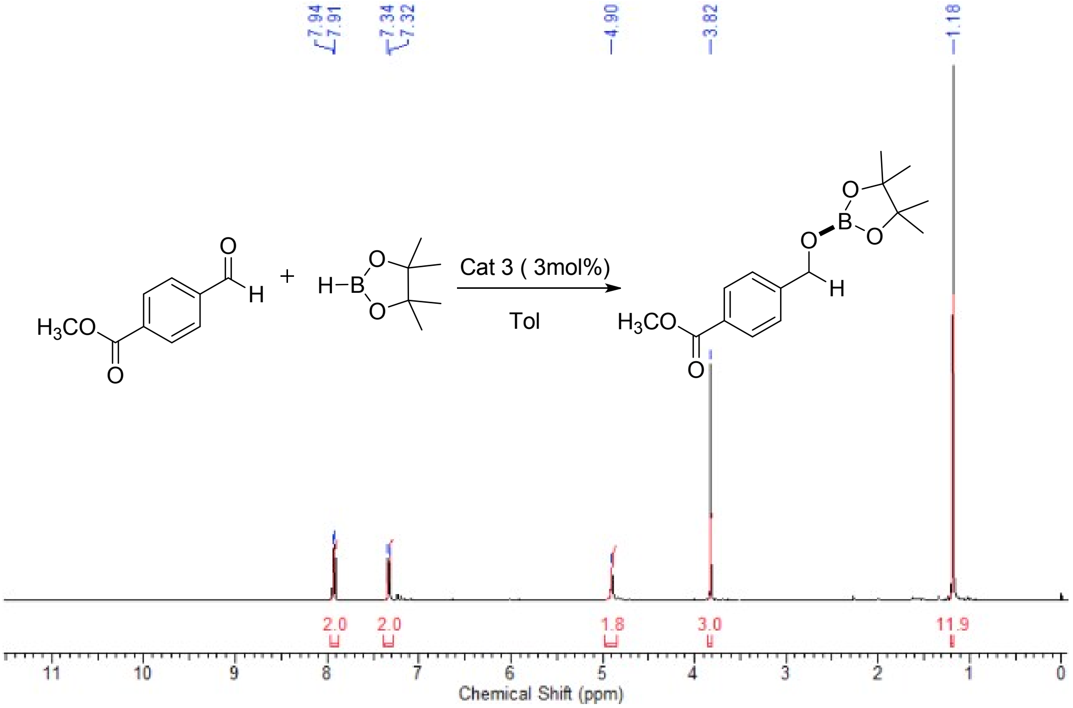

Figure FS105.^{1}H NMR spectrum (128.4 MHz, 25°C, $CDCl_3$) of chemo selective reduction of aldehydes.

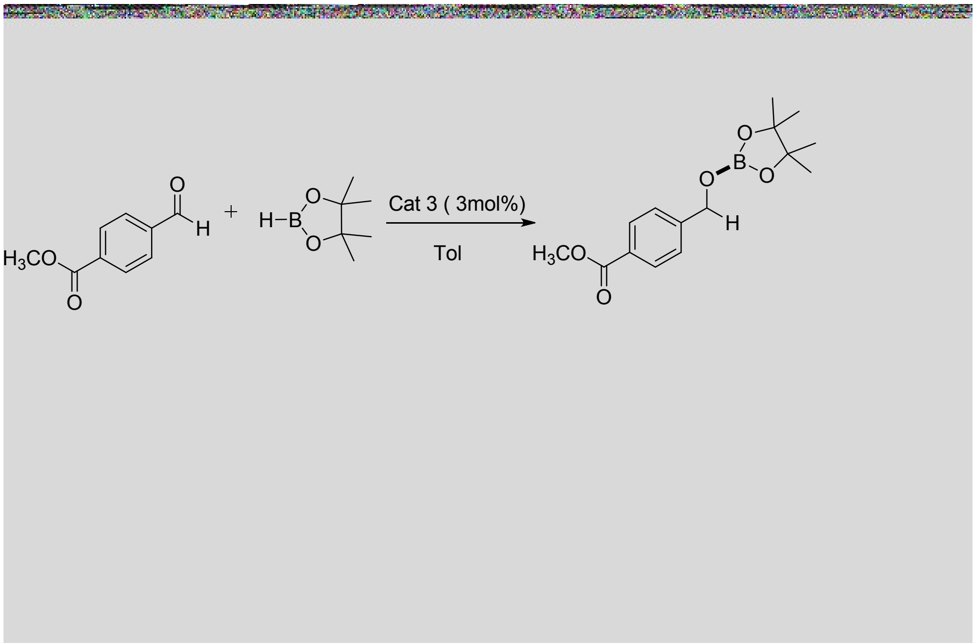

Figure FS106. ^{11}B NMR spectrum (128.4 MHz, 25°C, CDCl$_3$) of Chemo selective reduction of aldehydes**.**

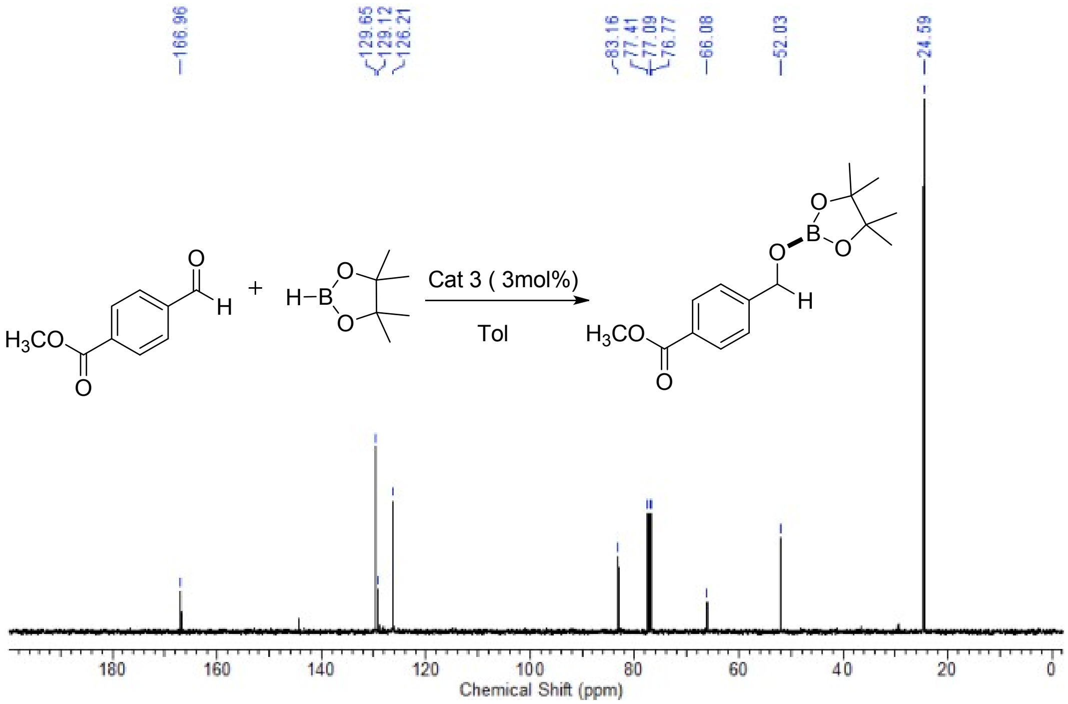

Figure FS107.^{13}C NMR spectrum (100 MHz, 25°C, CDCl$_3$) Chemo selective reduction of aldehyde**.**

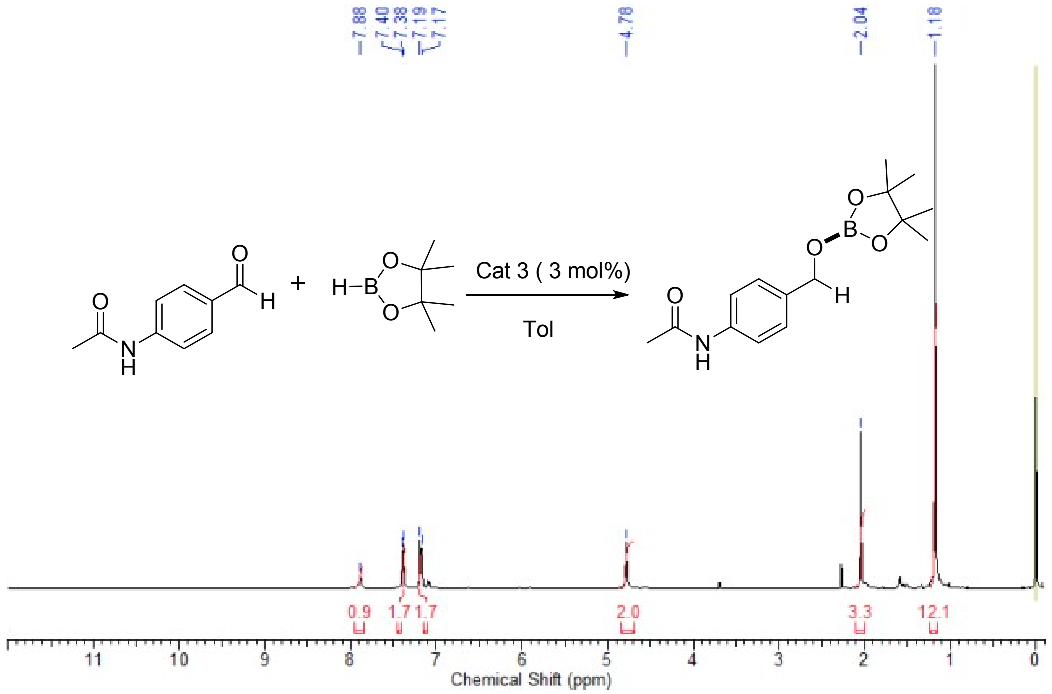

Figure FS108. ^{1}H NMR spectrum (128.4 MHz, 25°C, CDCl$_3$) of chemo selective reduction of aldehydes.

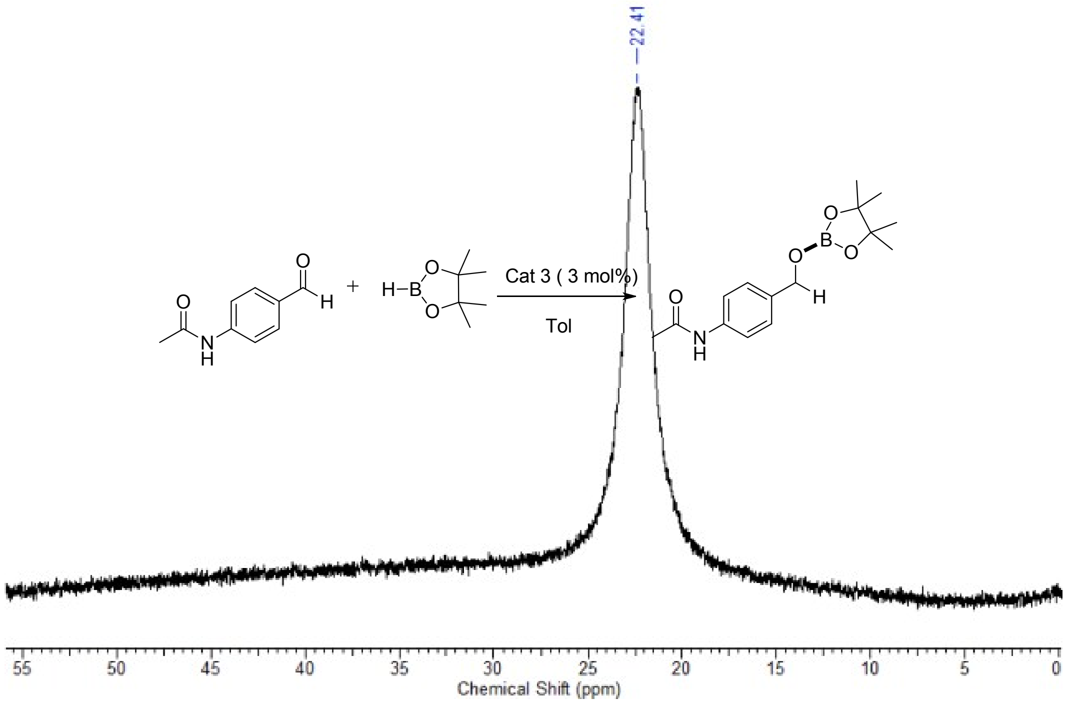

Figure FS109. ^{11}B NMR spectrum (128.4 MHz, 25°C, CDCl$_3$) of Chemo selective reduction of aldehydes.

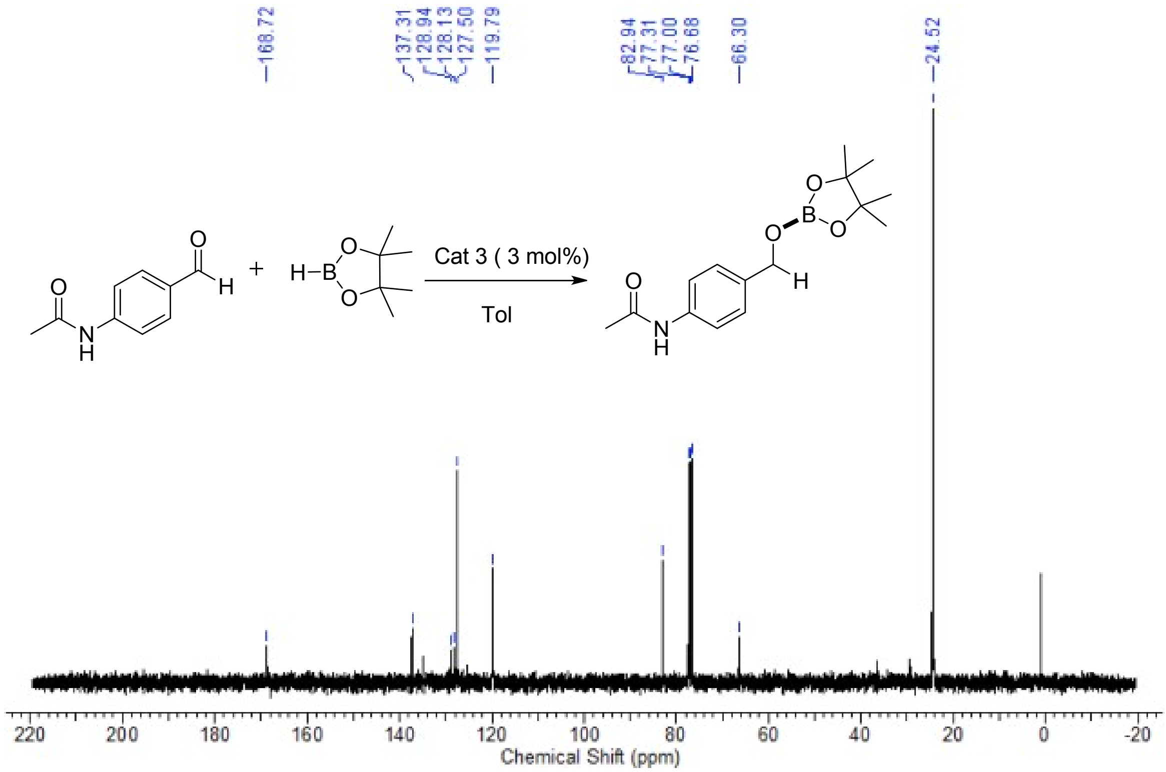

Figure FS110. ^{13}C NMR spectrum (100 MHz, 25°C, $CDCl_3$) Chemo selective reduction of aldehyde.

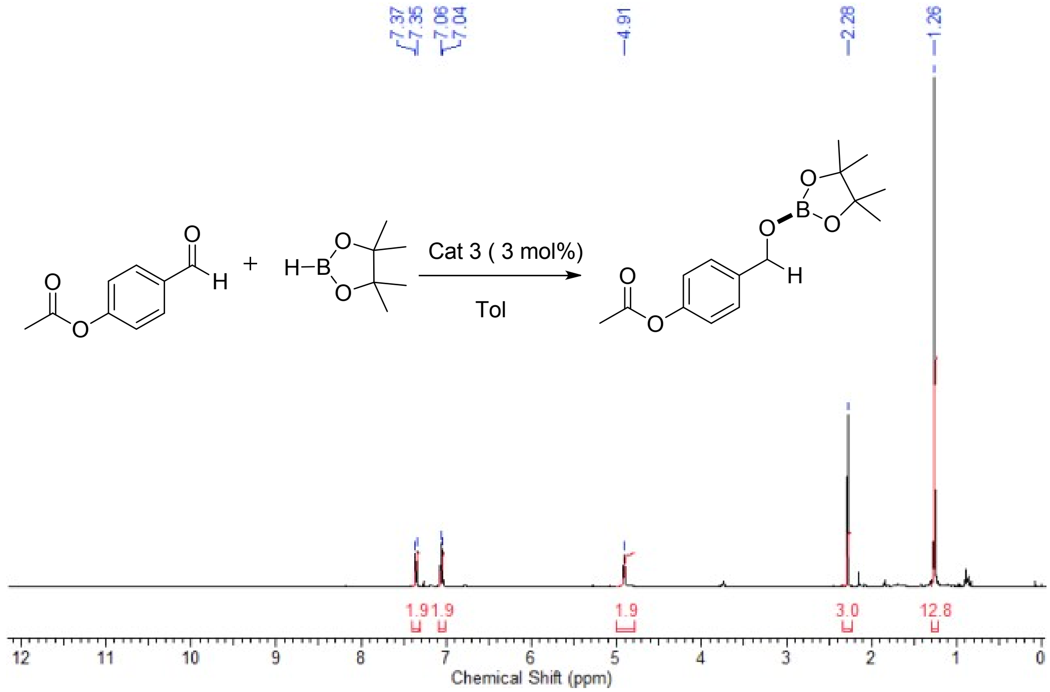

Figure FS111. ^{1}H NMR spectrum (128.4 MHz, 25°C, $CDCl_3$) of chemo selective reduction of aldehydes.

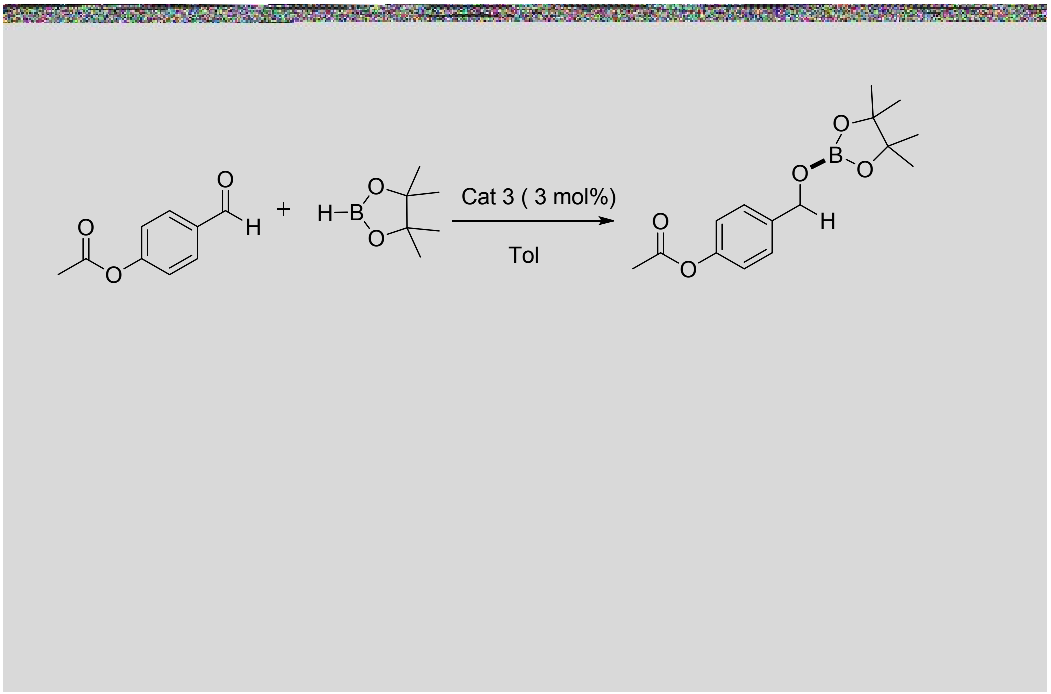

Figure FS112. ^{11}B NMR spectrum (128.4 MHz, 25°C, $CDCl_3$) of Chemo selective reduction of aldehydes**.**

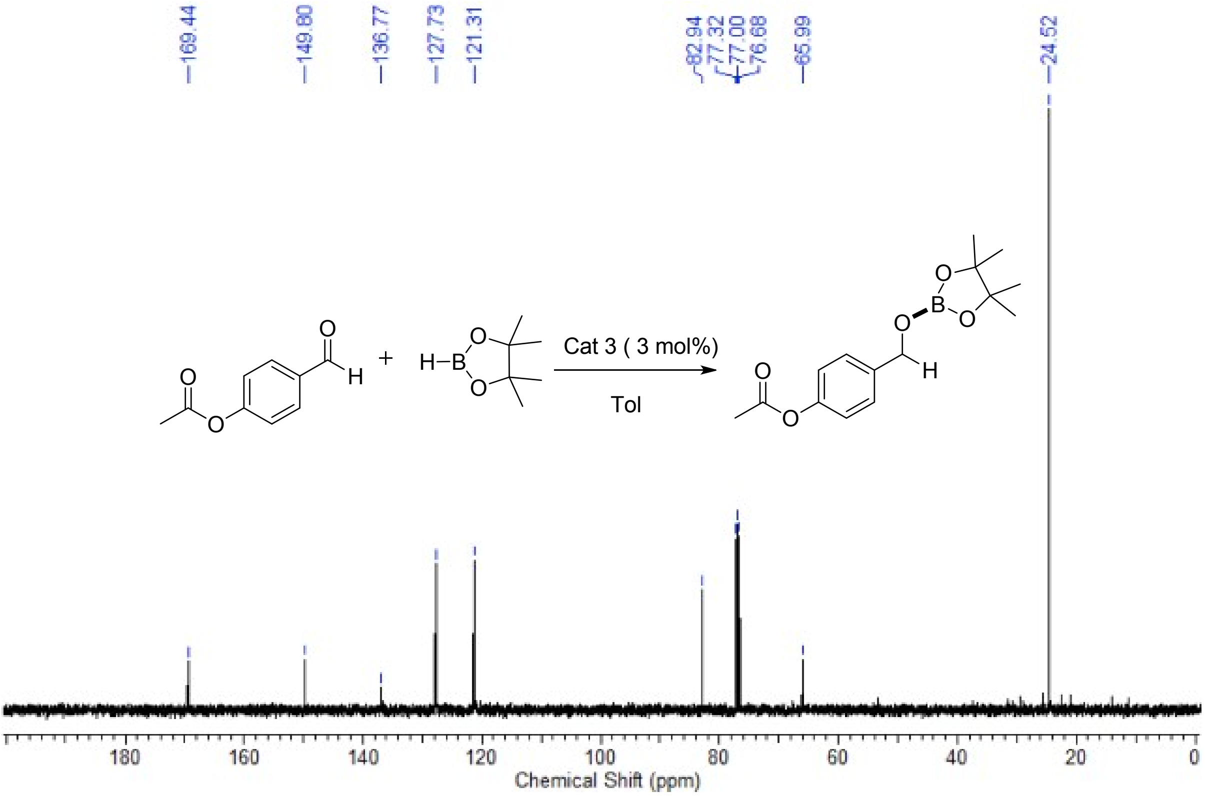

Figure FS113.^{13}C NMR spectrum (100 MHz, 25°C, $CDCl_3$) Chemo selective reduction of aldehyde**.**

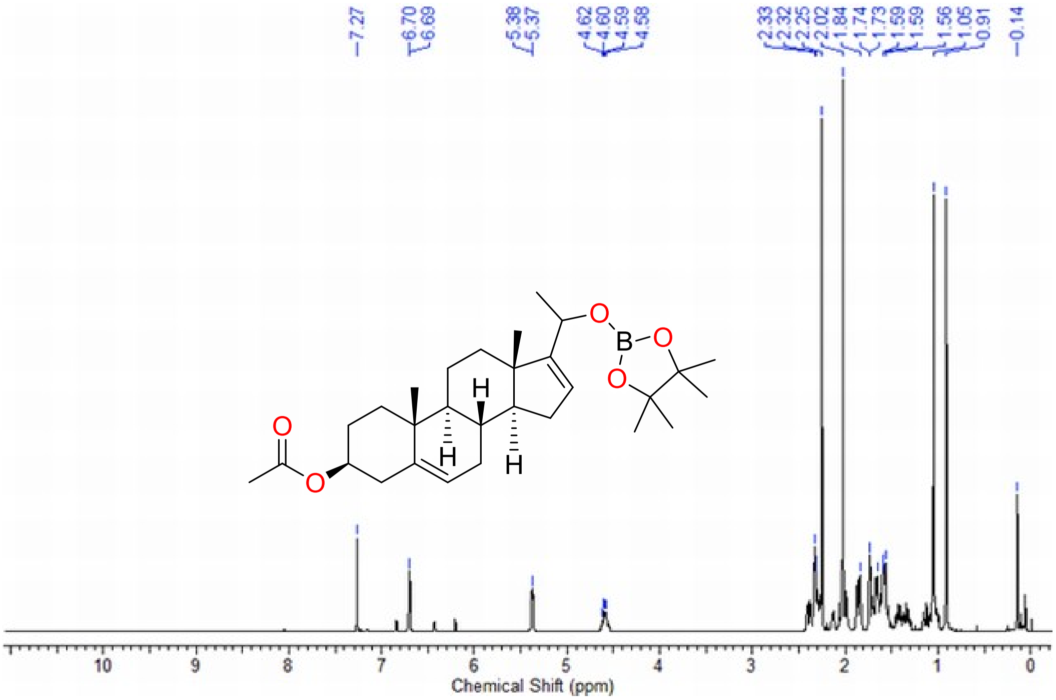

Figure FS114.^{1}H NMR spectrum (128.4 MHz, 25°C, $CDCl_3$) of chemo selective reduction of 16-dehydropregnolone acetate.

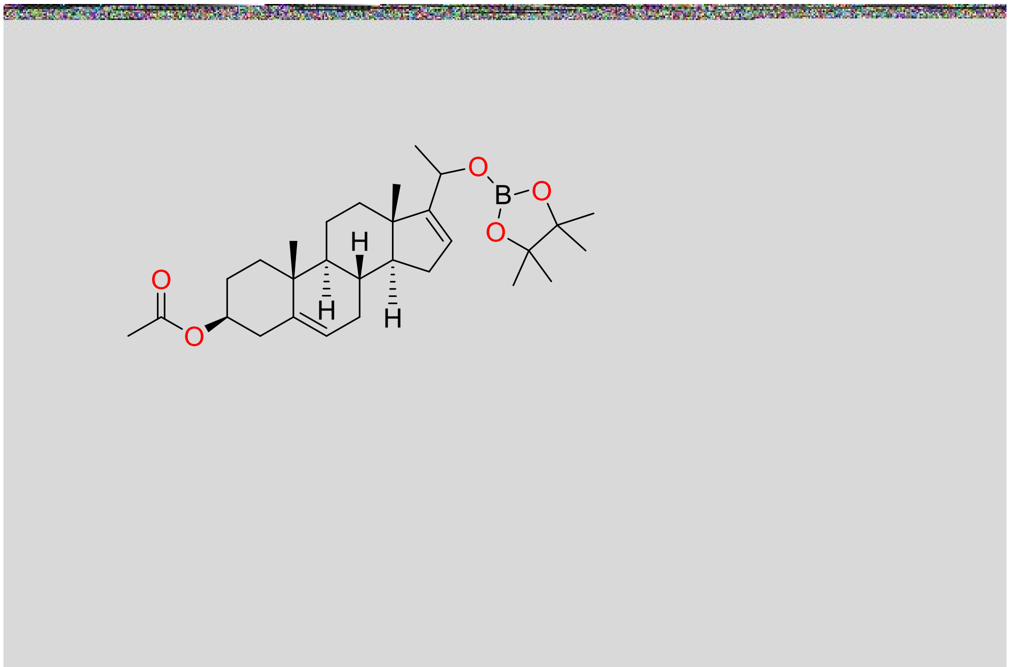

Figure FS115. ^{11}B NMR spectrum (128.4 MHz, 25°C, $CDCl_3$) of Chemo selective reduction of 16-dehydropregnolone acetate.

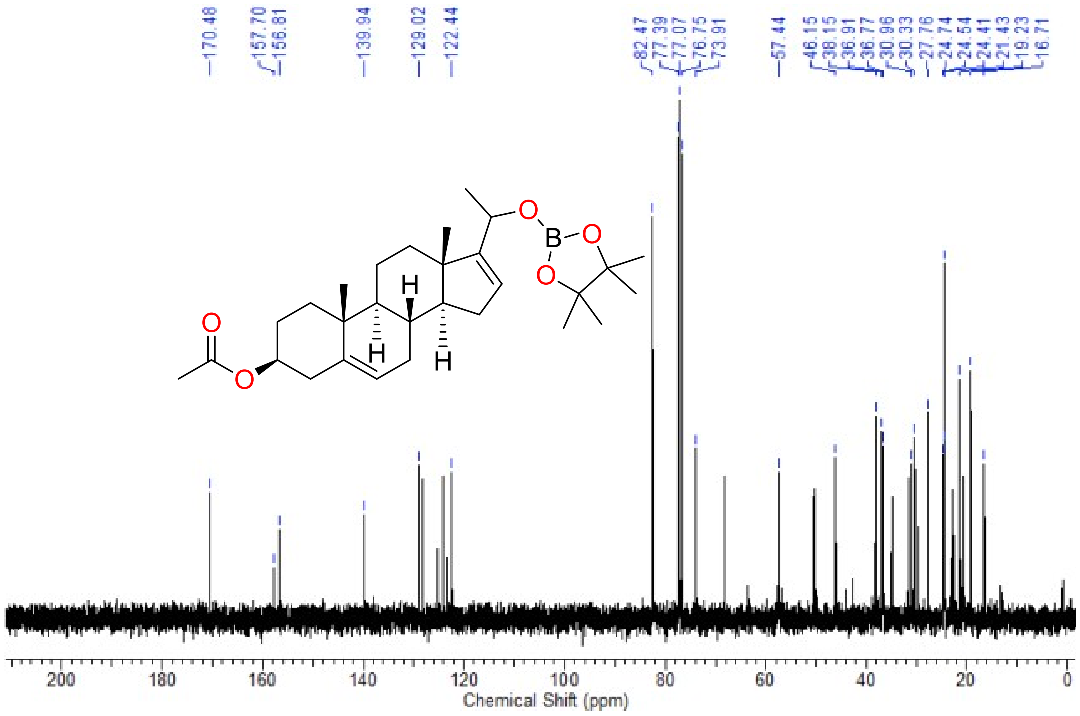

Figure FS116.^{13}C NMR spectrum (100 MHz, 25°C, CDCl$_3$) Chemo selective reduction 16-dehydropregnolone acetate.

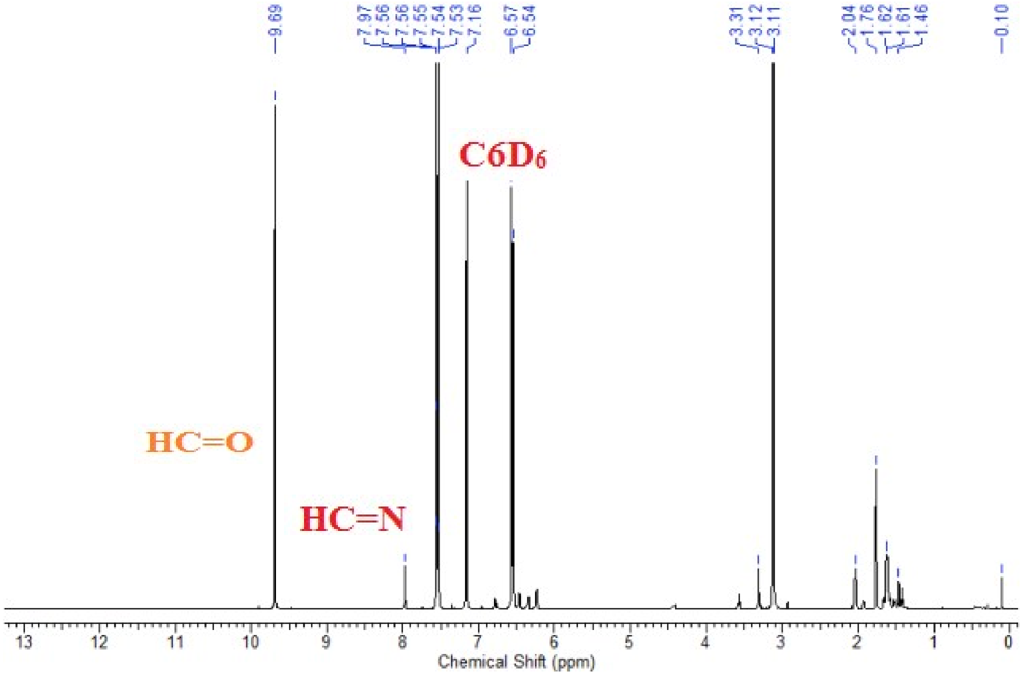

Figure **FS117.**^{1}H NMR spectrum (128.4 MHz, 25°C, CDCl$_3$) of complex **3** in presence of excess *p*-OMe Benzaldehyde

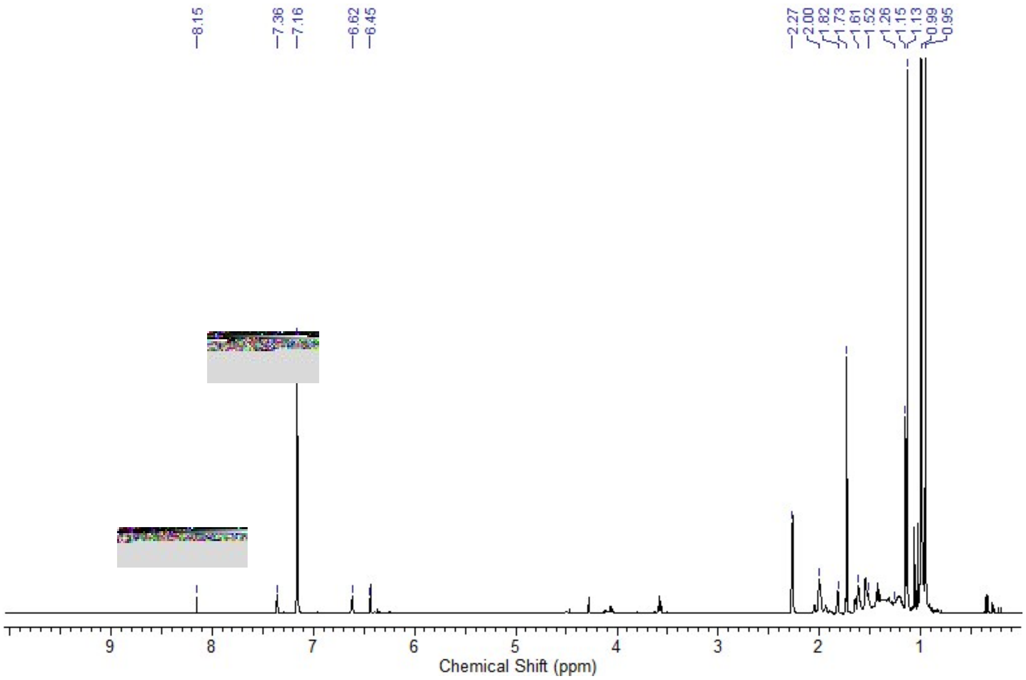

Figure **FS118.**^{1}H NMR spectrum (128.4 MHz, 25°C, $CDCl_3$) of complex **3** in presence of excess HBpin.

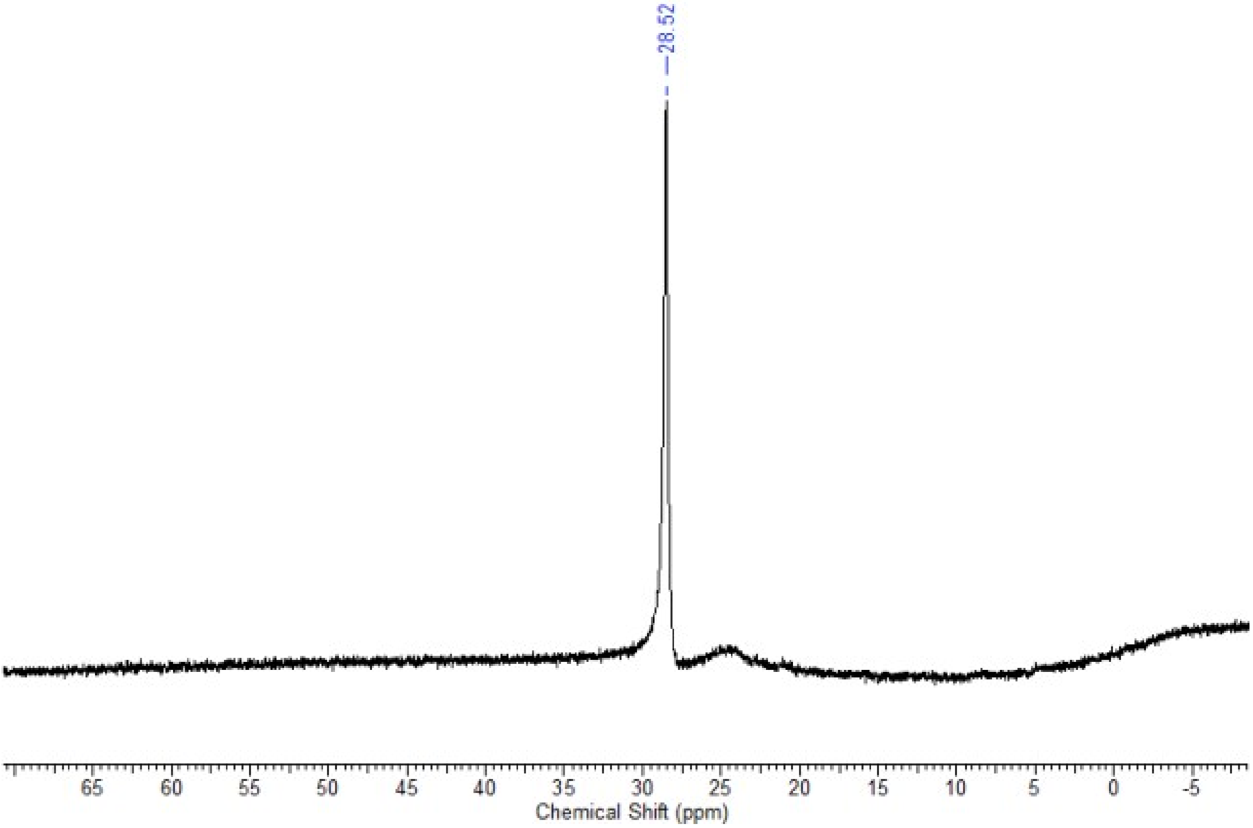

Figure FS119. ^{11}B NMR spectrum (128.4 MHz, 25°C, $CDCl_3$) of complex **3** in presence of excess HBpin.

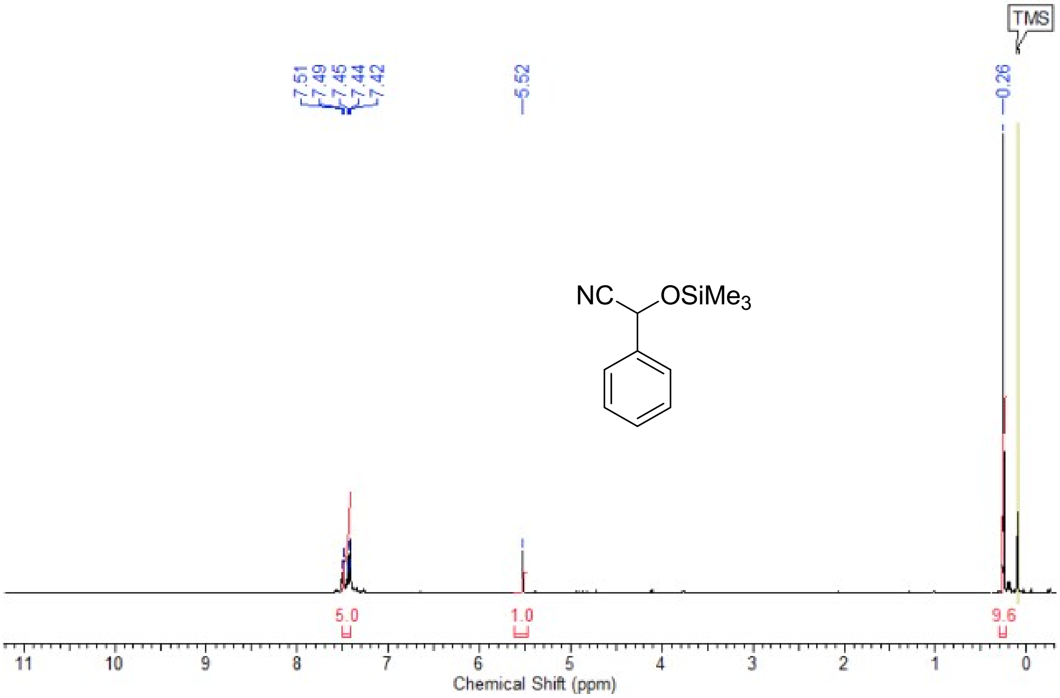

Figure FS120. ^1H NMR spectrum (400 MHz, 25°C, $CDCl_3$) of 2-phenyl-2 ((trimethylsilyl)oxy)acetonitrile.

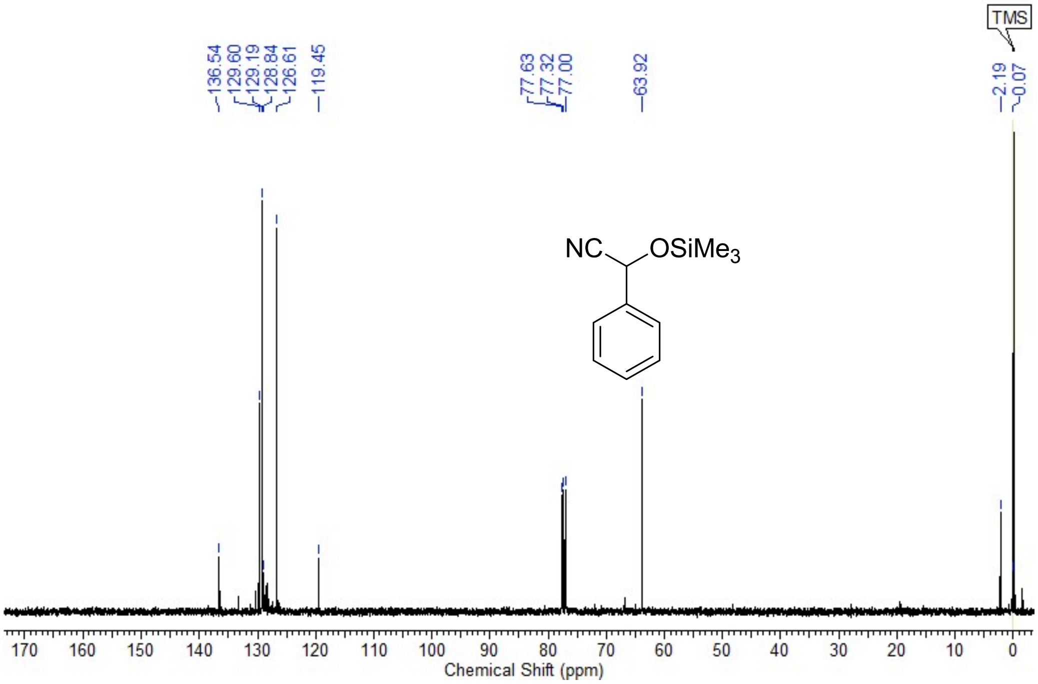

Figure FS121. ^{13}C NMR spectrum (100 MHz, 25°C, $CDCl_3$) of 2-phenyl-2-((trimethylsilyl)oxy)acetonitrile.

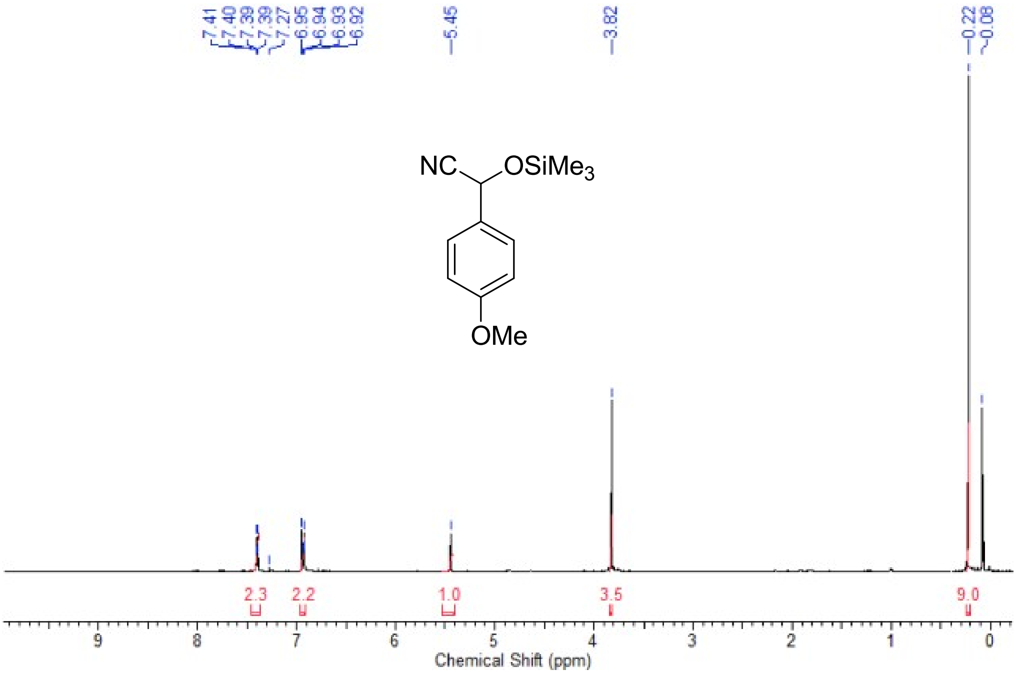

Figure FS122. ^{1}H NMR spectrum (400 MHz, 25°C, $CDCl_3$) of 2-(4-methoxyphenyl)-2-((trimethylsilyl)oxy)acetonitrile.

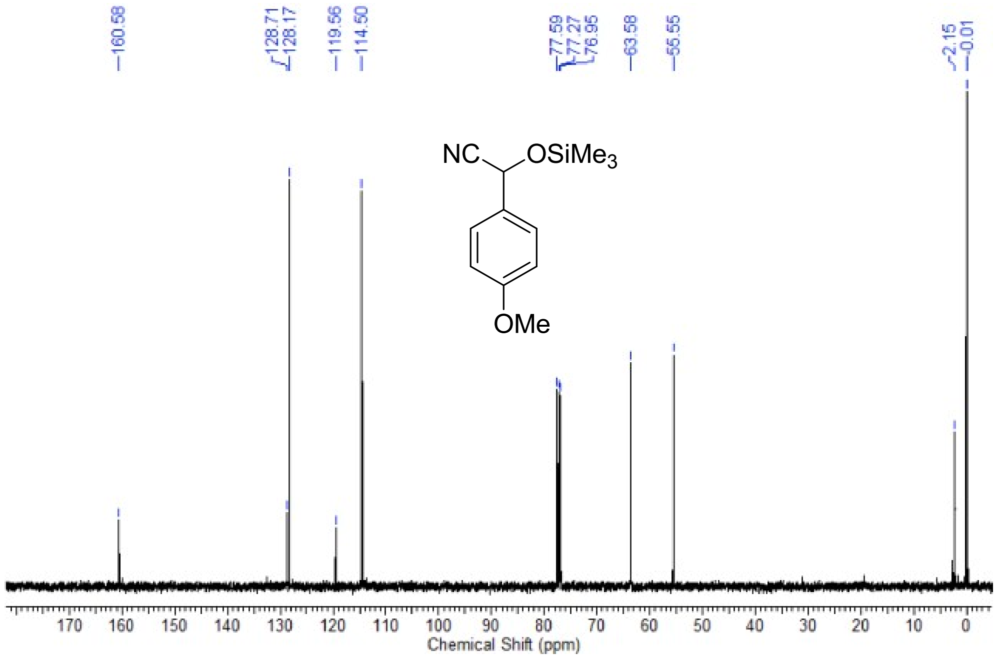

Figure FS123. ^{13}C NMR spectrum (100 MHz, 25°C, $CDCl_3$) of 2-(4-methoxyphenyl)-2-((trimethylsilyl)oxy)acetonitrile.

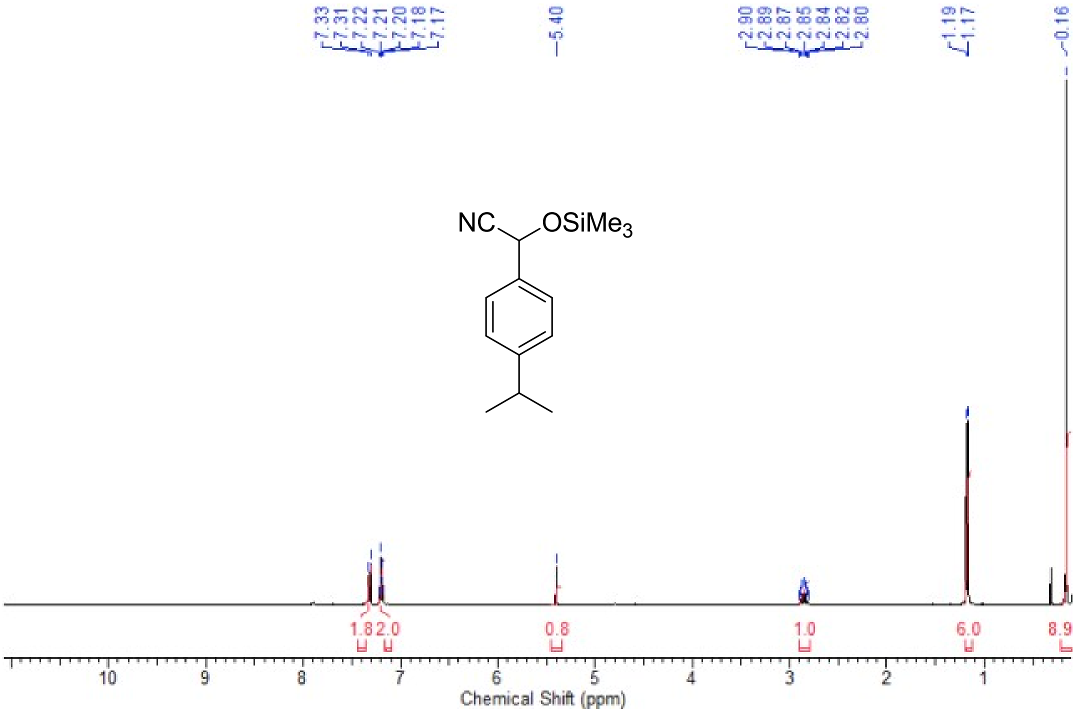

Figure FS124. ^{1}H NMR spectrum (400 MHz, 25°C, $CDCl_3$) of 2-(4-isopropylphenyl)-2-((trimethylsilyl)oxy)acetonitrile.

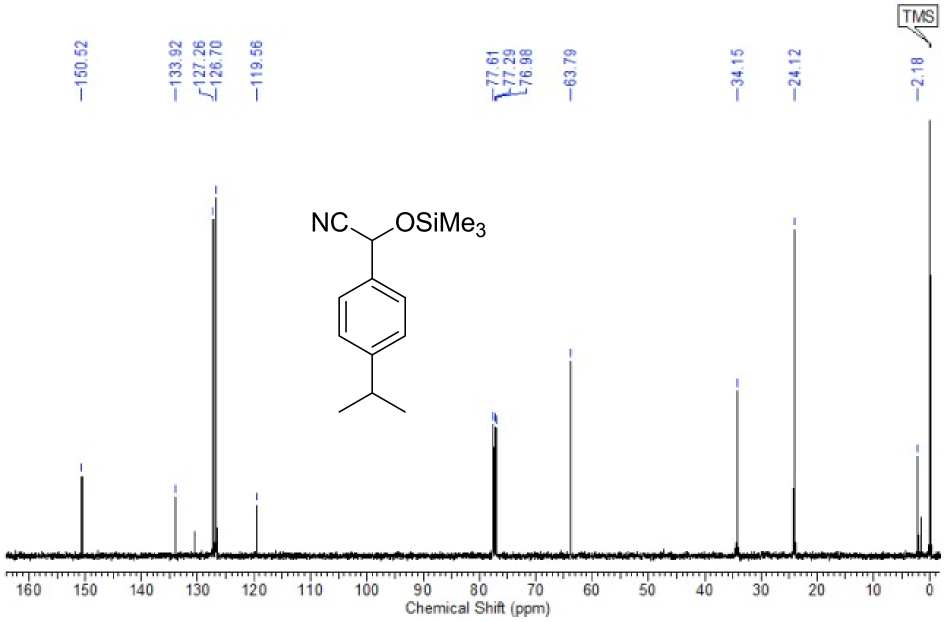

Figure FS125. ^{13}C NMR spectrum (100 MHz, 25°C, $CDCl_3$) of 2-(4-isopropylphenyl)-2-((trimethylsilyl)oxy)acetonitrile.

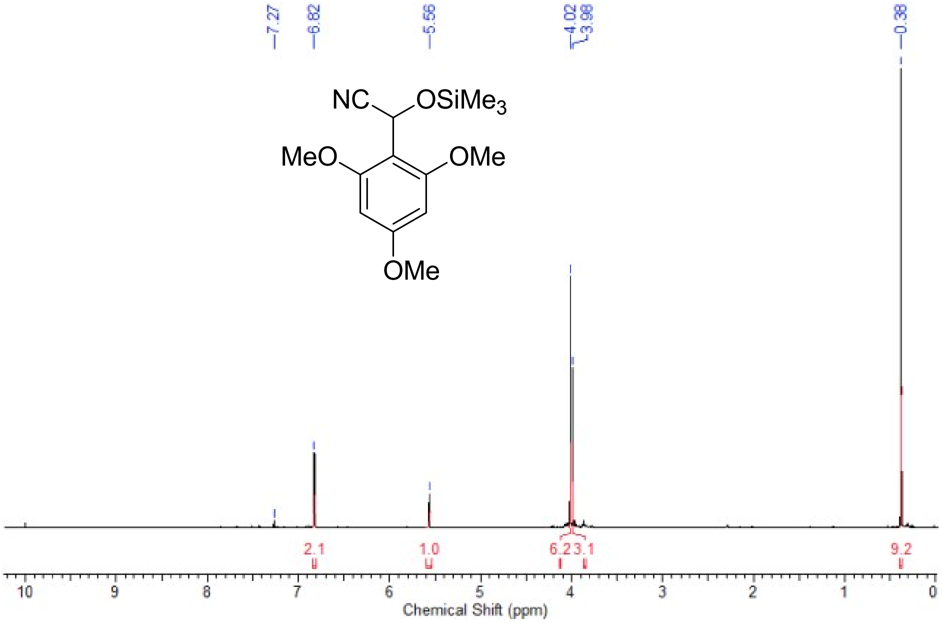

Figure FS126. ^{1}H NMR spectrum (400 MHz, 25°C, $CDCl_3$) of 2-(2,4,6-trimethoxyphenyl)-2-((trimethylsilyl)oxy)acetonitrile.

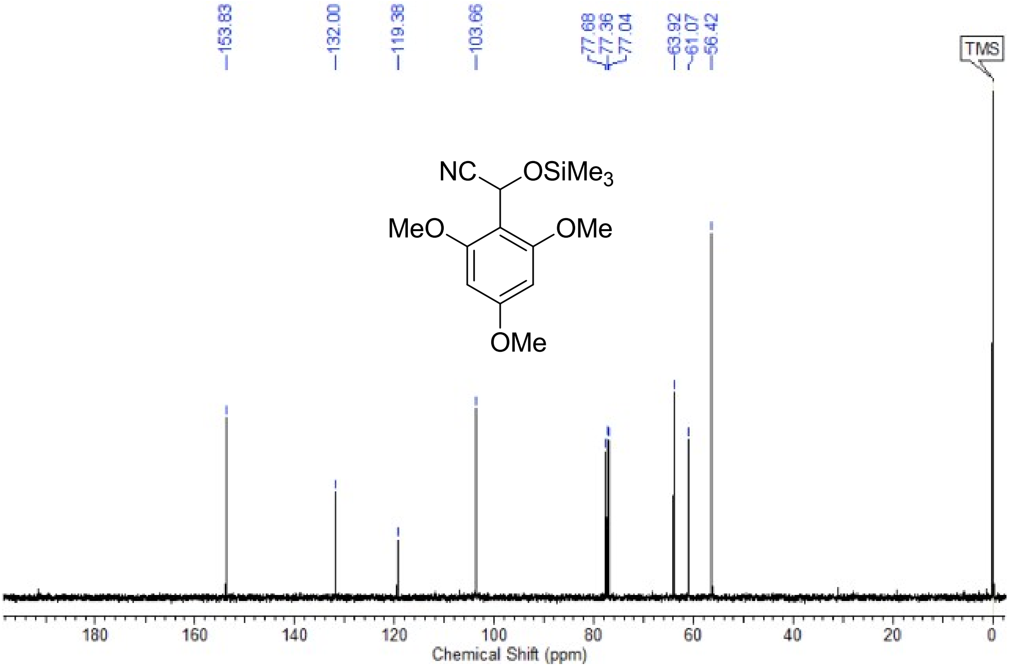

Figure FS127. ^{13}C NMR spectrum (100 MHz, 25°C, $CDCl_3$) of 2-(2,4,6-trimethoxyphenyl)-2-((trimethylsilyl)oxy)acetonitrile.

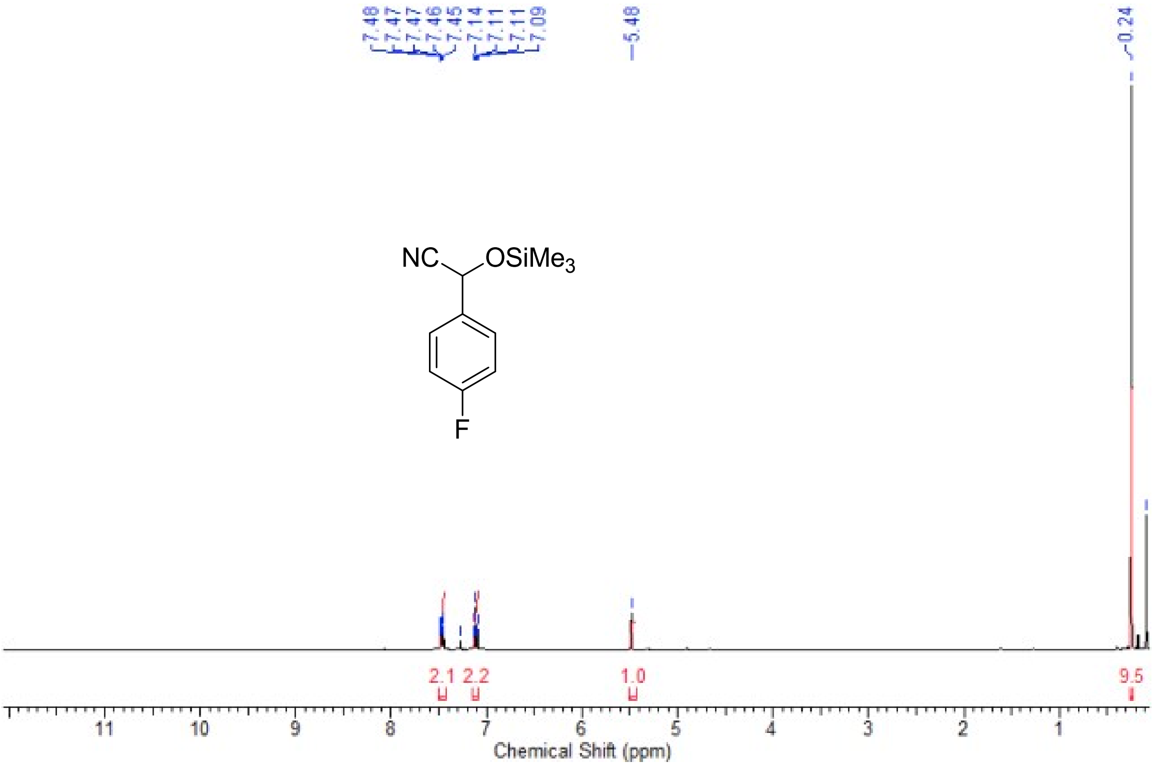

Figure FS128. ^{1}H NMR spectrum (400 MHz, 25°C, $CDCl_3$) of 2-(4-fluorophenyl)-2-((trimethylsilyl)oxy)acetonitrile.

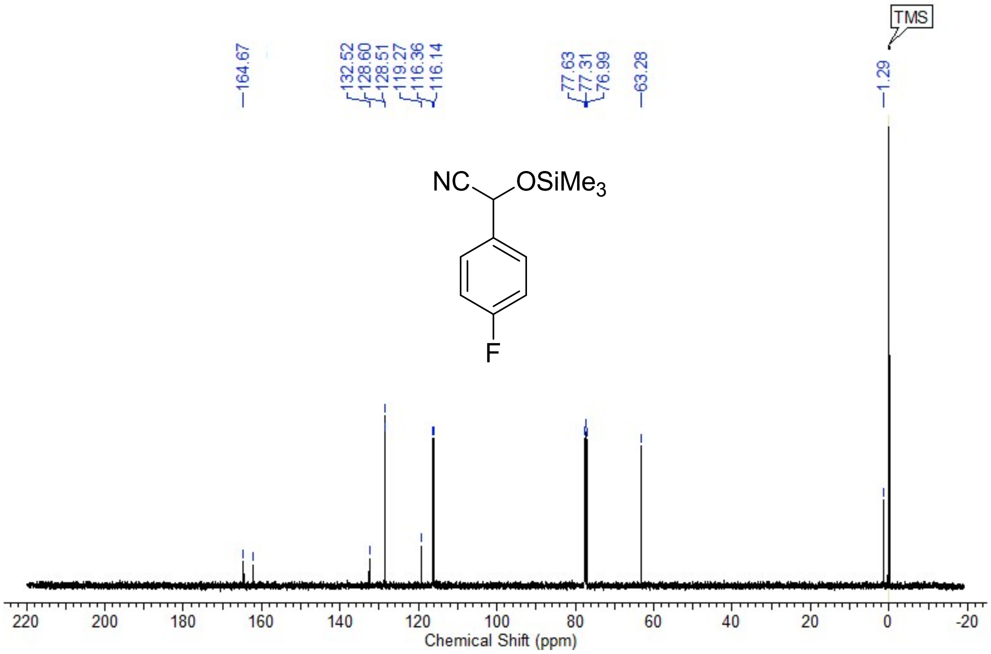

Figure FS129. ^{13}C NMR spectrum (100 MHz, 25°C, $CDCl_3$) of 2-(4-fluorophenyl)-2-((trimethylsilyl)oxy)acetonitrile.

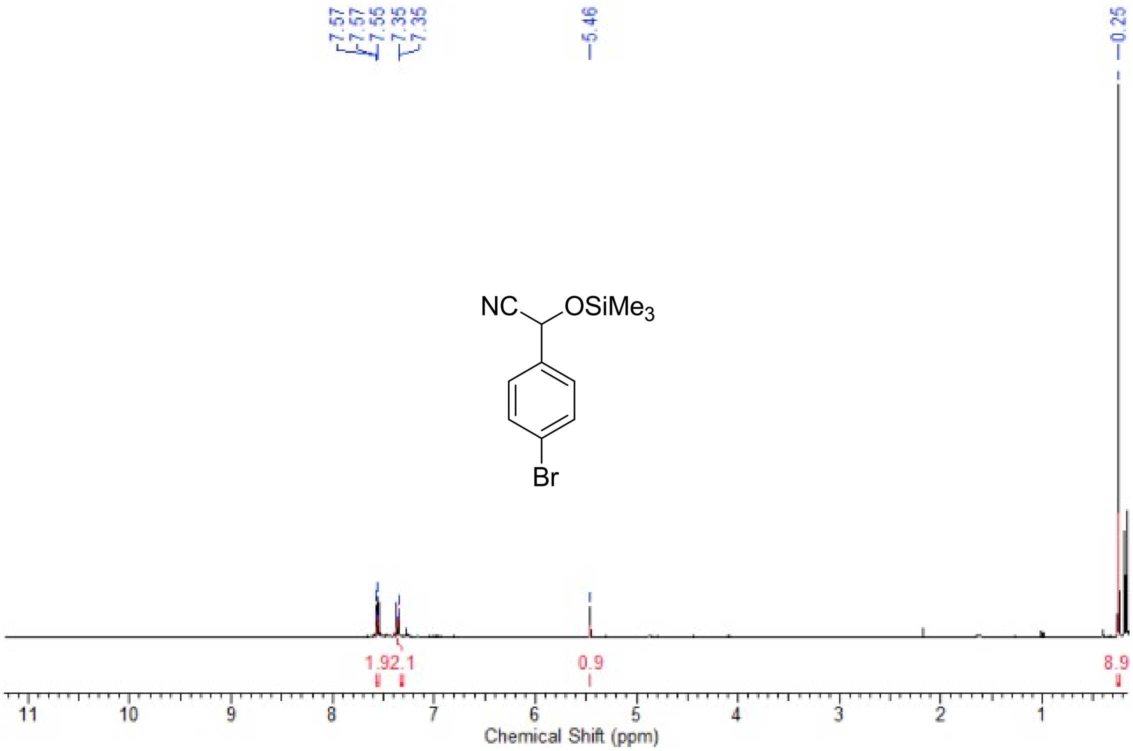

Figure FS130. ^{1}H NMR spectrum (400 MHz, 25°C, $CDCl_3$) of 2-(4-bromophenyl)-2-((trimethylsilyl)oxy)acetonitrile.

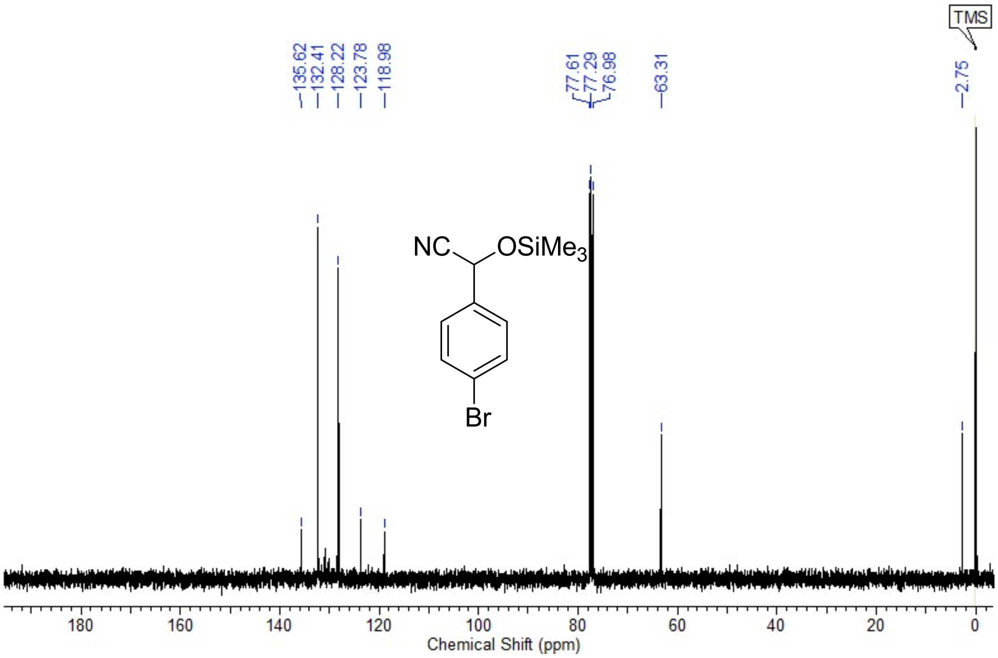

Figure FS131. ^{13}C NMR spectrum (100 MHz, 25°C, $CDCl_3$) of 2-(4-bromophenyl)-2-((trimethylsilyl)oxy)acetonitrile.

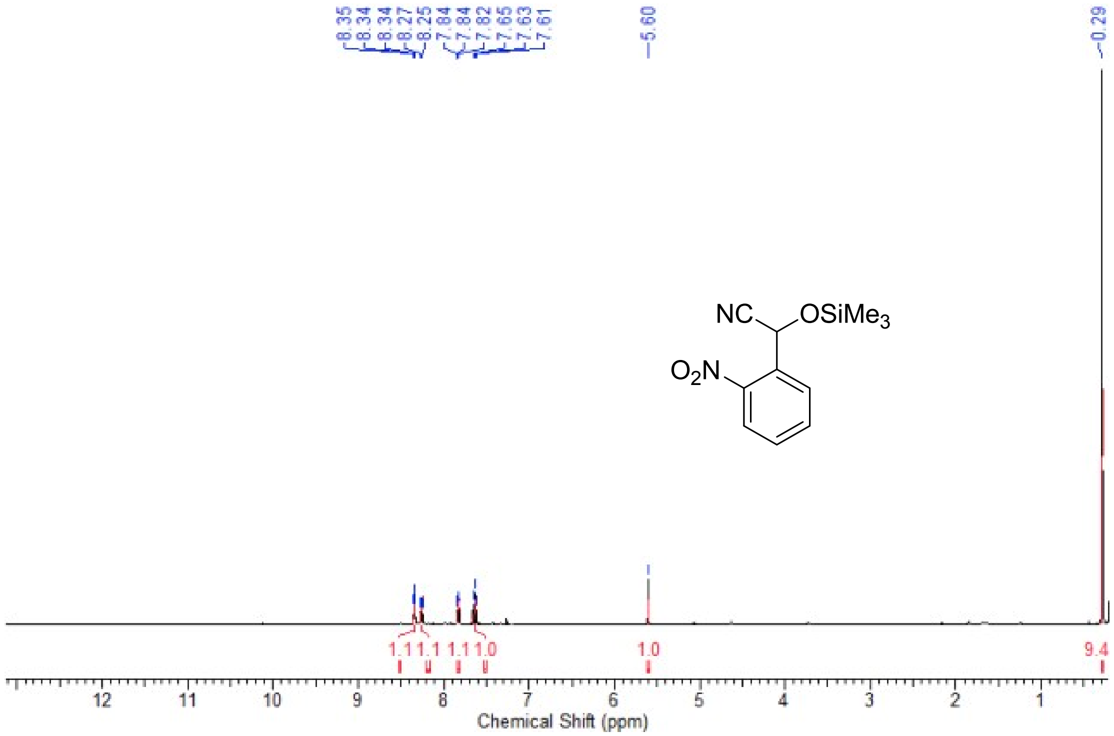

Figure FS132. ^{1}H NMR spectrum (400 MHz, 25°C, $CDCl_3$) of 2-(2-nitrophenyl)-2-((trimethylsilyl)oxy)acetonitrile.

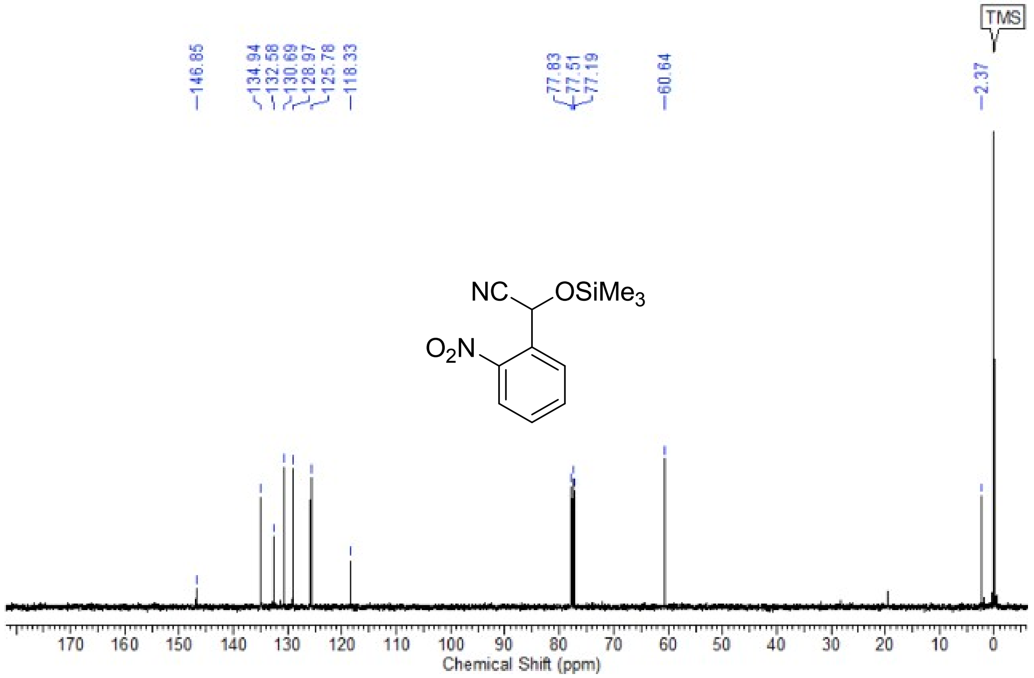

Figure FS133. ^{13}C NMR spectrum (100 MHz, 25°C, $CDCl_3$) of 2-(2-nitrophenyl)-2-((trimethylsilyl)oxy)acetonitrile.

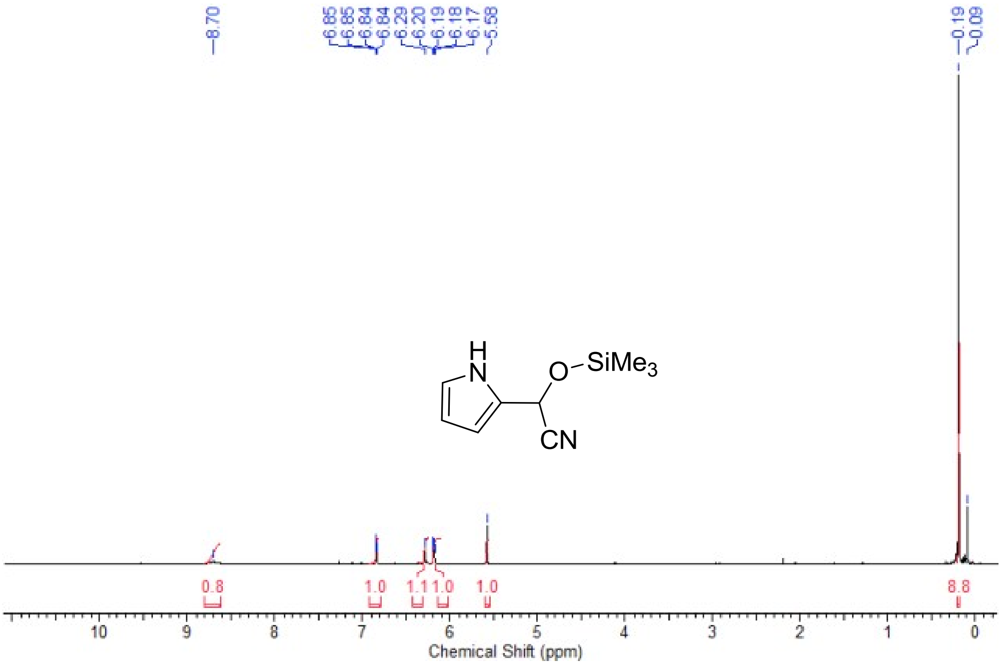

Figure FS134. ^{1}H NMR spectrum (400 MHz, 25°C, $CDCl_3$) of 2-(1H-pyrrol-2-yl)-2-((trimethylsilyl)oxy)acetonitrile.

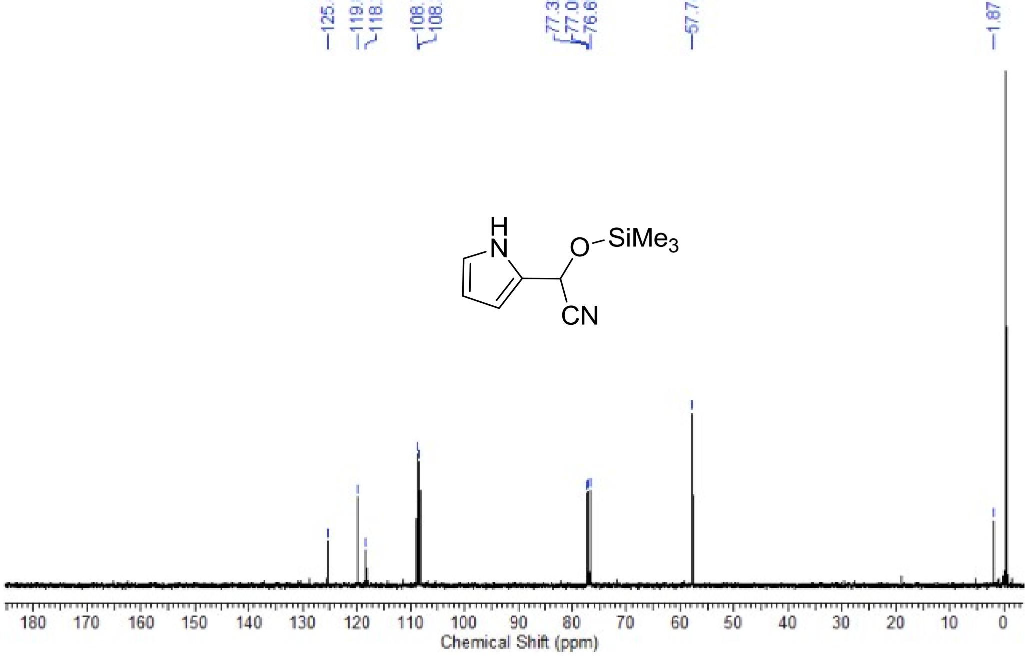

Figure FS135. ^{13}C NMR spectrum (100 MHz, 25°C, $CDCl_3$) of 2-(1H-pyrrol-2-yl)-2-((trimethylsilyl)oxy)acetonitrile.

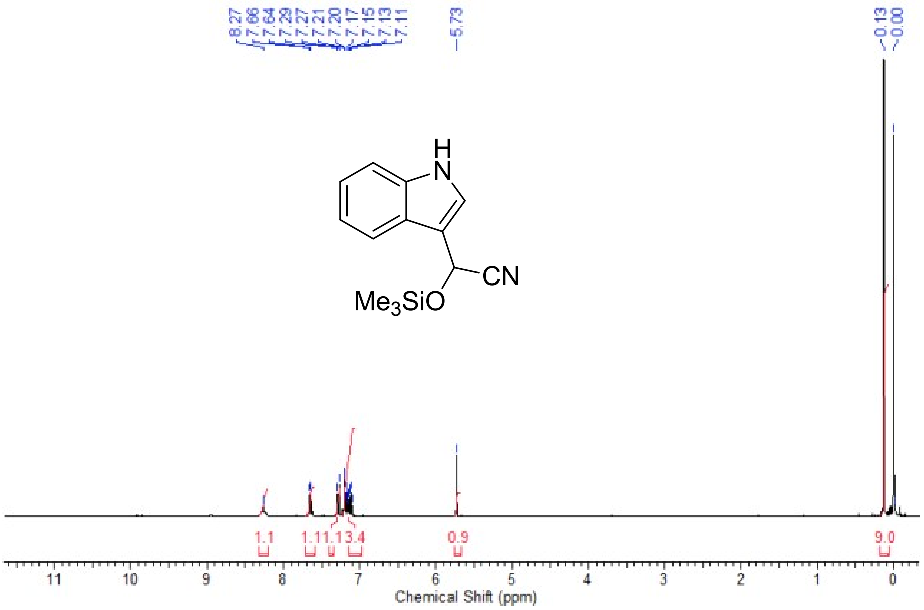

Figure FS136. ^{1}H NMR spectrum (400 MHz, 25°C, $CDCl_3$) of 2-(1H-indol-3-yl)-2-((trimethylsilyl)oxy)acetonitrile.

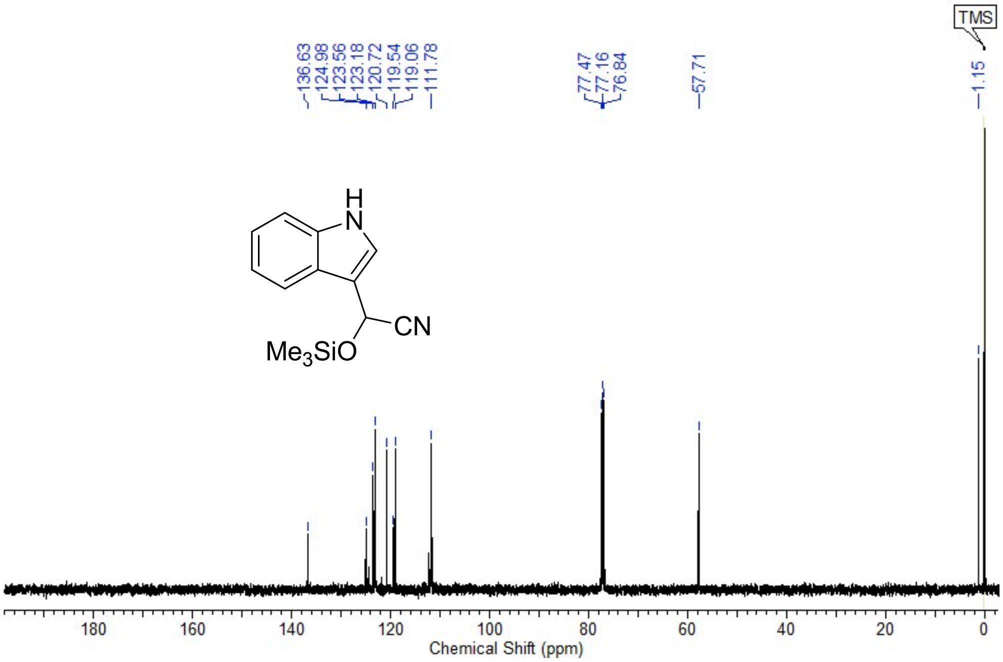

Figure FS137. ^{13}C NMR spectrum (100 MHz, 25°C, $CDCl_3$) of 2-(1H-indol-3-yl)-2-((trimethylsilyl)oxy)acetonitrile.

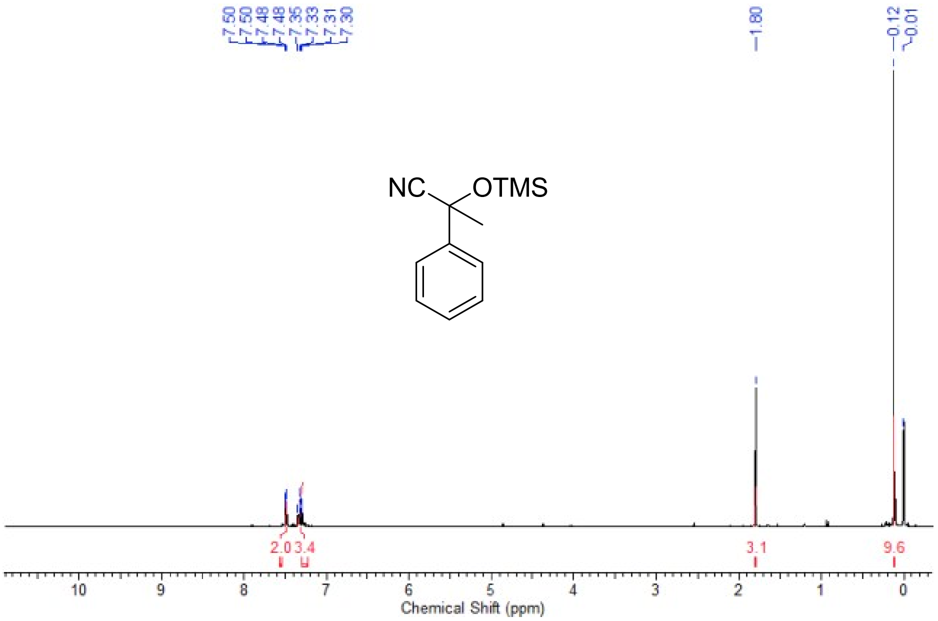

Figure FS138. ^{1}H NMR spectrum (400 MHz, 25°C, CDCl$_3$) of 2-phenyl-2-((trimethylsilyl)oxy)propanenitrile

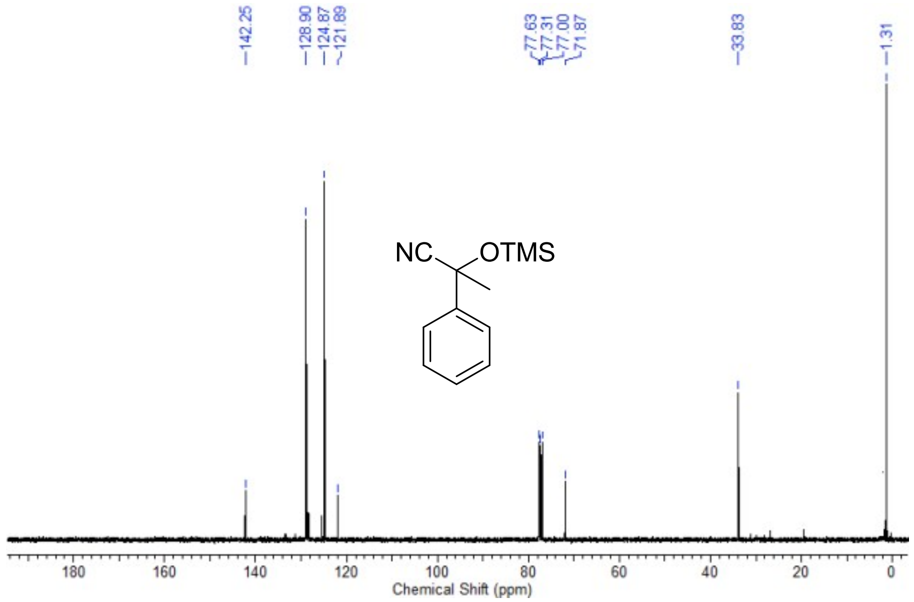

Figure FS139. ^{13}C NMR spectrum (100 MHz, 25°C, CDCl$_3$) of 2-phenyl-2-((trimethylsilyl)oxy)propanenitrile.

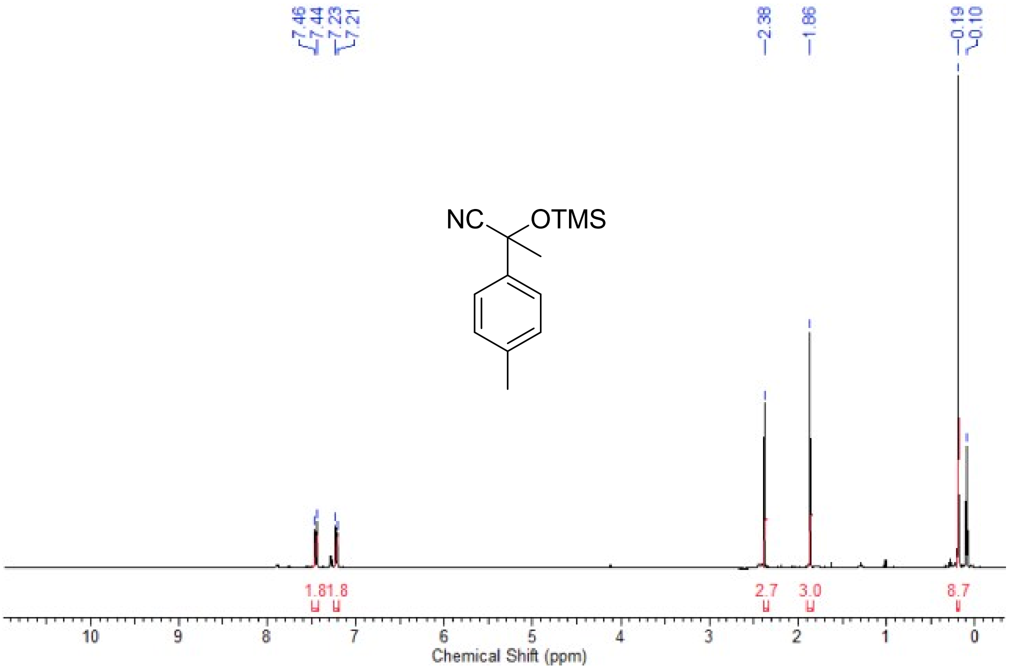

Figure FS140. ^{1}H NMR spectrum (400 MHz, 25°C, $CDCl_3$) of 2-(p-tolyl)-2-((trimethylsilyl)oxy)propanenitrile.

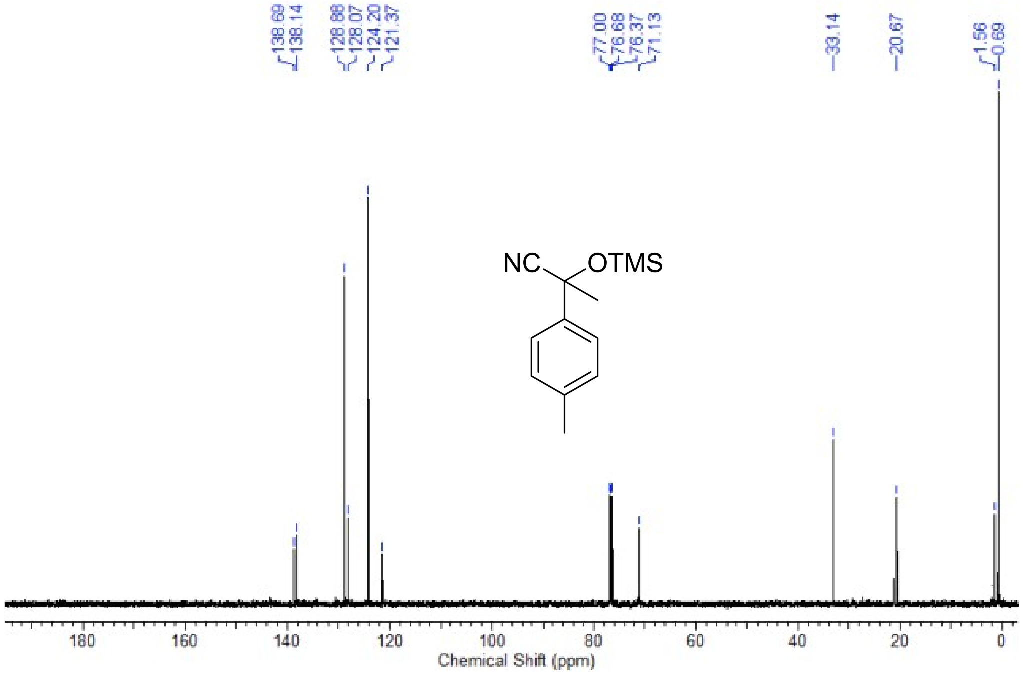

Figure FS141. ^{13}C NMR spectrum (100 MHz, 25°C, $CDCl_3$) of 2-(p-tolyl)-2-((trimethylsilyl)oxy)propanenitrile.

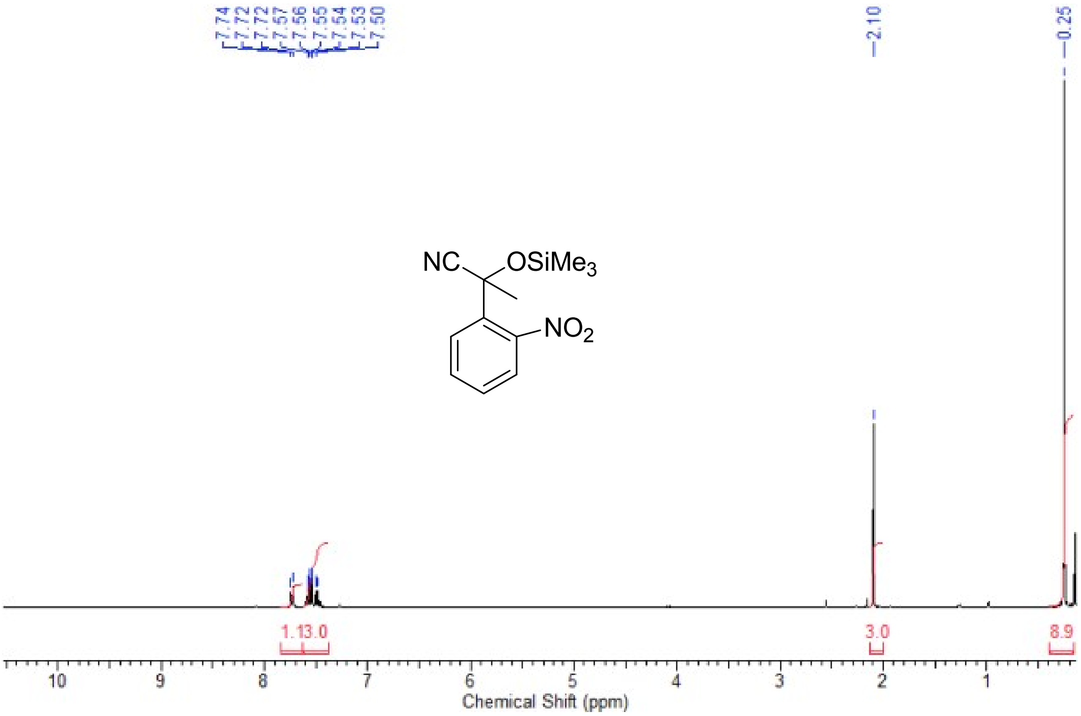

Figure FS142. ^{1}H NMR spectrum (400 MHz, 25°C, $CDCl_3$) of 2-(2-nitrophenyl)-2-((trimethylsilyl)oxy)propanenitrile.

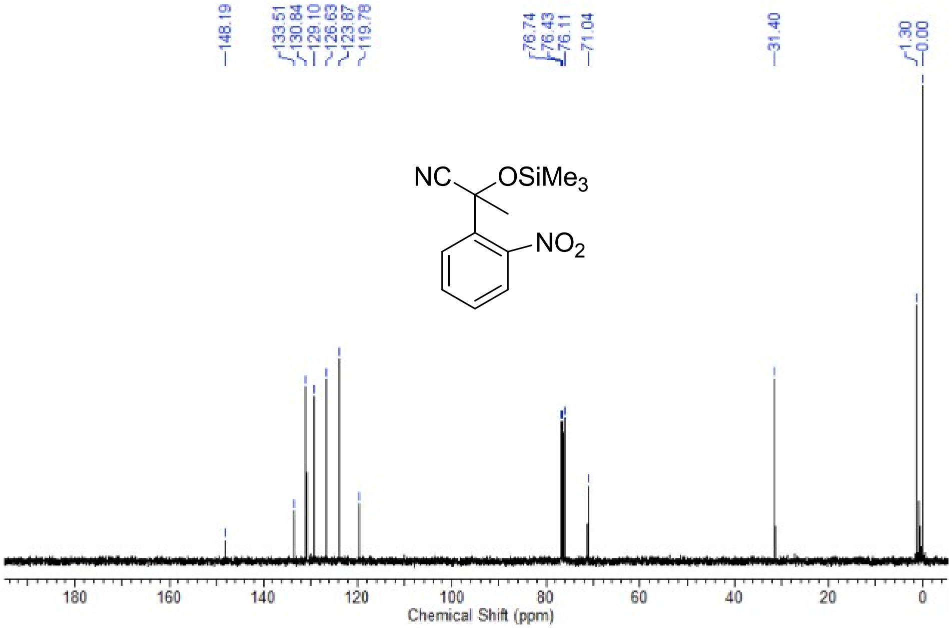

Figure FS143. ^{13}C NMR spectrum (100 MHz, 25°C, $CDCl_3$) of 2-(2-nitrophenyl)-2-((trimethylsilyl)oxy)propanenitrile.

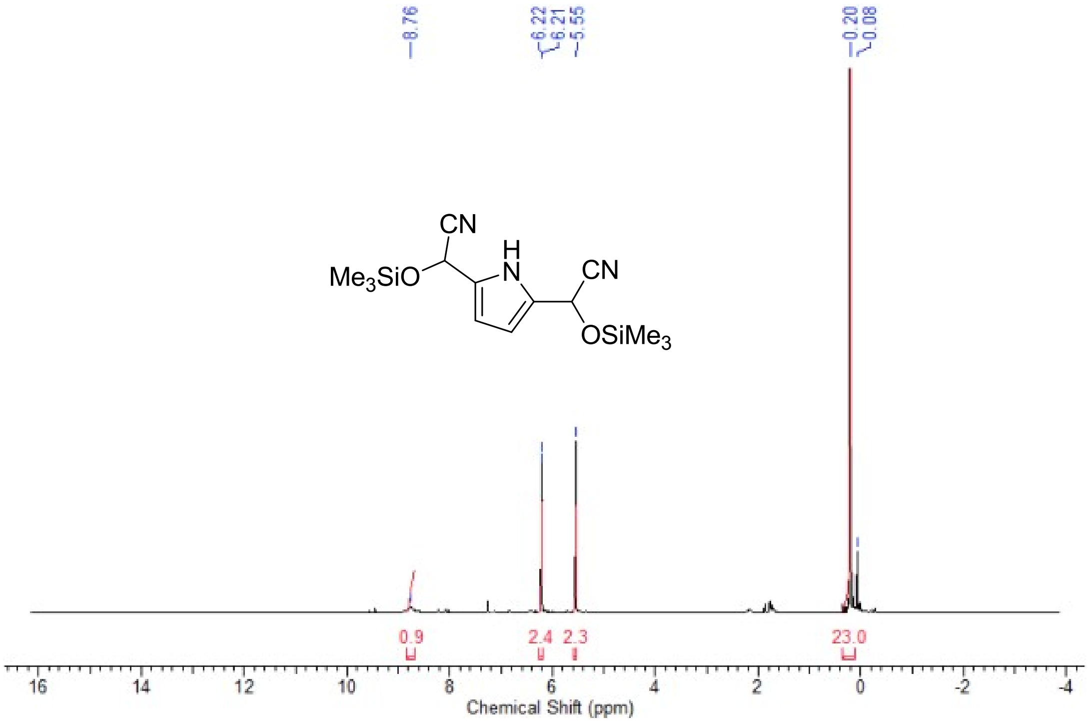

Figure FS144. ^{1}H NMR spectrum (400 MHz, 25°C, $CDCl_3$) of 2,2'-(1H-pyrrole-2,5-diyl)bis(2-((trimethylsilyl)oxy)acetonitrile).

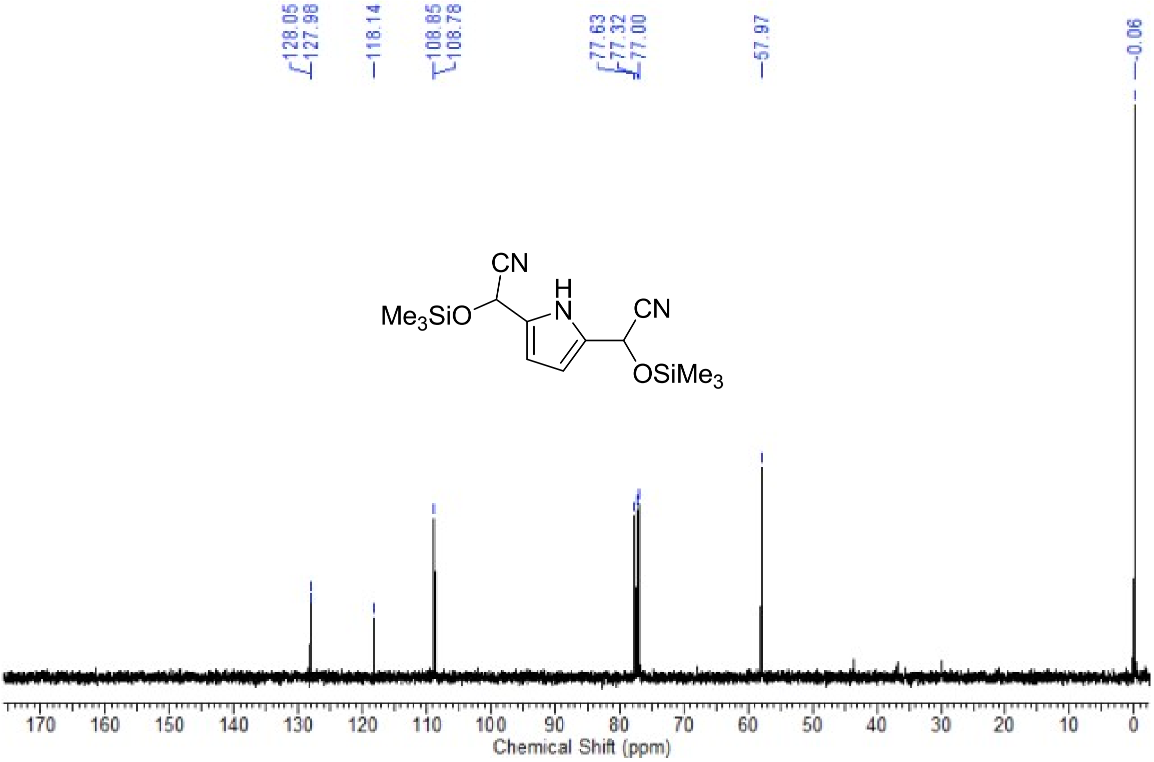

Figure FS145. ^{13}C NMR spectrum (100 MHz, 25°C, $CDCl_3$) of 2,2'-(1H-pyrrole-2,5-diyl)bis(2-((trimethylsilyl)oxy)acetonitrile).

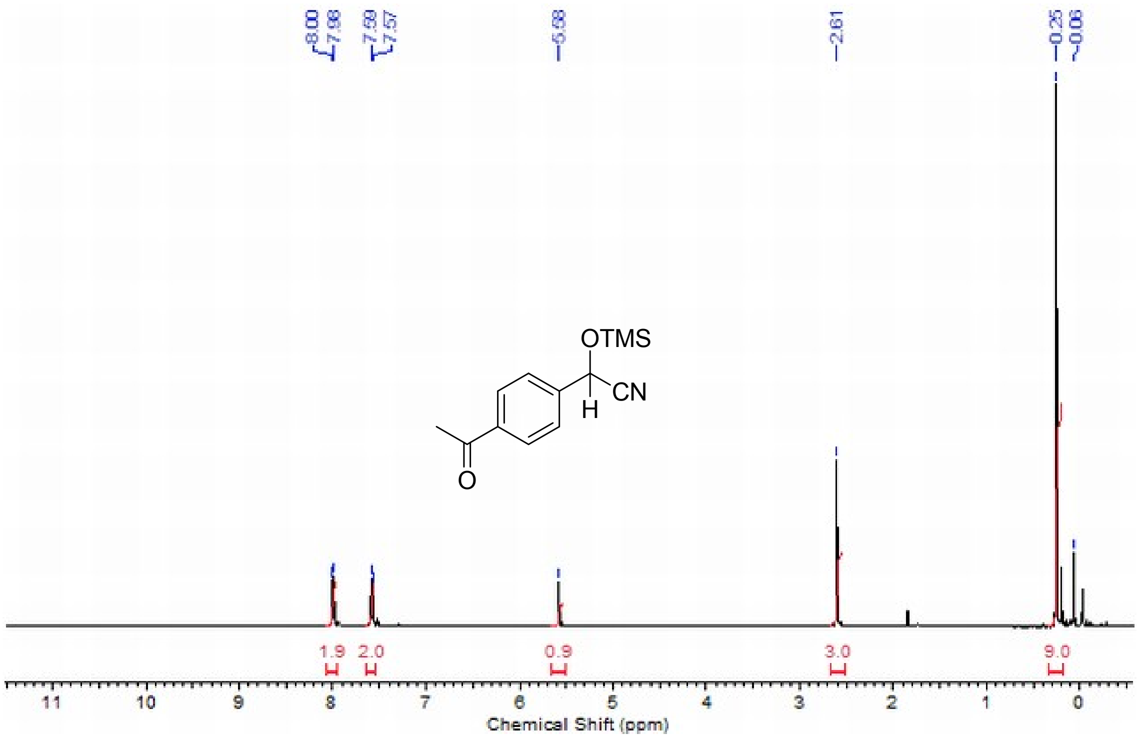

Figure FS146.^{1}H NMR spectrum (400 MHz, 25°C, $CDCl_3$) of chemo selective cyanosilylation of aldehydes.

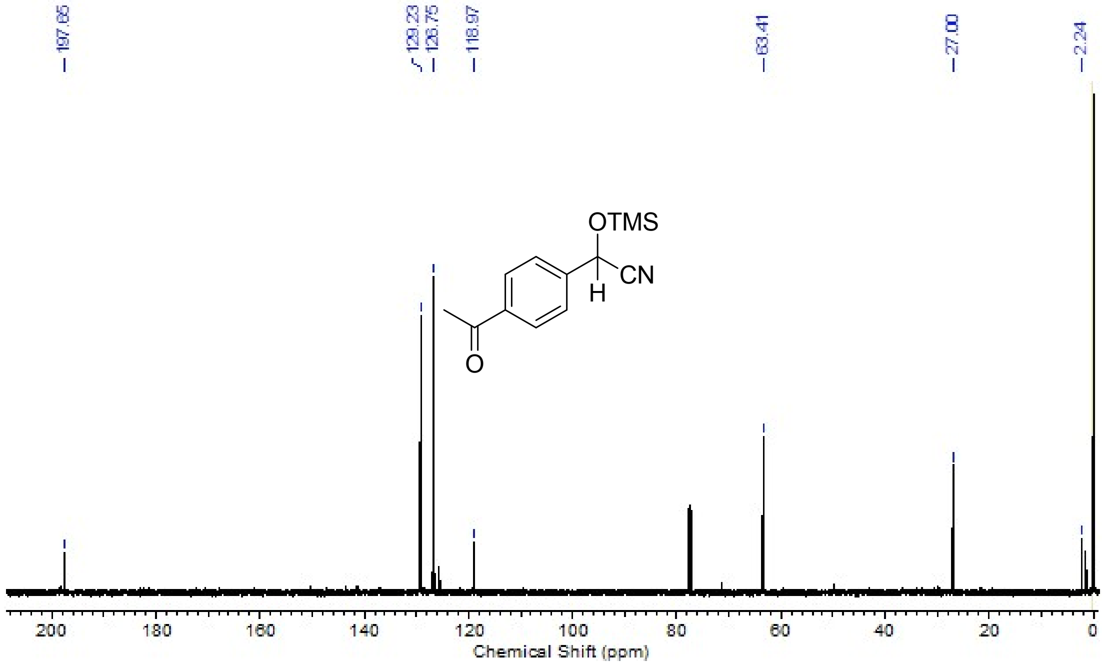

Figure FS147.^{13}C NMR spectrum (100 MHz, 25°C, $CDCl_3$) of Chemo selective cyanosilylation of aldehydes.

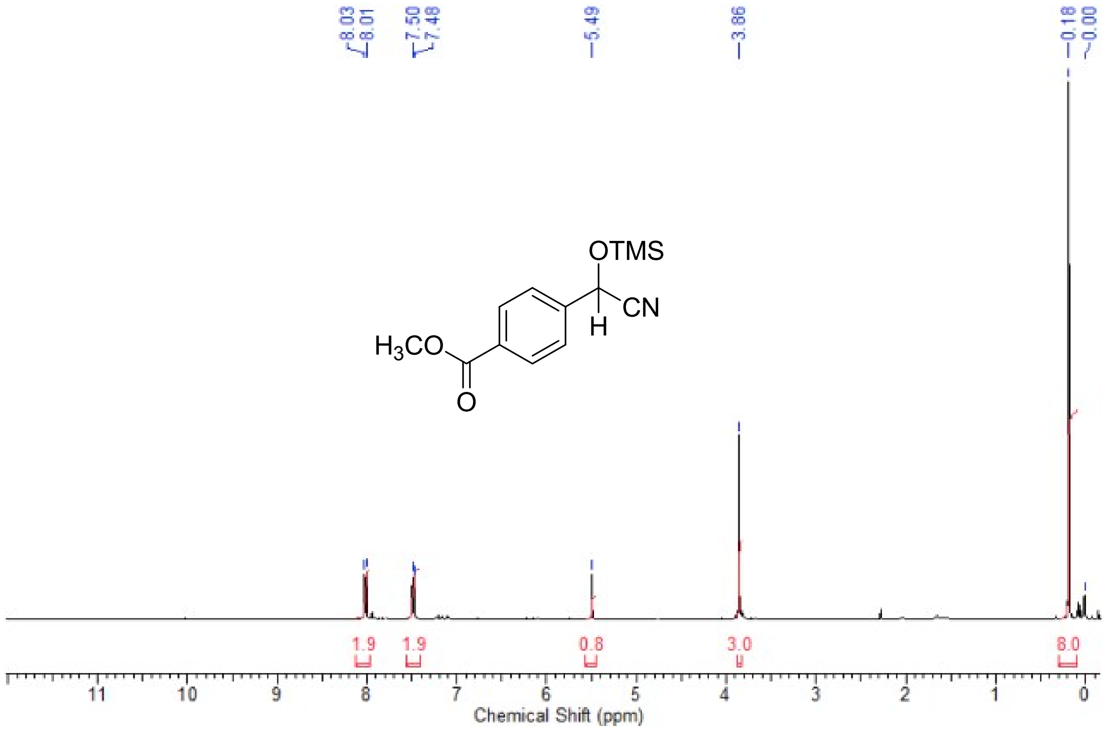

Figure FS148. ^1H NMR spectrum (400 MHz, 25°C, $CDCl_3$) of chemo selective cyanosilylation of aldehydes.

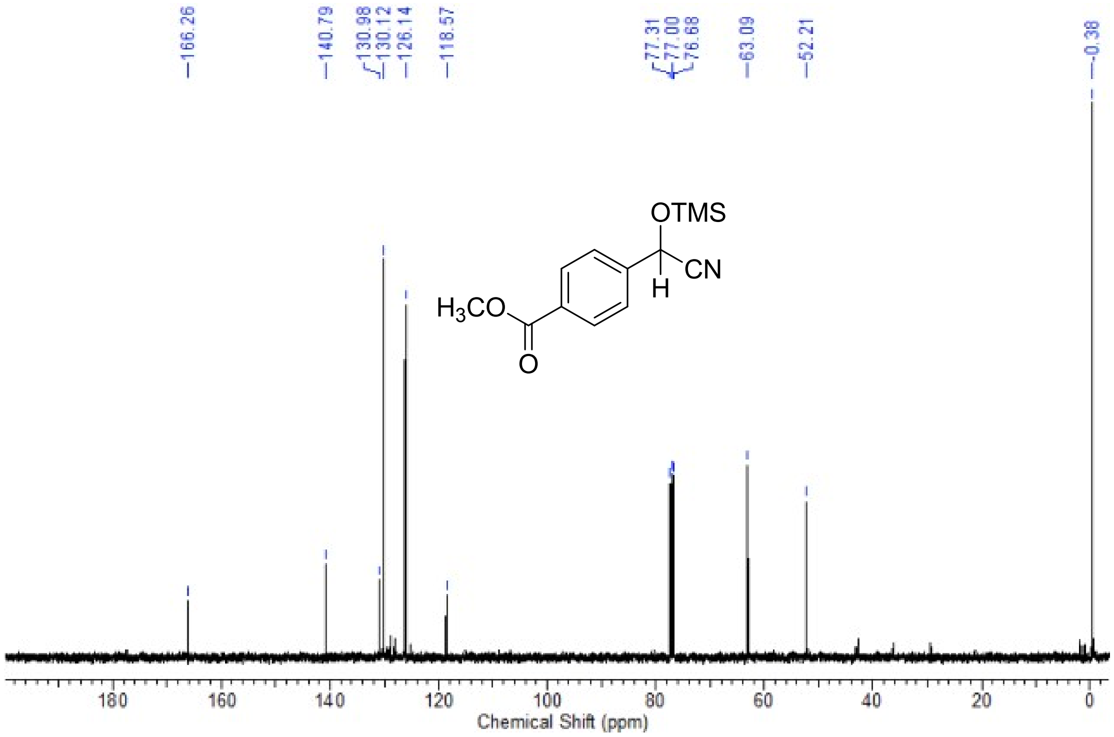

Figure FS149. ^{13}C NMR spectrum (128.4 MHz, 25°C, $CDCl_3$) of chemo selective cyanosilylation of aldehydes.

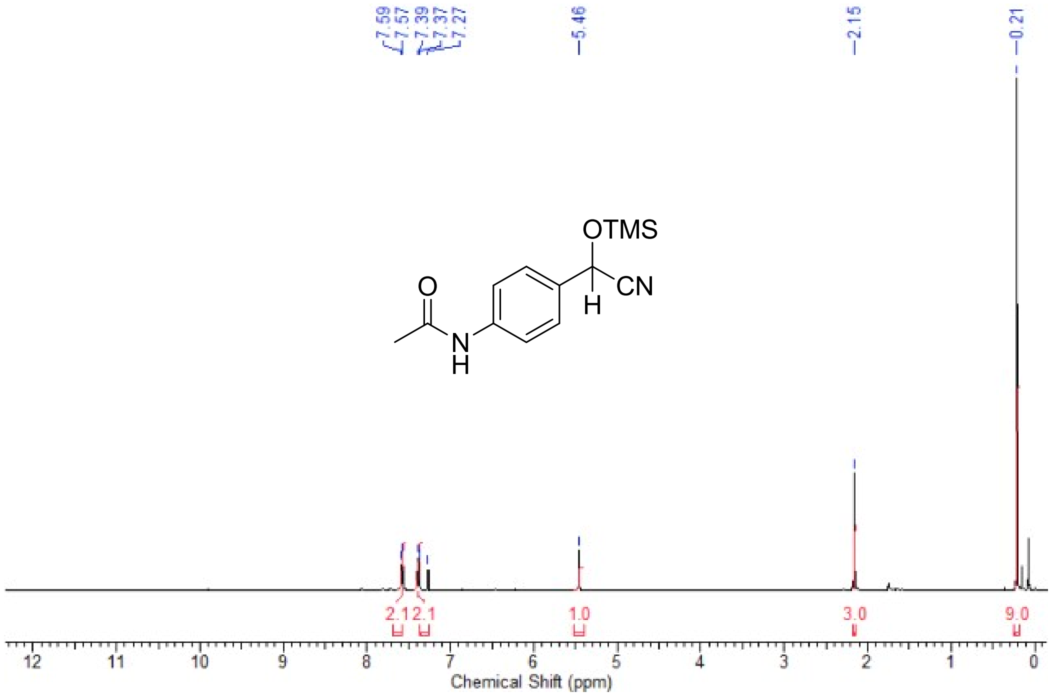

Figure FS150. ^{1}H NMR spectrum (128.4 MHz, 25°C, $CDCl_3$) of chemo selective cyanosilylation of aldehydes.

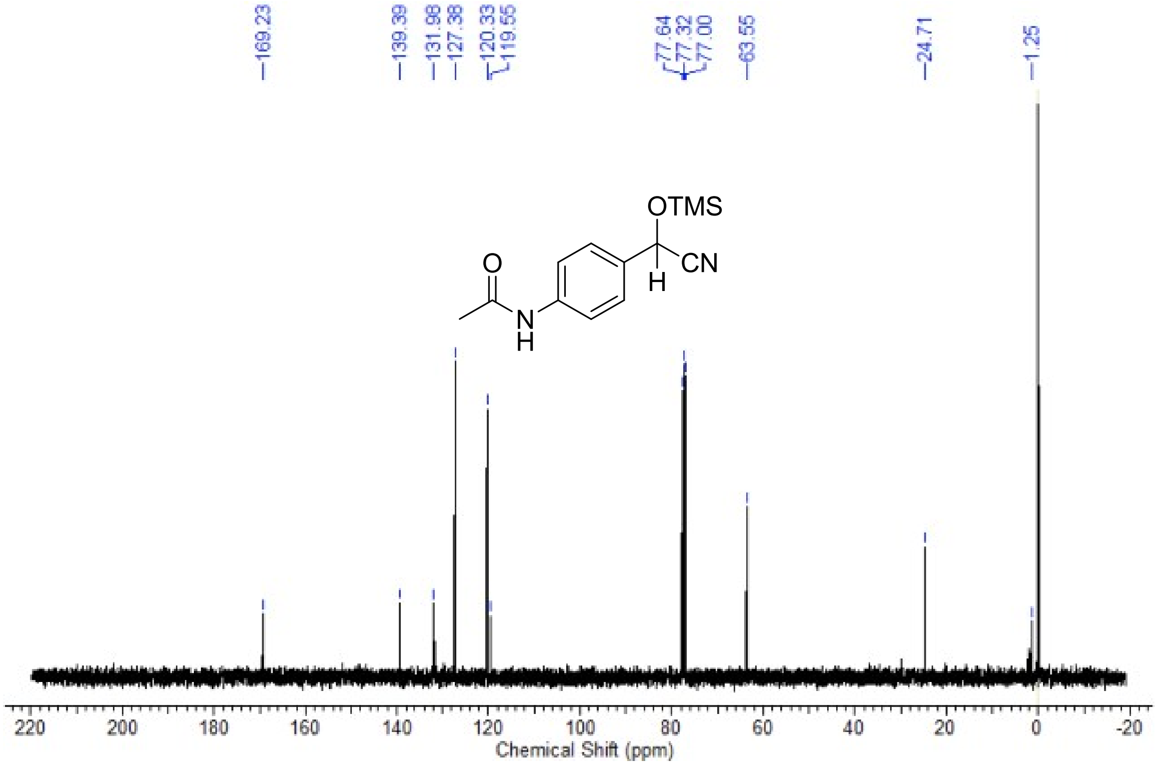

Figure FS151. ^{13}C NMR spectrum (128.4 MHz, 25°C, $CDCl_3$) of chemo selective cyanosilylation of aldehydes.

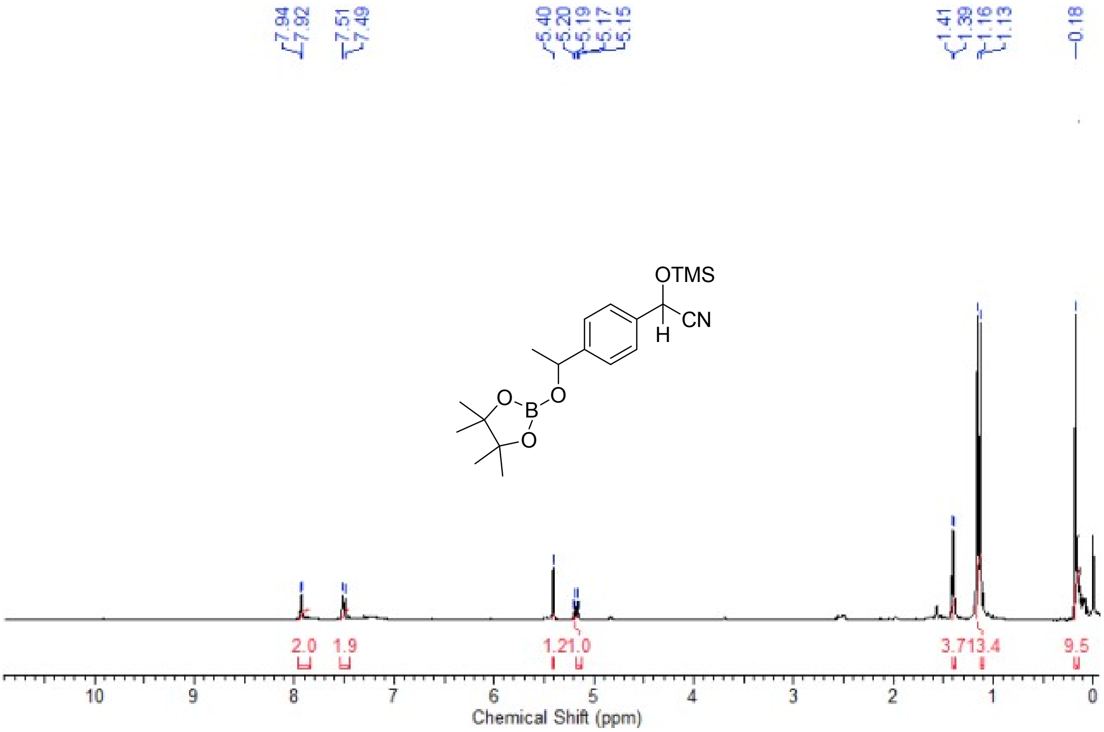

Figure FS152. ^{1}H NMR spectrum (400MHz, 25°C, CDCl$_3$) of sequential cyanosilylation and hydroboration of 4-acetyl benzaldehyde.

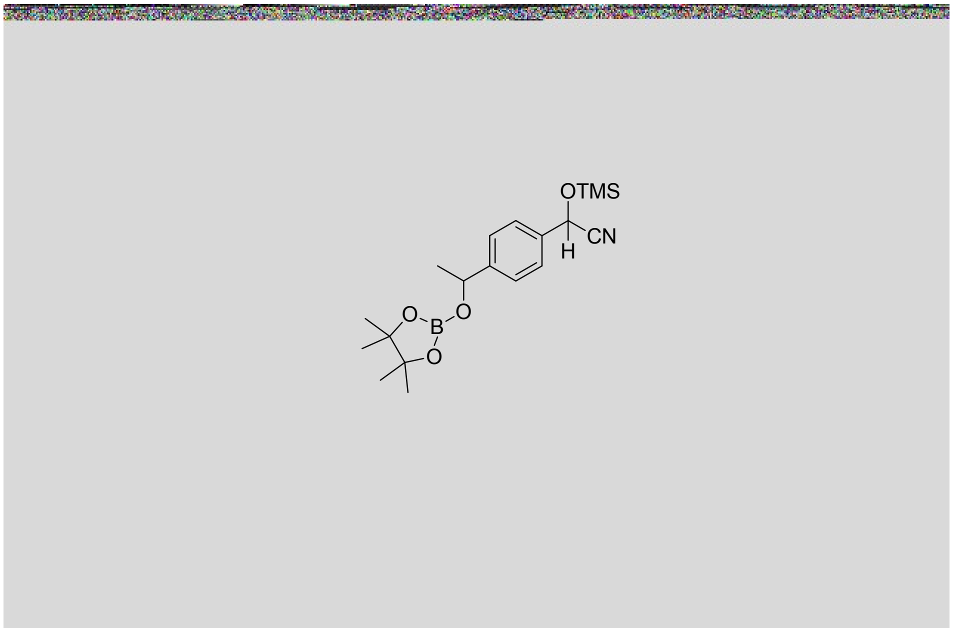

Figure FS153.^{11}B NMR spectrum (128.4 MHz, 25°C, CDCl$_3$) of sequential cyanosilylation and hydroboration of 4-acetyl benzaldehyde.

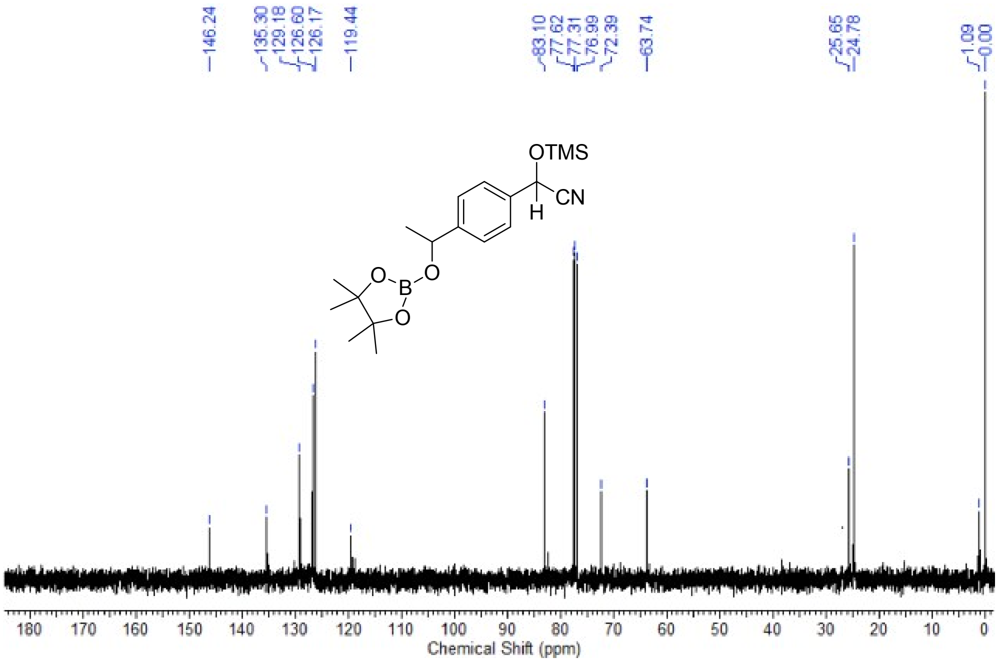

Figure FS154. ^{13}C NMR spectrum (100 MHz, 25°C, $CDCl_3$) of sequential cyanosilylation and hydroboration of 4-acetyl benzaldehyde.

References:

1. A. Altomare, M. C. Burla, G. Camalli, G. Cascarano, C. Giacovazzo, A. Guagliardi and G. Polidori, *J. Appl. Crystallogr*. 1994, **27**, 435-436.
2. G. M. Sheldrick, *Acta Crystallogr. Sect. A*: 2008, ***A64***, 112-122.
3. V. L. Weidner, C. J. Barger, M. Delferro, T. L. Lohr, T. J. Marks, *ACS Catal.* 2017, **7**, 1244.
4. S. Chen, D. Yan, M. Xue, Y. Hong, Y. Yao, Q. Shen, *Org. Lett*. 2017, **19**, 3382.
5. W. Yohsuke, Y. Takashi, *J. Org. Chem.* **2011**, **6**, 1957-1960.
6. Y. Li, J.Wang, Y. Wu, H Zhu, P. P. Samuel, H. W. Roesky*, Dalton Trans.* 2013, **42**, 13715–13722.
7. D. Martin, M. Soleilhavoup, G. Bertrand, *Chem. Sci.* 2011, **2**, 389 – 399.
8. M. Asay, C. Jones, M. Driess, *Chem. Rev.* 2011, **111**, 354 – 396.